Impact of Blockages on Mobile Users in 5G Millimeter-Wave Cellular Systems

Abdanaser Okaf

A Thesis
in
The Department
of
Electrical and Computer Engineering

Presented in Partial Fulfillment of the Requirements
For the Degree of
Doctor of Philosophy (Electrical and Computer Engineering) at
Concordia University
Montréal, Québec, Canada

May 3, 2022

CONCORDIA UNIVERSITY
SCHOOL OF GRADUATE STUDIES

This is to certify that the thesis prepared

By: **Abdanaser Okaf**

Entitled: **Impact of Blockages on Mobile Users in 5G Millimeter-Wave Cellular Systems**

and submitted in partial fulfillment of the requirements for the degree of

Doctor of Philosophy (Electrical and Computer Engineering)

complies with the regulations of the University and meets the accepted standards with respect to originality and quality.

Signed by the final examining committee:

Tiberiu Popa — Chair

Dr. Abdelouahed Gherbi — External Examiner

Dr. Dongyu Qiu — Thesis Supervisor

Dr. Mehmet Ali — Examiner

Dr. Yousef R. Shayan — Examiner

Dr. Roch Glitho — Examiner

Approved by

Dr. Wei-Ping Zhu, Graduate Program Director

May 3, 2022

Dr. Mourad Debbabi, Dean
Gina Cody School of Engineering and Computer Science

Abstract

Impact of Blockages on Mobile Users in 5G Millimeter-Wave Cellular Systems

Abdanaser Okaf, Ph.D.

Concordia University, 2022

The fifth-generation (5G), now being developed for use in the millimeter-wave (mm-wave) frequency bands, would enhance the Quality of Service (QoS) for the Mobile User (MU) in the near future. Despite the advantages of using mm-wave communications that are attained through the large bandwidth available in this band, it suffers from high penetration loss and low diffraction, which causes very high signal attenuation in free space. The signal's attenuation can also be due to the blockages, such as buildings, human presence, vehicles, etc. As a result, the signal propagation path could be interrupted by those blockages causing significant fluctuation in the handover (HO) probability. Thus, the foreseen mm-wave communication gains are achieved at the expense of varying HO probability. Therefore, the impact of blockages on the HO probability for a user with mobility is a crucial performance factor that needs to be analyzed and addressed in mm-wave cellular communication systems. This thesis analyzes the impact of different types of blockages on the HO probability for a MU with mobility in the 5G mm-wave cellular network, and it shows how blockages affect the resource allocation in mm-wave cellular system.

Firstly, we obtained the effect of a single static blockage with a fixed location in the 2-D plane on the HO probability for a MU moving radially away from the mm-wave base station (BS) at a certain speed. The mm-wave BSs, are assumed to be distributed according to a homogeneous Poisson Point Process (PPP). We considered the MU is moving at a uniform angle with a certain speed in the mm-wave cellular network. The results show that the blockage has a remarkable impact on the HO probability, depending significantly on its location and length, and MU direction and speed.

Secondly, we analyzed the impact of multiple static blockages, with a certain density, distributed according to PPP. The results show in this scenario that the density of the blockages plays a significant role in the HO probability for a user with mobility in a 5G

mm-wave cellular system.

Thirdly, we presented an analysis of the impact of self-blockage on HO probability in 5G mm-wave cellular networks. As expected, the results showed that self-blockage has a notable effect on the HO probability. The results show that the HO probability where self-blockage is incorporated in the system is different from the HO probability in case no blockages are incorporated in the system model.

Fourthly, we analyzed the impact of dynamic blockages on the system's performance in the mm-wave cellular network. The blocking probability of the link between the mm-wave BS and the MU due to dynamic blockages is calculated. We consider blockages and mm-wave BSs are distributed according to PPP, while the MU is assumed to make a displacement from the origin to another position. The arrival process of the blockages crossing the link between the tagged mm-wave BS and the MU is assumed to be Poisson with a certain density. The blockage duration is assumed to be independent of the blockage arrival process with exponential distribution. The results showed that the blocking probability gets higher when the blockages are moving at a high speed, and the density of the blockages gets higher as well.

Fifthly, we apply a classical HO scheme in mm-wave cellular networks to show how blockages affect resource allocation. We apply an adjustment of the number of reserved channels reserved exclusively for the HO requests based on a predefined threshold of the probability of blocking HO calls, to ensure the requirement of the QoS and hence the resource allocation is managed efficiently. The results show that a higher number of reserved channels is required to satisfy the minimum threshold of the blocking probability of HO calls. As a result, an optimized and balanced scheme between the blocking probability of HO calls and the blocking probability of originating calls in the mm-wave BS is required.

We conclude our research by providing the future plans of our research and the conclusion.

Acknowledgments

First of all, I am thankful to Almighty ALLAH. It would have been impossible to finish my thesis without His blessings.

Secondly, special thanks to my mother, wife, and son (Mohamed) for their support and encouragement during my Ph.D. study journey.

Thirdly, I would like to express my sincere gratitude and most profound appreciation to my brothers, sisters, relatives, and friends for their support.

Fourthly, I sincerely wish to thank my supervisor Prof. Dongyu Qiu, who gave me research guidance, suggestions and support to finish my thesis. It was an absolute pleasure for me to have such an exceptional scholar, and it was my honor to be his Ph.D. student.

Last and not least, I would like to thank the committee members, Prof. Glitho, Prof. Mehmet Ali, and Prof. Yousef R. Shayan, for their review of my dissertation and their constructive comments and feedback.

This thesis is dedicated to the soul of my dear father (Mohamed Ben Issa Okaf)

Contents

List of Figures

List of Abbreviations

5G	Fifth-Generation
6G	Sixth-Generation
QoS	Quality of Service
MU	Mobile User
HO	Handover
Mm-Wave	Millimeter-Wave
PPP	Poisson Point Process
BS	Base Station
Gbps	Gigabit-per-second
LOS	Line-of-Sight
NLOS	Non-Line-of-Sight
2-D	Two-Dimensional
Tx	Transmitter
Rx	Receiver
ROP	Random Object Process
SNR	Signal-to-Noise Ratio
RSRP	Reference Signal Received Power
Gbps	Gigabit-per-Second
GHz	Giga-Hertz
RWP	Random Walk Point
$\mathbb{R}^2$	Two-Dimensional Euclidean Plane

Chapter 1
Introduction

1.1 Introduction to Mm-Wave Communications:

The current requirements for high data rates in wireless services and the spectrum insufficiency ranging between 700 MHz and 2.6 GHz bands are emphatically motivating the use of the mm-wave frequencies. The use of mm-wave frequency bands would significantly impact the QoS of the 5G networks and overcome the global bandwidth shortage [1, 2]. Mm-wave carrier frequencies support vaster bandwidth allocations, resulting in higher data transfer rates. 5G mm-wave communication would allow service providers to significantly extend the channel bandwidths far exceeding the existing 20 MHz channels used by 4G customers [3]. Making the bandwidth full for the mobile radio channels will be reflected positively on the data capacity and decrease the latency for digital traffic, which would support much better QoS and motivate operators and the industrial sector to transition towards the 5G mm-wave communication cellular system.

According to [2], there has been a sharp increase in wireless data traffic for the past decade. The growth in wireless data traffic is estimated to increase at a rate of more than 50 percent annually per subscriber. This trend in the data traffic is expected to accelerate steadily in the next decade with the rise in the popularity of video, and the Internet-of-Things [3, 4]. As a result of the need to address this challenge, the global wireless industry has put all energies into transitioning to the 5G of cellular technology.

This technology will employ the mm-wave frequencies to offer unprecedented spectrum and multi-Gigabit-per-second (Gbps) data rates to the MU's. The shift in the technology from the 4G to the 5G networks, which employ the mm-wave frequencies, would greatly improve the performance of the MU [5, 6]. For instance, it is estimated that 1 GHz wide channels at 28 or 73 GHz are capable of offering several Gbps of data rate to the MU [2]. However, mm-wave communications also pose a new challenge, which is represented by the impact of the blockages that could cause severe signal attenuation and degrade the data speeds and quality reaching the MU under the 5G networks [7,8]. There is a need to address the impact of blockages on users with mobility in mm-wave cellular systems, such as vehicles, aircraft, buildings, etc. Even human traffic could be a significant challenge that would adversely alter the QoS of the MU.

1.2 Motivations and Problem Statement:

Analyzing the system performance of mm-wave cellular networks in the presence of different types of blockages, is a crucial task to understand network behavior. Lately, there has been a growing demand for high data rates in wireless communication systems. The latter promoted and motivated the researchers and industrial sector to transition towards mm-wave bands where a vast spectrum range is available to provide a multi-gigabit per second data rate transmission. Therefore, to satisfy such demand, it is highly recommended to operate at mm-wave bands (30 GHz-300 GHz) as a solution to overcome this problem. However, migration to the mm-wave operating frequencies has various issues and challenges that need to be addressed for a successful transition. The propagation characteristic of the mm-wave signals is one of the main challenges influenced by blockages, such as buildings, cars, and even small objects such as human bodies. During user mobility, such blockages can interrupt the signal path between the mm-wave BS and MU. The signal interruption due to blockages could force MU to make frequent handovers in order to access another Line-of-sight (LOS) mm-wave BS. That depends mainly on the type, shape, and location of the MU's blockage and speed. However, blockages can be classified into three types, which will be described extensively in chapter II, namely:

1. Static Blockage.
2. Dynamic Blockage.
3. Self-Blockage.

Regardless of whether the blockage is static or dynamic, it plays a crucial role in the performance of the mm-wave cellular system. The prime objective of the models that incorporate blockages in prior work was to analyze the system's performance and to study the impact of blockages on stationary MU in the mm-wave cellular systems. However, prior work did not include an analysis of blockage impact on the system performance for a user with mobility in an mm-wave cellular system. Moreover, apart from the blockage type, blockage frequency, and blockage duration due to MU mobility, blockages affect the performance of the mm-wave system and are critically important for studying the performance of the system overall.

1.3 Research Objectives:

The main objective of this research is to study and analyze the impact of different types of blockages on the performance of the MU with mobility in a 5G mm-wave cellular network to capture the performance-related metrics and to compare the results of this analysis with the results in the case of no blockage of the traditional 4G cellular systems. This is to facilitate and simplify the theoretical analysis, which would be complicated, and to capture the potential impact of the blockages due to user mobility considering the three types of blockages; static, dynamic, and self-blockage. Another goal of this research is to use the analysis of the impact of different types of blockages on HO probability as a starting phase in designing an efficient HO scheme to minimize the blocking probability of HO requests in the target mm-wave BS, aiming for continuity of service without any signal interruptions or forced termination. The following aspects are summarized objectives that proposed as part of the research activities:

- Analyzing the impact of static blockages on HO probability for a user with mobility in 5G mm-wave cellular network.

- Analyzing the impact of self-blockage on HO probability for a user with mobility in 5G mm-wave cellular network.

- Analyzing the impact of dynamic blockage on blocking probability for a user with mobility in 5G m-wave cellular network.

- Applying a classical HO scheme based on HO priority strategy in mm-wave cellular networks to show how blockages affect the resource allocation.

1.4 Research Contributions:

This research aims at analyzing the impact of different types of blockages on the performance of the MU in the 5G mm-wave cellular network. We particularly focused on the impact of blockages on HO probability for a user with mobility in 5G mm-wave cellular networks. That would enhance and ensure efficient use of channel resources and guarantee

the minimum quality of service (QoS) requirements.

The main contributions of this research can be summarized as follows:

1.4.1 Impact of Static Blockages on HO Probability for A User with Mobility in Mm-Wave Cellular Network

We analyzed the impact of static blockages on HO probability for a user with mobility in different scenarios. Firstly, we captured the impact of a single static blockage on the HO probability with different displacements and directions of the MU. In this scenario, the blockage's location is assumed to be fixed with predefined coordination. Secondly, we extended our analysis by capturing the impact of multiple static blockages on HO probability for a user with mobility in the 5G mm-wave cellular network. In this scenario, the center of blockages is assumed to be distributed according to Poisson Point Process (PPP) at a uniform.

The following paper has been published based on the first scenario of this work:

A. Okaf and D. Qiu, "Analysis of Blockage Impact on Handover Rate for User with Mobility in 5G mm-Wave Cellular Network," 2020 International Symposium on Networks, Computers and Communications (ISNCC), 2020, pp. 1-6, [9].

1.4.2 Impact of Self-Blockage on HO Probability for A User with Mobility in Mm-Wave Cellular Network

We studied the self-blockage impact on HO probability for a MU with mobility. We considered that the own body of the MU could block the link between the MU and the mm-wave BS, which depends mainly on the blocking angle that results from the body of the MU.

The following paper has been published based on this work:

A. Okaf, A. Saied and D. Qiu, "Analysis of Self-Blockage Impact on Handover Probability for User with Mobility in 5G Mm-Wave Cellular Network," 2021 International Symposium on Networks, Computers and Communications (ISNCC), 2021, pp. 1-5, [10].

1.4.3 Impact of Dynamic Blockages on Blocking Probability for A User with Mobility in Mm-Wave Cellular Network

Dynamic blockages is another type of blockages that need to be considered in designing an mm-wave cellular system. For this purpose, we studied the impact of dynamic blockages on the blocking probability for a user with mobility in mm-wave cellular systems.

The presence of dynamic blockages results in a higher probability of blocking the LOS link for some time while the blockage crosses the LOS link, which could cause an increase of the HO probability and the ping-pong effect. In this analysis, we assumed that the MU makes a displacement from the origin to another location. The arrival process of the blockages crossing the mm-wave BS-MU link is based on Poisson with intensity α. In contrast, the blockage duration is assumed to be independent of the blockages arrival process and is exponentially distributed with mean $\frac{1}{\mu}$. Therefore, the blocking event follows an exponential on-off process with α and μ being the blocking and unblocking rates, respectively.

The following article has been submitted with respect to this work:

Abdanaser Okaf and D. Qiu,"Impact of Dynamic Blockages on Blocking Probability in Mm-Wave Cellular Systems", 2022 IEEE Global Communications Conference: Wireless Communications, (Submitted)

1.4.4 Impact of Blockages on Resource Allocation in Mm-Wave Cellular Networks

We address the problem of resource allocation in mm-wave cellular systems in the presence of blockages. We apply a classical HO scheme based on HO priority strategy in mm-wave cellular system to show how the blockages affect resource allocation. Adjusting the number of reserved channels for HO requests aims to minimize the blocking probability of HO requests and guarantees the QoS requirement. We show how adjusting the number of reserved channels for HO requests could maintain the minimum requirements of QoS, so that channel resources are used efficiently, and a predefined threshold of blocking probability of HO requests is satisfied.

The following article has been submitted with respect to this work:

Abdanaser Okaf and D. Qiu,"Impact of Blockages on Resource Allocation in Mm-Wave

Cellular Networks" IEEE Access, (Submitted)

1.5 Thesis Organization

This research is divided into six chapters with the abstract. The first chapter covers the introduction, the motivation, the problem statement, and the objectives. The rest of this thesis is organized as follows:

- The second chapter presents a background and literature review of mm-wave communication, including; the reflection and penetration loss in mm-wave communication, blockages impact in 5G mm-wave cellular systems, and HO probability and mobility management in 5G mm-wave cellular systems.

- The third chapter analyzes the impact of a single static blockage on HO probability for users with mobility in a 5G mm-wave cellular network.

- The fourth chapter covers an analysis of the impact of multiple static blockages on HO probability for user with mobility in 5G mm-wave cellular networks.

- The fifth chapter presents an analysis of the impact of self-blockage on HO probability for users with mobility in a 5G mm-wave cellular network. It also presents the impact of dynamic blockages on the blocking probability.

- Chapter six addresses the problem of resource allocation management in mm-wave cellular systems in the presence of blockages by applying a classical HO scheme based on HO priority strategy to show the impact of blockages on resource allocation in mm-wave cellular systems.

- Conclusions and future work are drawn in chapter seven. The thesis is concluded with all appendixes and references.

Chapter 2
Background and Literature Review

2.1 Preliminaries and Background of Mm-Wave Communications:

Thanks to the abundant bandwidth in mm-wave frequencies, mm-wave communication is considered one of the best candidates for the 5G cellular communication systems compared to traditional cellular communication systems that work at sub-6 GHz bands [4]. Despite the bandwidth availability, several critical challenges are related to mm-wave signals. The limited availability of the LOS link is the most challenging in mm-wave communications. This is due to its susceptibility to blockages of the Non-Line-Of-Sight (NLOS) link resulting from higher penetration losses, and reduced diffraction in mm-wave signals [5]. In contrast to microwave cellular systems, at shorter mm-wave wavelengths, such blockages can be caused by any object, for instance, human bodies, buildings, vehicles, etc. Due to mobility, this makes wireless channels frequently fluctuate from the NLOS link to the LOS link and vice versa, which leads to rapid channel variations that directly impact the link and, consequently, the HO probability.

This chapter introduces a brief literature review of the issues and challenges related to mm-wave communications that need to be addressed. It begins by presenting the characteristics of mm-wave communication and an abbreviation of the previous work related to the reflection and penetration loss in mm-wave signals to understand the signal degradation and interruption due to blockages in mm-wave communications. It also gives a brief background on the impact of blockages on the performance of mm-wave communication systems. Moreover, it offers a short literature review of the HO management in 5G mm-wave cellular networks in the presence of blockages.

2.2 Characteristics of Mm-Wave Communication

In order to efficiently use mm-wave frequency bands, it is necessary to comprehend the mm-wave communication characteristics. The mm-wave communication has more special characteristics than traditional microwave communication, including extensive bandwidth, huge path loss, sparse channel, and blockage impact. The propagation characteristics of signals at mm-wave frequency bands impose more challenges to establishing reliable connections. The following subsections briefly present the propagation characteristics of

mm-wave communication:

2.2.1 Large Bandwidth

One of the most important characteristics of mm-wave communication is the vast bandwidth. It has a frequency band ranging from 30 GHz to 300 GHz, bringing more focus from industry and academia because of the large amount of unused spectrum in the mm-wave frequency band [2]. More precisely, the mm-wave frequency band retains more than 20 GHz of the available spectrum, which is 20 times more than that assigned for the current Wi-Fi and cellular networks. This band is distributed into the following sub-bands, as illustrated in figure (2.1):

- 1.4 GHz bandwidth at the 39 GHz frequency band.
- 2.1 GHz bandwidth at the 37 frequency GHz.
- 7 GHz bandwidth at the 60 GHz frequency band.
- More than 10 GHz at the E frequency band (71–76 GHz, 81–86 GHz, and 92–95 GHz).

It is expected that these frequency bands to be utilized in future generations of wireless networks, such as the fifth-generation (5G) and the sixth-generation (6G), to meet the huge demand for the high-speed data transmission rate [1–4, 11, 12].

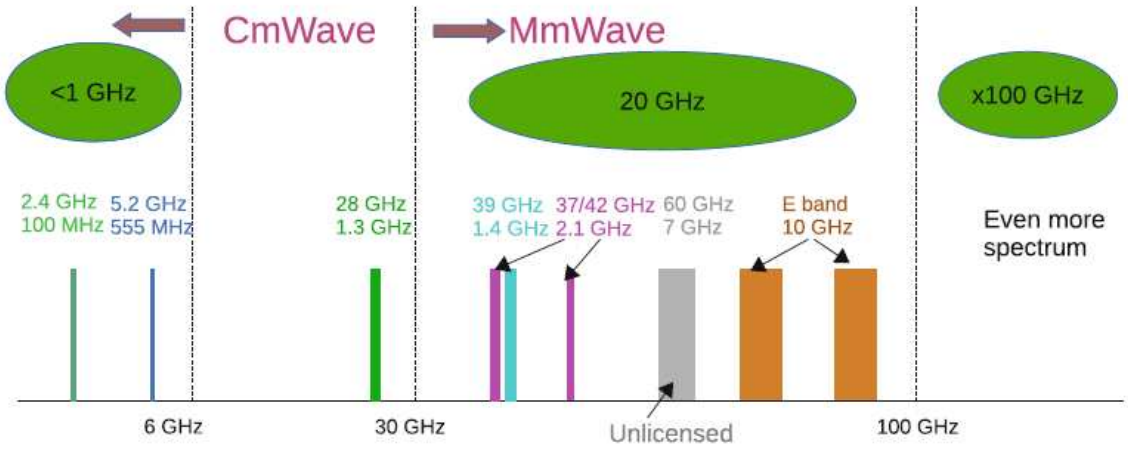

Figure 2.1: Spectrum distribution at the mm-wave frequency band.

2.2.2 Huge Path Loss

Mm-wave communication suffers from significant path loss. It can be shown that by Friis law formula [13] in the following simple mathematical calculation.

The received power, P_r, in the ideal free space transmission case follows:

$$P_r = P_t G_t G_r \left(\frac{\lambda}{4\pi}\right)^2 r^{-\alpha} \tag{2.1}$$

Where,

P_t: is the transmit power.

r: is the distance between the transmitter and the receiver.

λ: is the wavelength of the carrier frequency.

α: represents the path loss exponent.

G_t and G_r: represent the antenna gains of the transmitter and the receiver, respectively.

From equation (2.1), it is clear that the received power depends mainly on the wavelength of the carrier frequency. Since mm-wave signal wavelength is much smaller than the wavelength of the microwave signal. Consequently, the aperture of the mm-wave antenna element is smaller than that of the microwave antenna. That leads to less RF power can be captured by the element of the mm-wave antenna at the receiver side. Therefore, the path loss at the mm-wave frequency band is much higher than that at the microwave frequency band.

By considering an mm-wave frequency at the unlicensed 60 GHz band and the microwave frequency at 2.4 GHz band, according to the equation (2.1), the mm-wave signal will suffer from 28 dB extra path loss as compared to that microwave signal. Moreover, the mm-wave communication suffers from higher noise power than the microwave communication due to the large bandwidth. Considering the received power and noise power, mm-wave communication suffers from severe signal-to-noise ratio (SNR) loss.

In addition to the ideal case of the free space transmission, rain attenuation and the absorption resulting from the atmospheric add more path loss to the mm-wave communication. It is shown that the attenuation resulting from the heavy rain scenario is about 7 dB/km, whereas the attenuation resulting from atmospheric absorption, based on measurement results at the frequency of 28 GHz, is about 1 dB/km [14].

In fact, various measurement studies have been conducted to capture channel propagation characteristics and path loss models for mm-wave communication, including path loss exponent and the shadowing factor, to understand the behavior of the mm-wave signals. For example, propagation measurements have been conducted in [15] using an omnidirectional antenna. It was shown that the path loss exponent is 3.4, and the shadowing factor is 9.7 for the 28 GHz band. Another study in [16] was conducted to measure reflection coefficients and penetration losses for common building materials at 28 GHz in and around buildings in New York City. The results show that materials used for outdoor buildings, such as tinted glass, have a high reflection coefficient of 0.896 compared to materials used for indoor buildings with a low reflection coefficient. The work in [17] presents propagation measurements in the presence of human activity for a 60 GHz channel. The results show that a human body for a single person can shadow the direct link between the transmitter (Tx) and the receiver (Rx) and cause attenuation of more than 20 dB for approximately 100 milliseconds (ms). On the other hand, a group of people could cause fading in durations of 300 ms or more. Several measurements for the indoor and outdoor environment have been conducted at 60 GHz. For example, short-range office measurements, conducted in [18], showed that fade durations in line-of-sight (LOS) environments were about 550 ms with average attenuations between 6 dB and 18 dB. In contrast, the results obtained from outdoor measurements in a street canyon using omnidirectional antennas show that attenuation could exceed 40 dB when the LOS path is blocked [19]. Another experiment was conducted in [20] at 28GHz using omnidirectional antennas in an urban environment in the presence of pedestrians and vehicles for a small mm-wave BS. The results show that 12 dB to 25 dB attenuation of the LOS path. Many experiments were carried out to capture and analyze the characteristics of the propagation of mm-wave signals, for example, but not limited to in [21], [16], [22]. However, these experiments did not provide an accurate statistical characterization of the blockage dynamics that can be used as a reference for analyzing the performance of the mm-wave communication system [21]. On the other hand, these experiments provide insights into the channel propagation characteristics and path loss models for mm-wave communication in the presence of blockages. Recently, the study in [7] presented the result of a measurement conducted on human bodies in an anechoic chamber at different mm-wave frequencies, specifically at 15, 28, and 60 GHz. The experiment was conducted on 15

humans of different sizes and weights. The results showed that the losses are proportional to the size of the human body with respect to the radio link. It also shows that as the height of the transmitting mm-wave antenna increases, the blockage loss decreases.

2.2.3 Sparse Channel

Channel sparsity is one of the characteristics of mm-wave communication. Microwave communication is characterized by high diffraction at lower-frequency bands that maintain a number of paths in the channel. The channel in mm-wave communication is relatively sparse, and there are only fewer paths in the channel than the mm-wave channel. The following points show the number of paths in mm-wave communications and the performance of these paths in realistic scenarios:

- **Number of paths:**

  Generally, the clustered paths are consist of one dominant LOS propagation path and a few NLOS propagation paths. The NLOS propagation paths are usually obtained from reflectors with a high ability to reflect the mm-wave signals. Human bodies and materials of some structures are examples of strong reflectors. Several experiments and measurements are conducted to demonstrate and show whether the mm-wave channel is sparse or not. For example, there are less than five paths on average at the unlicensed 60 GHz band in conference room scenarios.

- **performance of paths:**

  Due to the reflection and a longer signal propagation path, the NLOS path suffers from higher path loss than the LOS path. That is based on the results obtained from extensive experiments conducted in different scenarios to capture the performance of the NLOS mm-wave paths.

  For example, measurement results based on a ray-tracing method inside an office show that the first-order of the reflected NLOS path experience between 5–10 dB SNR loss if we compare this result with the LOS path. While the SNR of the second-order of the reflected NLOS path experience 0–20 dB less than that of the LOS path [16].

Besides the drawbacks of the channel sparsity that affect the network coverage and

may reduce it, the channel sparsity has some advantages in addressing problems related to channel estimation in mm-wave communications. For example, a large antenna array generates narrow beams with high antenna gains to resist and counteract the path loss at high frequency in the mm-wave bands. Recently, the work in [23] reported the fading evaluation in different mm-wave bands where the measurements were carried out through a campaign conducted in different scenarios in an indoor environment, where it is characterized by rich-multipath scattering. The measurements were carried out under LOS and NLOS conditions for a broad range of frequencies and different fading models. The findings of this work concluded that due to many reflecting and dispersing elements in an indoor environment, the well-known fading models available in the literature can be used to characterize short-term fading statistics of the standardized 5G mm-wave bands.

2.3 Impact of Blockages on Mm-Wave Cellular Systems

Different from microwave signals, mm-wave signals suffer from high penetration loss. This is because the mm-wave signal's wavelength is much shorter than the dimensions of the objects in the environment. That imposes significant challenges for mm-wave communications. The experience of high penetration loss in mm-wave communication contradicts microwave communication and makes blockage a thorny issue that needs to be addressed. There are several forms of common blockage in mm-wave communications, and the link in mm-wave communication may have three types of blockages, namely:

1. Static Blockage: This type of blockage is due to permanent structures such as buildings and static objects. It could cause permanent signal interruption and block the LOS link during the MU movement. However, it could play a small role in open and rural areas, but it could play a significant role in urban areas.

2. Dynamic Blockage: This type of blockage is due to mobile objects such as human bodies and vehicles. It could cause frequent signal interruptions and block the LOS link frequently.

3. Self-Blockage: This type of blockage is due to the MU's own body that could block the LOS link to the mm-wave BS.

Very limited studies in the literature presented the impact of different types of blockages on a user's mobility performance in mm-wave cellular systems. Studies were carried out by Bai et al. in [24] and [25], proposing a stochastic model for a stationary MU to capture the impact of static blockages on the system. Several performance metrics have been quantified using tools from random shape theory and a stochastic geometry approach. The results show that the coverage probability and connectivity are a function of blockages' metrics, such as blockages density and size. It showed that static blockages could cause a notable decrease in LOS link quality in the urban area, unlike an open area such as a public park. With regard to dynamic blockages, an analytical model in [26] characterizes the blocking created by humans by assuming that blockages are to be randomly distributed. A Markov model presented in [21] for blockage events based on measurements on a single mm-wave BS-MU link. Likewise, the authors in [27] present the blockage measurements with different statistical models. A self-body blocking model is presented in [28] to evaluate the impact of self-blockage in mm-wave cellular networks using a tool from stochastic geometry. Notably, all previous studies proposed analytical models for a stationary MU. However, these analytical models are not applicable to a user with mobility. The presence of blockages in the link between mm-wave BS and MU may cause a significant reduction in the LOS link, which may cause variations in the HO probability and, consequently, change the performance of the system overall. The occurrence of high-frequency interruptions and lengthy blockage duration has a further adverse impact on the quality of data received by the MU. As a result of the potential adverse impacts of the blockages on the effectiveness of the 5G mm-wave Cellular Systems, it becomes critical to find means to address this challenge [29]. As a result, all different types of blockages potentially reduce efficiency in data quality offered by the 5G mm-wave frequencies.

2.4 Handover in Mm-Wave Cellular Systems

Handover (HO) is a process of switching the current channel, including frequency, time slot, spreading code, or combination of them, associated with the current BS to another channel associated with another BS while a call of an MU is in progress as shown in figure

(2.2). In this figure, a MU is moving from the old BS to the new BS. The mean signal strength of the old BS decreases as the MU moves away from it. Similarly, the mean signal strength of new BS increases as the MU approaches it.

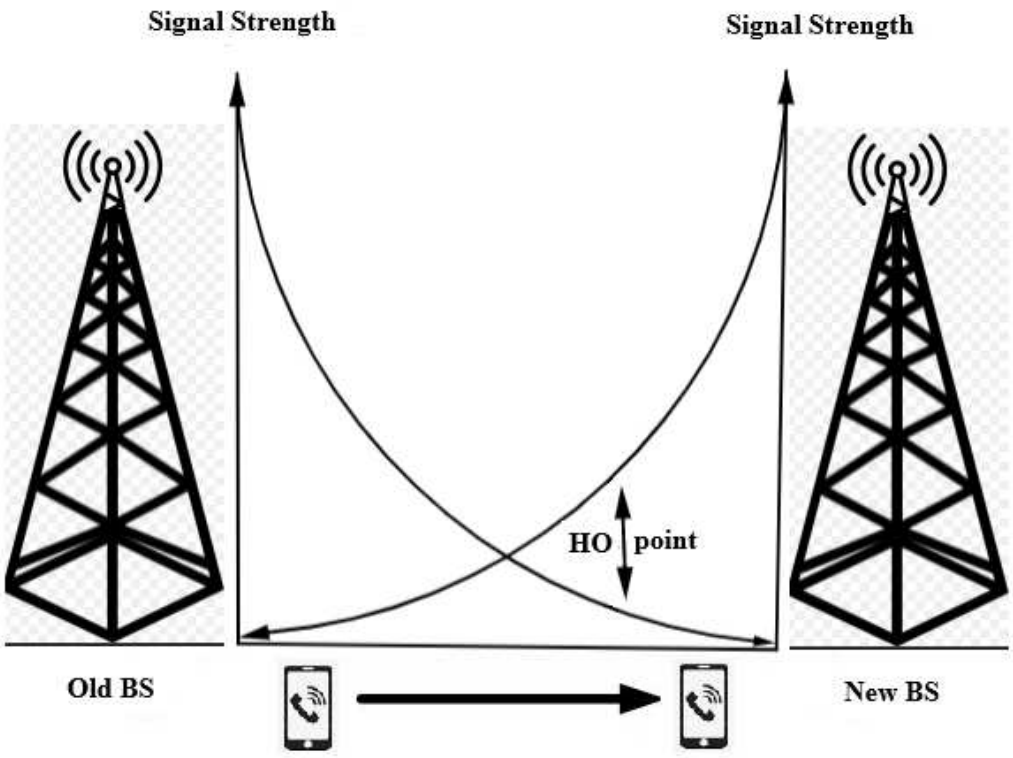

Figure 2.2: HO process in traditional cellular network.

HO is often initiated when the MU crosses a cell boundary, where the quality of the received signal in the current channel deteriorates. Since the mm-wave communication signal suffers from high penetration loss, the received signal's strength may degrade significantly due to interruption by a blockage that crosses the link between the MU and the mm-wave BS, such as human bodies or vehicles, etc. There are two categories of HO. Hard and soft HO, wherein the hard HO, the current resources are released before new resources are used, while in soft HO, both existing and new resources are used during the HO process. However, a hard HO may occur when the old connection is forced terminated because of blockage interruption before a new connection to a new mm-wave BS is established.

To diminish the redundant HOs in traditional cellular networks, two parameters, hysteresis, and threshold, are introduced in 3GPP [30]. For a particular MU, HO is triggered

if the Reference Signal Received Power (RSRP) of the tagged serving BS is lower than a predefined threshold, and the RSRP of the target BS is stronger than that of the serving BS by hysteresis. Such an approach, however, is not appropriate for implementation in mm-wave cellular systems due to the small size of the mm-wave BSs, where a high dense deployment of mm-wave BSs is required, and the fast change of the mm-wave channel quality resulting from the presence of blockages in the LOS link between the mm-wave BS and the MU.

In fact, there are various approaches used for performing HO, which are described in the following subsection:

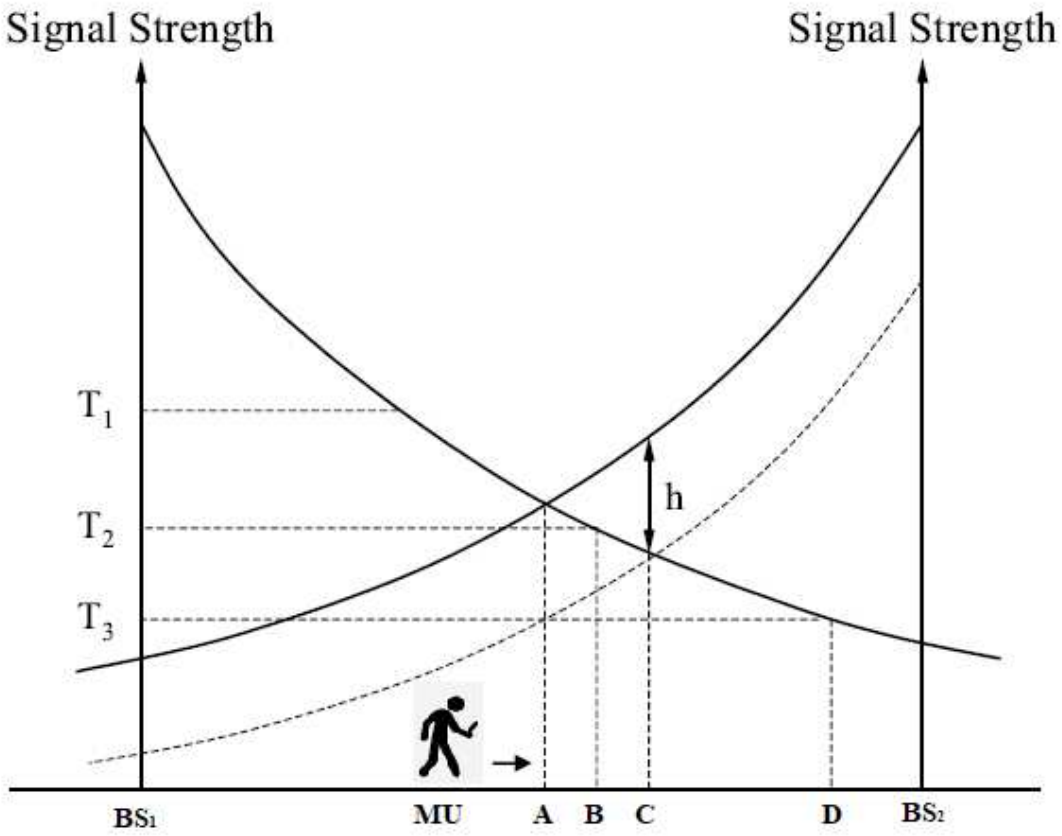

Figure 2.3: Signal strength and hysteresis between two adjacent BSs for potential HO.

2.4.1 Relative Signal Strength

This approach selects the BS whose signal is the strongest at all times, where the HO decision is taken based on the mean measurement of the received signal. Frequent unnec-

essary HOs could happen in this approach when the received signal of the current BS is still at an acceptable level.

2.4.2 Relative Signal Strength with Threshold

This approach allows a MU to make a HO only if the received signal from the current BS is less than a predefined threshold and the other is stronger than that threshold, where the signal strength is sufficiently weak.

The threshold depends relatively on the signal strengths of the two BSs at the point at which the two received signals are equal. When the threshold is assumed to be higher than T1, as shown in figure (2.3), the schemes based on this approach perform exactly like the schemes based on the relative signal strength approach, so the HO occurs at position A. If the threshold is assumed to be lower than T2 in figure (2.3), the HO would be delayed until the current received signal strength becomes higher than the threshold at position B. The delay at T3 could be very long, such that the MU could draft far away from the current BS. As a result, the link quality from the first BS (BS_1) could be reduced, and it might be dropped. Besides that, the co-channel interference might be increased. Therefore, using this approach to the HO scheme may create an overlapping of the coverage areas of the cells.

2.4.3 Relative Signal Strength with Hysteresis

In this approach of the HO scheme, the user is allowed to make a HO only if the received signal from the new BS is stronger enough by a hysteresis margin, h, from the current BS, as shown in figure (2.3), where the HO would occur at point C. The advantage of using this scheme is diminishing the ping-pong effect resulting from the rapid fluctuations of the channel condition, reducing unnecessary HOs.

2.4.4 Relative Signal Strength with Hysteresis and Threshold

In this approach of the HO scheme, the MU makes a HO only if the received signal from the current BS is dropped below the threshold, and the received signal from the new BS becomes stronger than the current BS by a given hysteresis margin, as shown in figure (2.3). The HO will occur at point D if the threshold is T3.

2.4.5 Prediction Techniques

Predicting the future value of the received signal strength is used to take the HO decision in this approach. It aims to reduce unnecessary HOs using all previous techniques. The authors in [31] proposed a smart HO scheme based on a reinforcement learning policy to reduce the frequent HOs in the mm-wave cellular network while maintaining user QoS requirements. This work shows that the number of HOs is significantly reduced by utilizing such an HO technique compared with traditional HO policies without learning. Another study in ([32]) proposes a Fuzzy Logic based system. The system in this model can take efficient HO execution decisions to reduce the occurrence of the ping-pong effect.

2.5 HO Schemes in Single Traffic Systems

The probability of blocking new calls and terminating ongoing calls are essential criteria for the MU in the traditional cellular systems in general and in mm-wave cellular systems in particular. The HO scheme has a significant impact on the performance of the MU in the mm-wave cellular system, where the cell size is relatively small compared to traditional cellular systems in the presence of blockages. The following section describes several existing HO schemes that address the call HO problem. Namely, non-priority, priority, and queuing HO schemes:

2.5.1 Non-Priority Scheme

Consider a system that has many cells. Each cell has M channels. In this scheme, all M channels are shared by both new and HO request calls. Therefore, originating calls and HO calls have equal access to all channels, and no priority is given to any one of them. Therefore, the blocking probability for both HO and originating calls is equal. Figure (2.4) shows a generic system model for the non-priority HO scheme.

2.5.2 Priority Scheme

This scheme gives priority to HO requests by assigning K channels exclusively for HO calls among the M channels in the cell, as shown in figure (6.1). Therefore, (M-K) channels are shared for both originating and HO calls, while K channels are solely reserved for HO

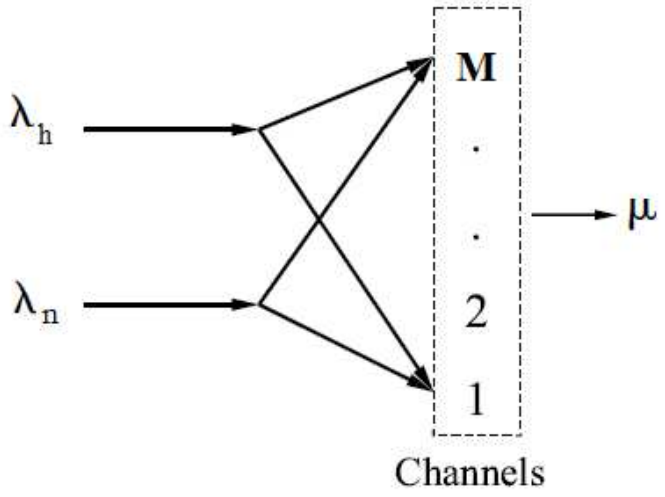

Figure 2.4: A generic system model for non-priority HO scheme.

calls. Hence, the blocking probability for HO requests is less than the blocking probability for the originating requests [33].

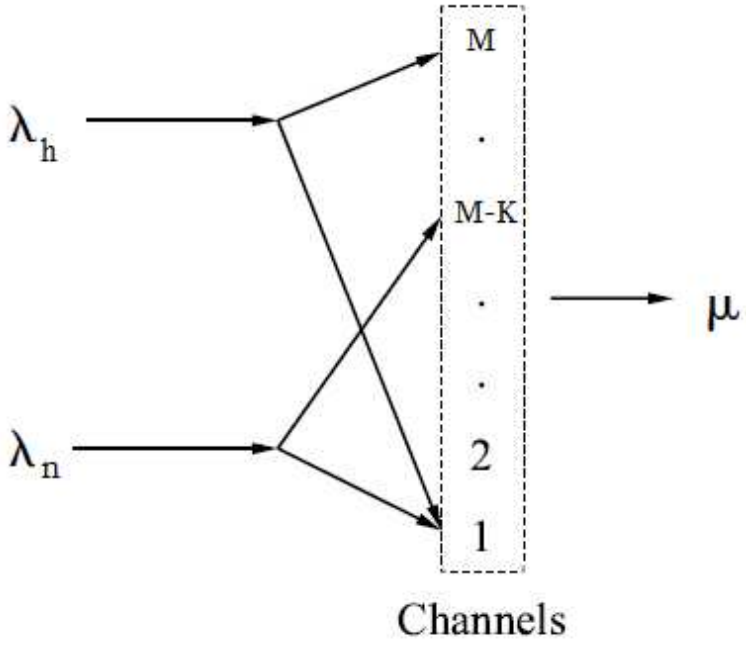

Figure 2.5: A generic system model for priority HO scheme.

2.5.3 HO Priority with Queuing Scheme

This scheme is similar to the priority scheme, except that queuing of HO requests is allowed. Therefore, the blocking probability for the HO requests in this scheme is less than that in the priority scheme [34]. Figure (2.6) shows a generic system model for priority with queue HO scheme.

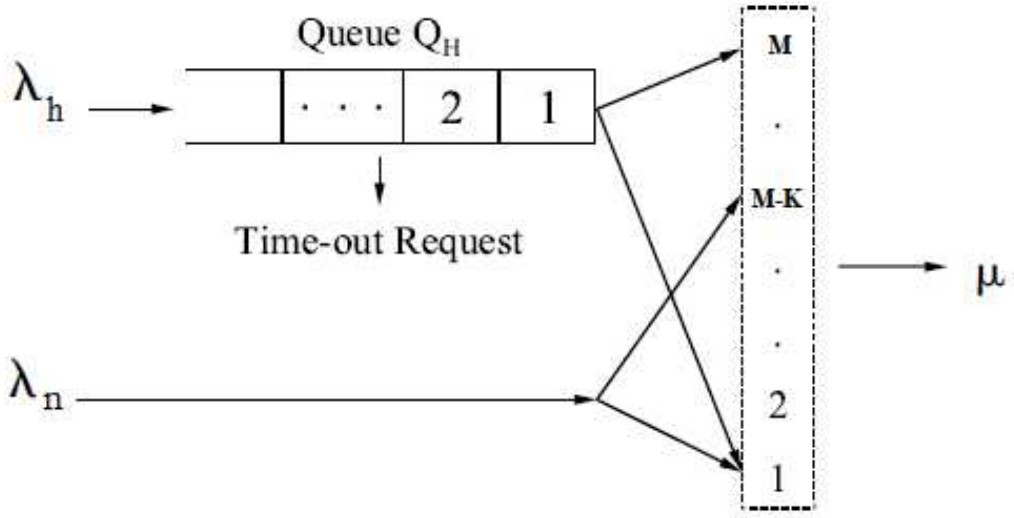

Figure 2.6: A generic system model for priority with queue HO scheme.

2.6 HO probability and Resource Management in Mm-Wave Cellular Systems

In the context of HO rate and mobility management, there is a large body of literature studying the HO rate and HO algorithms in different models. The study in [35] provides a stochastic geometric framework for the analysis of the HO rate for mobility of an MU using Random Walk Point Model (RWP). The work in [36] analyzes the effect of user mobility in multi-tier heterogeneous cellular networks, where the HO rate for an MU moving from one position to another is analyzed in an irregular cellular network, whereas the BSs are distributed according to homogeneous Poisson Point Process (PPP). It is assumed that a fraction of HO's result in connection failures. The latter is used as a sensitive indicator for the system to analyze the coverage probability. Unluckily, previous studies did not analyze the blockages' impact on the HO rate. The work in [29] studies the

effect of mobile blockages on mm-wave cellular networks for static MU. It is developing an LOS dynamic blockage model and evaluates some metrics, such as; the probability, duration, and frequency of blockage events by considering all the links to the MU LOS and NLOS. The results in this work provide the satisfaction intensity of BS to meet the requirements of the QoS in mm-wave cellular networks to provide reliable service with minimum latency.

One of the biggest challenges in mm-wave communications is the ping-pong effect resulting from unnecessary HOs when the link between the MU and mm-wave BS is interrupted by blockage for a short time due to mobility. The study in [37] proposed an algorithm by classifying the MU speed. Once the MU is classified as fast, no HO will be executed as long as the MU remains at its speed. Similar techniques could be applied in mm-wave communication, considering the propagation characteristic of mm-wave signals. Regardless the HO decision is taken by the network controller, or the HO is performed autonomously by the MU [38], such algorithms can efficiently reduce the signaling overhead that could result from frequent HOs due to the ping-pong effect. Another study introduced a dwell-time threshold to take into account the history of the MU before taking any HO decision [39]. The work in [40] provides a performance evaluation for a MU in an mm-wave cellular system. The MU is moving with a certain speed in a given path to collect the cumulative information that the MU could receive as a function of the length of its path. This work considers the mobility of the MU, and the blockages are incorporated with different densities. To the best of our knowledge, there is no direct study in the literature addressing the impact of blockages on the HO probability for a user with mobility in mm-wave cellular systems. Therefore, blockages' impact on the HO probability needs to be carefully considered in designing an efficient HO management scheme and planning the 5G mm-wave cellular system, including the impact of blockages on the HO probability in different scenarios, static, dynamic, and self-blockage.

Chapter 3
Impact of Single Static Blockage on HO Probability for Mobile Users

3.1 Introduction:

Millimeter-wave (mm-wave) communication is considered a promising candidate for the future generation of cellular systems [4]. The bandwidth needs to be wider to meet the growing demand for data traffic. That can be achieved by utilizing the mm-wave frequency bands where a huge spectrum is available, which can deliver high data rates than the frequency bands utilized in traditional cellular systems. However, mm-wave communication systems are quite susceptible to different types of blockages because of higher penetration losses and the lower diffraction in mm-wave signals. Since the mm-wave connection is vulnerable to blockages, the LOS link between the MU and the mm-wave BS frequently fluctuates between the LOS and NLOS states. Consequently, the HO probability changes accordingly. Therefore, to maintain connection stability without interruption, the impact of blockages on HO probability needs to be analyzed and hence addressed.

HO probability can be defined as the probability serving BS that is no longer the best candidate when a MU makes a displacement with a certain distance of d and direction of ω. In other words, HO probability is the probability that MU is closer to the neighbor BS in one movement period, such that the MU switches to the neighbor BS.

In this chapter, we use concepts from random shape theory similar to [24]. Random shape theory is associated with stochastic geometry, which deals with arbitrary distributions of objects in space [41, 42].

We model any blockage that could take any dimension as a line segment in the 2-D space. These objects could have random lengths and orientations, where the centers of these blockages are located according to a spatial Poisson Point Process (PPP). The main objective of this chapter is to analyze the impact of static blockages on a MU in the 5G mm-wave cellular network. More precisely, in this chapter, we only focus on the impact of a single static blockage on the HO probability for a MU in 5G mm-wave cellular networks.

3.2 Assumptions and System Model

We consider one tier mm-wave cellular network in the down-link. We assume that all the mm-wave BSs in this tier have the same transmit power $\boldsymbol{P}$. The MU is associated to the closest LOS mm-wave BS (i.e. no blockage lies in the link between mm-wave BS and

MU). A single static blockage is assumed to be dropped in a predefined location within the transmission range of the MU with the tagged mm-wave BS, such that it lies inside a circle of radius r. The blockage is modeled as a line segment with given coordinates of its vertices, as shown in figure (3.1). Since the propagation and penetration losses are very high in mm-wave communication, we assumed that no signal will be received from any blocked mm-wave BS in the NLOS link and, hence any mm-wave BS lying beyond the blockage will be neglected and no signal will be considered in the MU side.

Thanks to its tractability and applicability, (PPP) Φ of intensity λ has been adopted to model the location of mm-wave BSs in the Euclidean plane ($\mathbb{R}^2$). Therefore, the number of mm-wave BSs in a specific area A is a Poisson random variable, with mean $A\lambda$. We assume that the initial position of the MU at the origin and all mm-wave BSs are distributed in the $\mathbb{R}^2$ plane according to PPP. As the propagation and penetration losses are very high in mm-wave communication, therefore, the received signal from blocked mm-wave BS in the NLOS link will be neglected. Consequently, no HO will occur to the blocked BS during the MU transition.

We assume that the mobile user makes a movement with a speed of distance $\boldsymbol{d}$ per time unit, from the original position P_1 towards a new position P_2. As can be seen in figure (3.1), the MU at location P_1 is initially associated with the closest LOS mm-wave BS, which is BS_t at connection distance r. The MU makes a displacement of d in a time unit at an angle of ω with respect to the connection direction. The HO only occurs if there is another LOS mm-wave BS that becomes closer to the MU than the tagged mm-wave BS after this displacement. In other words, if any other LOS mm-wave BS becomes closer than a distance R after a displacement of d, MU will make a HO to the new candidate mm-wave BS. Otherwise, it remains associated with the tagged mm-wave BS and HO will not occur.

The probability of HO, $\mathbb{P}\left(HO|d,\omega\right)$, for a MU moving at distance d in a time unit at angle of ω with respect to the connection direction, where the mm-wave BSs are distributed according to PPP with density of λ is given by:

$$\mathbb{P}\left[HO|d,\omega\right] = 1 - exp(-\lambda A) \tag{3.1}$$

Where A is the visible excess area resulted from MU moving from location P_1 to location

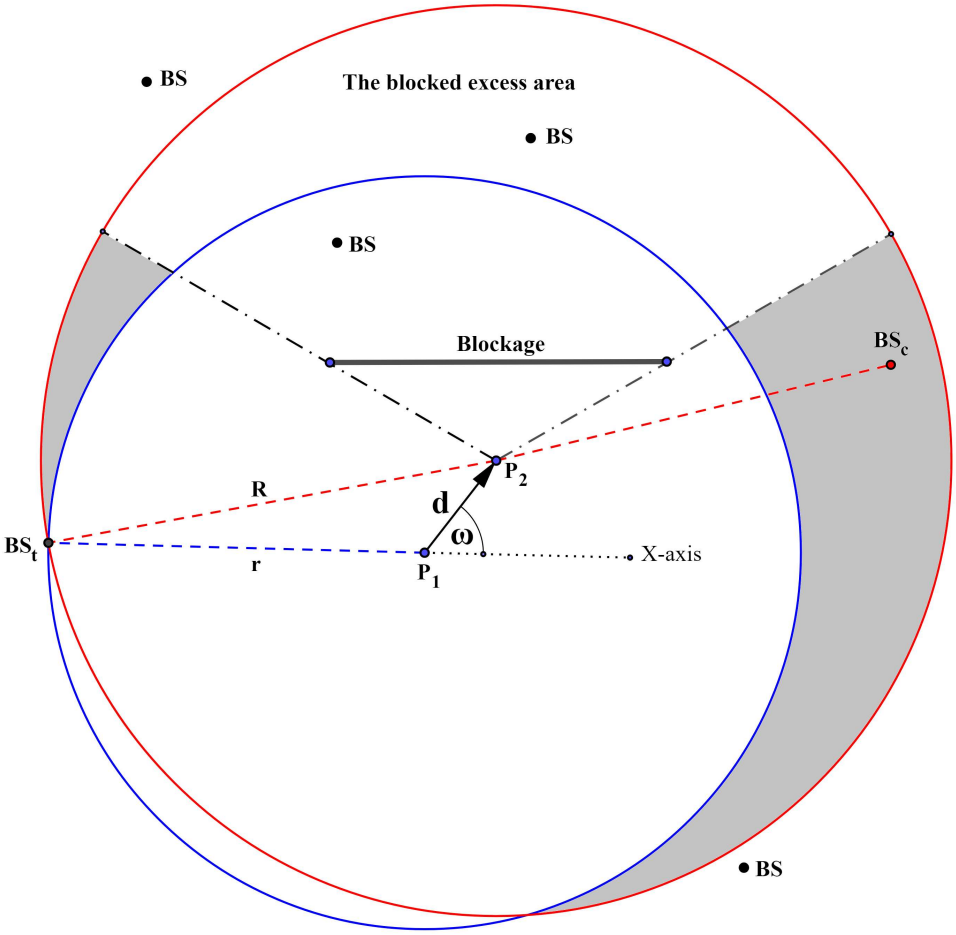

Figure 3.1: System model, where the mobile user is associated to closest LOS BS in presence of the blockage.

P_2 and inside the circle with radius R, see figure (3.1). Note that the new non-visible excess area blocked by the blockage will not be considered. However, the visible excess area depends mainly on the speed and direction of the MU, and the location and the length of the blockage.

Figure (3.2) shows the general case where no blockage is incorporated in the system. When the MU moves, another circle with radius R, centered at P_2, will be formed besides the circle of radius r, centered at P_1, which is formed when the MU was located in the initial location. Both circles intersect at BS_t. The MU movement forms an excess area denoted by A'. This area A' can be calculated as follows:

Let S_γ denotes the area of the sector between the arc of angle γ and the origin of the circle with radius R. Let S_ω represents the area of the sector between the arc of angle ω and the origin of the circle with radius r. Let $A\tau_1$ denotes the area of triangle with sides R, r, and d, and let $A\tau_2$ symbolizes the area of the other triangle with the same side lengths. Hence, A' is given by:

$$A' = S_\gamma + A_{\tau_1} + A_{\tau_2} - S_\omega \tag{3.2}$$

Because of the symmetry, both triangles, $A\tau_1$ and $A\tau_2$, have exactly the same area. Denote $A\tau = \tau_{P_1P_2P_3} = \tau_{P_1P_2P_4}$. Therefore, A' is given by:

$$A' = S_\gamma + 2A_\tau - S_\omega \tag{3.3}$$

$$A' = \pi R^2 - R^2\left[\omega - \sin^{-1}\left(\frac{d\sin\omega}{R}\right)\right] + rd\ sin\ \omega - r^2(\pi - \omega) \tag{3.4}$$

Proof: See Appendix A.

In order to calculate the total visible excess area that resulted from MU movement, we need to calculate the blocked area beyond the blockage and then subtract it from A'.

Let A'' denote the blocked area. Therefore, the visible axcess area is given by:

$$A = A' - A'' \tag{3.5}$$

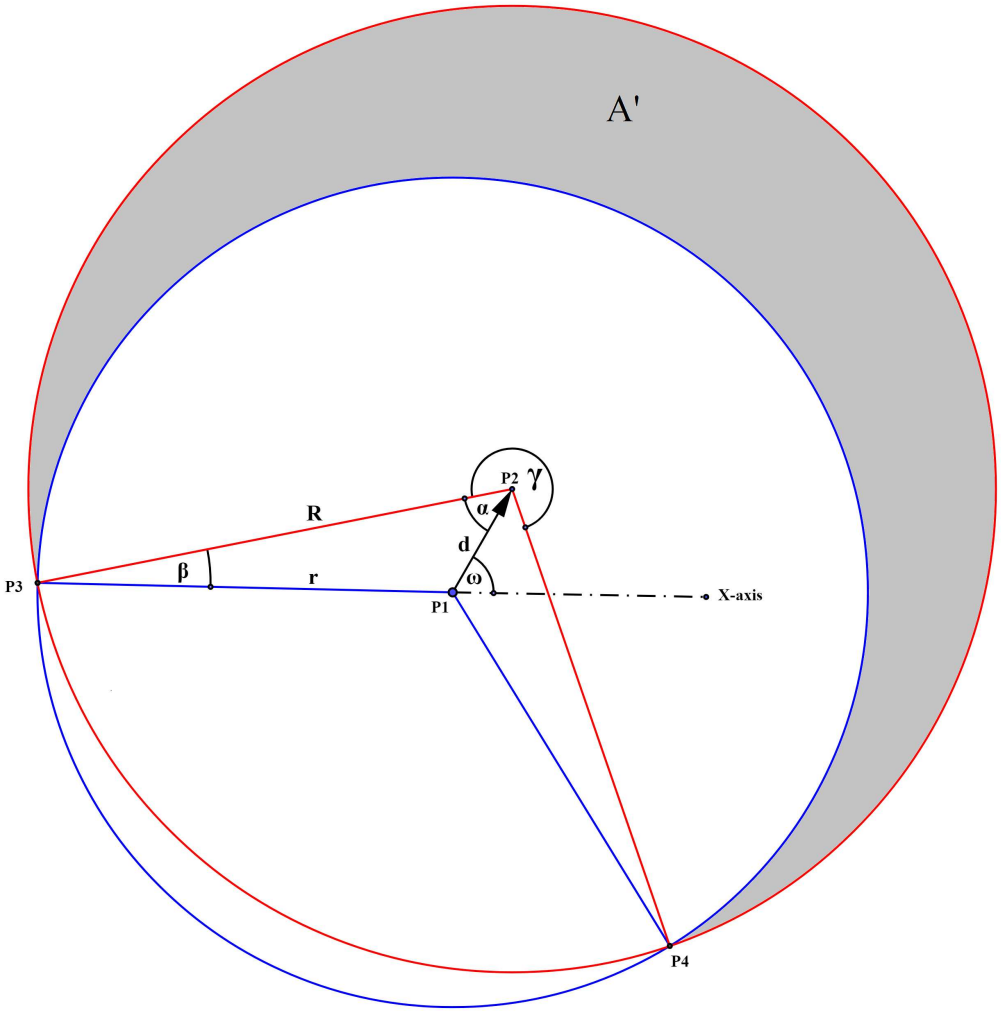

Figure 3.2: The excess area resulted from the MU movement in case of no blockage and the relationship between r, R, and d.

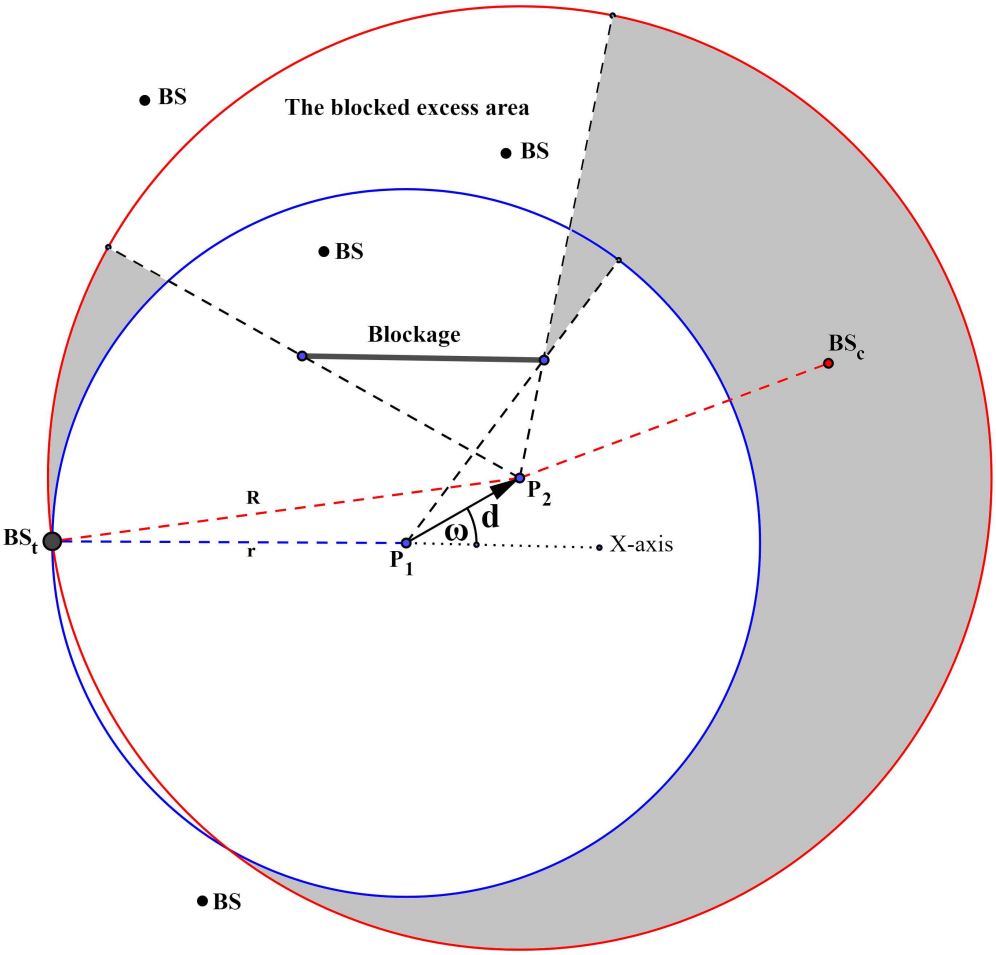

Figure 3.3: Another example of the excess area resulted from the MU movement, where it is moving in a different direction.

Note that A'' can be calculated numerically since the coordinates of the blockage's vertices are assumed to be fixed and known.

In the case of the MU is moving in a uniform direction, distributed on $\omega \in [0, 2\pi)$, the visible excess area can be classified into several different cases depending on the angle ω, and the location and the length of the blockage. In fact, there are a total of 9 cases. Due to the page limit, just two cases have been presented in this paper, as shown in figure (3.1) and figure (3.3). See appendix B for the remaining 7 cases. Note that the visible excess area could be inside the circumference of the circle with radius r when the MU is moving in a different direction, not towards the blockage, as in figure (3.3).

The HO probability for an MU moving distance d in time unit, at a uniform angle distributed on $\omega \in [\omega_{min}, \omega_{max})$, is given by:

$$\mathbb{P}\left[HO\right] = 1 - \int_{\omega_{min}}^{\omega_{max}} f_W(\omega) \;\; exp(-\lambda A)\; d\omega \tag{3.6}$$

Since ω has a uniform distribution, the probability distribution function (PDF) of ω is given by:

$$f_W(\omega) = \frac{1}{\omega_{max} - \omega_{min}} \tag{3.7}$$

Therefore, HO probability in (3.6) can be further simplified as derived below:

$$\mathbb{P}\left[HO\right] = 1 - \;\frac{1}{\omega_{max} - \omega_{min}}\; \int_{\omega_{min}}^{\omega_{max}} exp(-\lambda A)\; d\omega \tag{3.8}$$

Furthermore, using the theorem of total probability, the HO probability for a MU moving distance d in time unit, at a uniform angle distributed on $\omega \in [0, 2\pi)$, is given by:

$$\mathbb{P}[HO] = \sum_{k=1}^{n} \mathbb{P}[\omega_k]\; \mathbb{P}[HO_k|\omega_k] \tag{3.9}$$

Where n is the number of cases for the visible excess area that depends on the angle ω, and the location and the dimensions of the blockage. $\mathbb{P}(\omega_k)$ is the probability that ω, in case k, is within the interval of $[\omega_k, \omega_{k+1})$, and it is given by:

$$\mathbb{P}[\omega_k] = \mathbb{P}[\omega \in [\omega_k, \omega_{k+1})] \tag{3.10}$$

Since the MU is moving in a uniform direction in the interval of $\omega \in [0, 2\pi)$, therefore, $\mathbb{P}(\omega_k)$ can be calculated as follows:

$$\mathbb{P}[\omega_k] = \frac{\omega_{k+1} - \omega_k}{2\pi} \tag{3.11}$$

3.3 Results and Discussion

The analytical and simulation results in figures (3.4), (3.5) and (3.6) show the impact of a single static blockage on HO probability in an mm-wave cellular network in different mobility scenarios. We assumed that the distance between MU and tagged mm-wave BS, in the initial position, is r = 40m, and the coordinates of blockage's two vertices are (20, 25) and (-20, 25), respectively. We also assumed that the MU is moving at a fixed speed of $\boldsymbol{d}$ per time unit. The analytical results have been validated through Monte Carlo simulation, where M (independent runs) has been performed and averaged in each case. Thereafter, the HO probability is obtained using the total probability theorem for all cases.

Figure (3.4) shows the result where the MU is moving radially away from the tagged mm-wave BS (i.e., $\omega = 0$). It can be seen that the blockage has a slight impact on HO probability at the moderate speed of MU, while it has almost no impact at very low and high speeds. The reason behind that is that it is related to the position of the blockage, where the blocked excess area is getting very small when the MU is moving away very fast in the radial direction.

Figure (3.5) shows a comparison between the HO probability in case there is no blockage, and in case one static blockage is incorporated into the system. In this scenario, the MU is assumed to move at a fixed speed of $\boldsymbol{d}$ per time unit in a uniform direction on $\omega \in [0, 2\pi)$.

As depicted in figure (3.5), the blockage has a significant impact on the HO probability. It might be expected that as the MU is moving faster, the HO probability gets

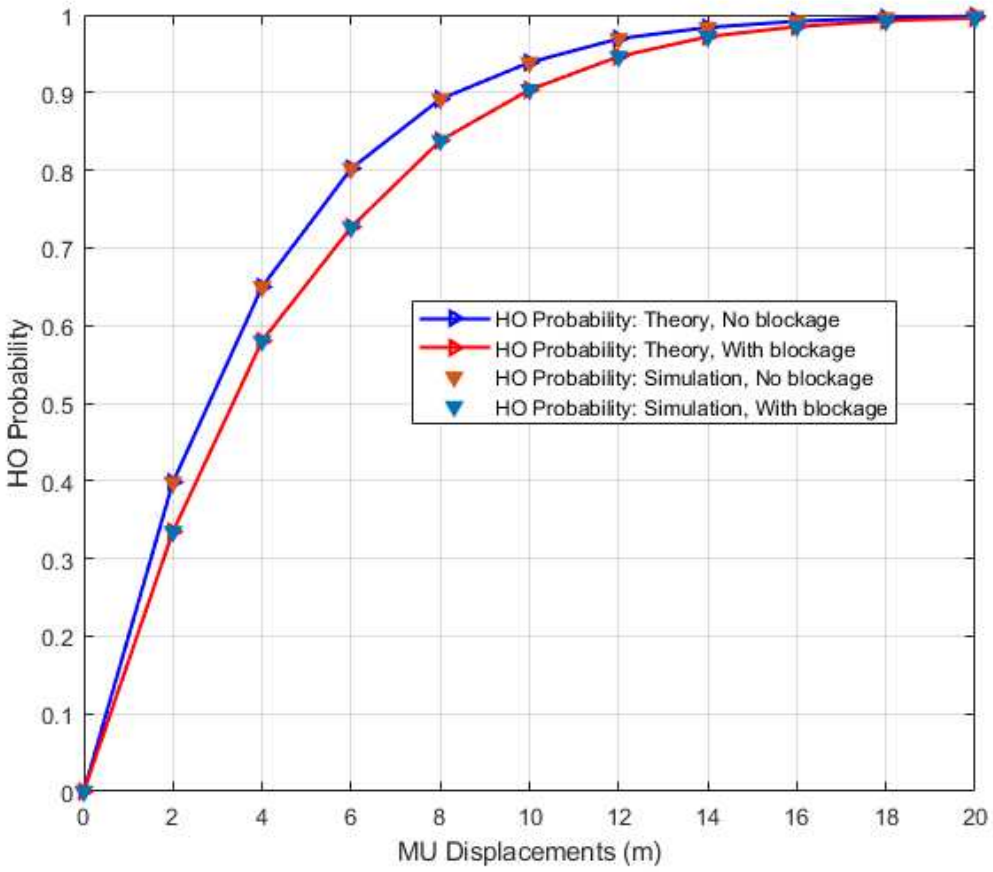

Figure 3.4: HO probability VS MU speed, with and without blockage and MU moving radially.

higher. Furthermore, it can be noticed that the HO probability, in case the blockage is incorporated into the system, is less than that when there is no blockage in the system. This result can be interpreted based on the fact that when the MU moves faster in a uniform direction, the blocked area gets larger, which makes the visible excess area smaller, consequently reducing the probability of having a candidate mm-wave BSs in this area. In other words, the less the visible excess area, the less probability of having mm-wave BSs on that area, which means less probability of HO.

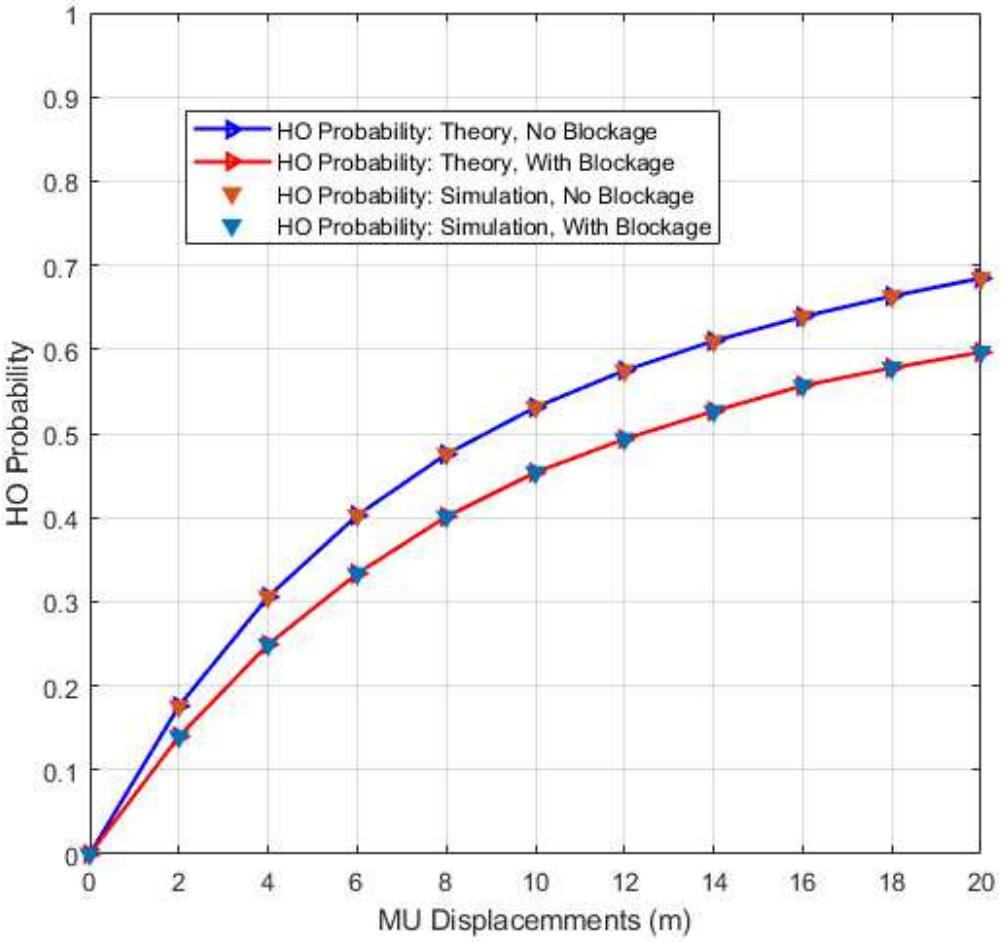

Figure 3.5: HO probability VS MU speed, with and without blockage and MU moving uniformly.

Another comparison is depicted in figure (3.6) between the HO probability in case of one static blockage is incorporated in the system and case of no blockage in the system with different mm-wave BSs densities. The densities of mm-wave BSs vary from $\lambda = 1\times10^{-3}$ to $\lambda = 1\times10^{-2}$ BS/m^2. The result clearly shows that as the density of mm-wave BSs gets high, the HO probability also gets higher. The reason behind this result is that as the

density of the mm-wave BSs gets higher, as there is probability of having more mm-wave BSs in the visible excess area, which means a higher likelihood of having HO. On the other hand, the blockage causes a reduction in the visible excess area and an increase in the blocked area, which diminishes the probability of having HO in the mm-wave cellular system. In all results, there is an exact matching between the analytical and simulation results, which proves the validity of the expression of the HO probability in the presence of a static blockage.

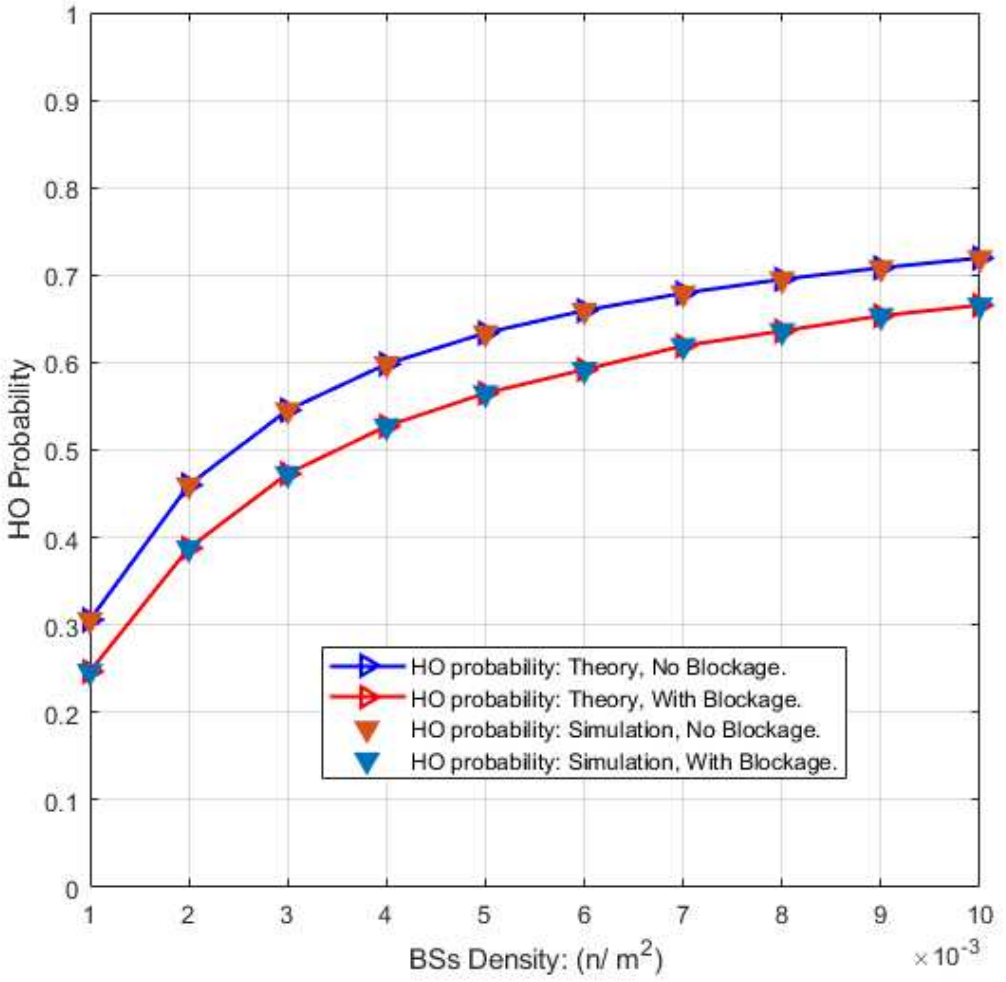

Figure 3.6: HO probability VS BS density, with and without blockage and MU moving uniformly.

Chapter 4
Impact of Multiple Static Blockages on HO Probability for Mobile Users

4.1 Introduction

Coverage in mm-wave cellular networks is difficult to foretell due to fluctuations in path loss in the presence of blockages. One critical deterioration is blockage of the LOS propagation path [3]. Blockages not only minimize the power of the received signal, but also affect MU association with the tagged mm-wave BS, e.g., an MU may associate with a distant unblocked mm-wave BS rather than a closer blocked mm-wave BS. As a result, MU attends frequent HOs, which depends mainly on the blockages' size and density and the propagation path length between the MU and the tagged mm-wave BS. Permanent structures, such as buildings, trees, and other static structures, known as static blockages, have a significant impact on mm-wave signal propagation characteristics [24], [28]. These propagation characteristics impose a new burden and challenge for establishing a reliable connection at the mm-wave cellular network. Efficient use of mm-wave communication in 5G cellular networks requires a sound understanding of its characteristics, including the blockage effect. In numerous standard propagation models, blocking is integrated by adding a log-normal distributed random variable in the path-loss computations, with a variance obtained from empirical measurements. Regrettably, such an approach does not predict the intuitive outcome that blocking the propagation path is more likely as the transmission path is longer and in the presence of different blockages size.

Several studies have been proposed to analyze the impact of static blockages on stationary MU. Unfortunately, these studies have not included the effect of blockages on a user with mobility. When the MU makes a displacement, the LOS propagation path may interrupt with an object that could lie between the tagged BS and MU. It might cause a ping pong HO effect. That might be for a short period of time when this object intersects with the propagation path for dynamic blockages. However, several scenarios need to be considered in the analysis in order to understand the impact of different blockages on HO probability.

The main objective of this chapter is to study and analyze the impact of multiple static blockages on HO probability for a user with mobility in a 5G mm-wave cellular network. In the previous chapter, we only studied the impact of a single static blockage on HO probability. Consequently, there is a necessity to consider multiple blockages in the analysis of the system model that would be compatible with the realistic scenario.

4.2 System Model and Problem Formulation

4.2.1 System Model

Because of its advantages of analytical tractability, we adopt the homogeneous Poisson Point Process (PPP), which is one of the most widely used 2-D spatial models, to characterize and model the distribution of mm-wave BSs and blockages with densities of λ_{BS} and λ_b, respectively. In this analysis, similar to [24], we used a Random Object Process (ROP) to model the distribution of the blockages, where the center points of the blockages are from a PPP. Since mm-wave signals are very susceptible to blockages, we assume that any blockage intersecting with the propagation path between the mm-wave BS and the MU will block the link. Consequently, the MU will not establish a new connection with any mm-wave BS and associate with it as long as this mm-wave BS is located behind a blockage. Moreover, if the MU is associated with an mm-wave BS and a blockage crosses the propagation path to this mm-wave BS, the MU will lose its connectivity and disconnect from it. The latter will impose the MU to switch to another mm-wave BS with a LOS propagation path. As a result, the HO will occur.

HO probability is difficult to predict in the presence of different types of blockages. This chapter only focuses on the impact of multiple static blockages on HO probability, and we neglect all other types of blockages in future work.

We consider the HO scenario for one tier mm-wave cellular network where the MU is moving from its initial location at the origin (P_1) to a new location (P_2) at a certain distance and direction. Mm-wave BSs are assumed to be distributed in the 2-D plane according to PPP with a density of λ_{BS}, in area $\boldsymbol{A}$. Therefore, the number of mm-wave BSs in an area A is a Poisson random variable with mean $\lambda_{BS}\boldsymbol{A}$. The blockages are modeled as line segments, as in [24], with length of L_i, centered at X_i. Each line segment with a uniform distribution of its length between $[L_{min}, L_{max})$, and orientation, θ_b, has also a uniform distribution between $[\theta_{min}, \theta_{max})$. Seeking simplicity, we assume that the MU associates to the closest LOS mm-wave BS at a distance of r, which means no LOS mm-wave BS closer than r. HO probability is defined as the probability that there is at least one LOS mm-wave BS becomes closer to the MU than the tagged mm-wave BS, after a MU displacement of d with a direction of ω with respect to the connection direction.

4.2.2 Problem Formulation

In the mm-wave cellular system, stationary MU is mainly in two states, either in coverage or in outage state. In coverage state means the MU associated to a mm-wave BS, whereas in outage state means the MU, for some reason, is not associated to any mm-wave BS. However, the MU with mobility could have a transition state from one mm-wave BS to another mm-wave BS when the MU occurs HO to maintain the connectivity to the network. In fact, there are three scenarios could happen after the MU displacement from the initial location, P_1, to the new location, $P2$, which can be classified as follows:

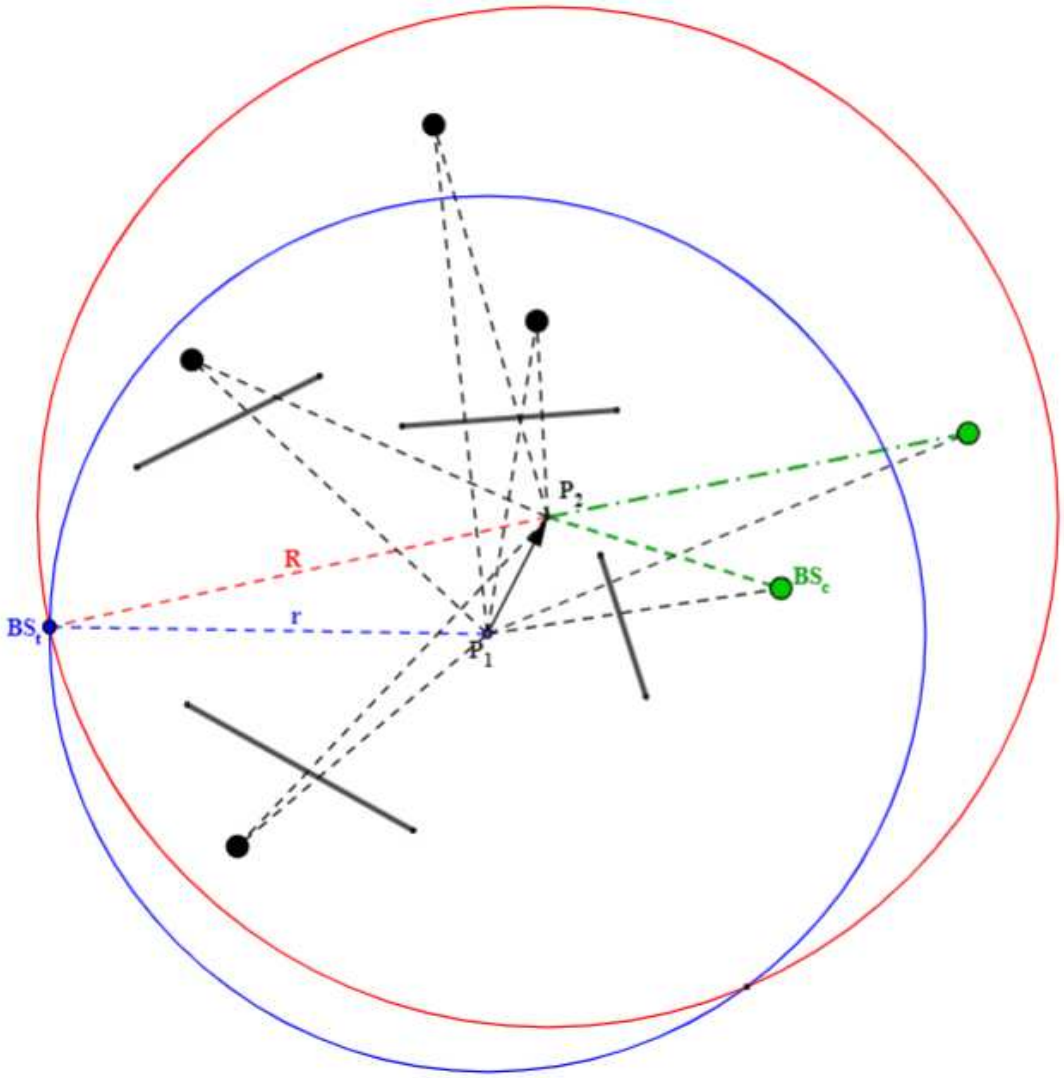

Figure 4.1: The first scenario where the link between the tagged mm-wave BS and the MU from the new location, P2, is LOS.

1. The first scenario: No HO occurs. After MU displacement and due to the block-

ages, there will be no visible "LOS" mm-wave BS closer to the MU than the tagged mm-wave BS, and the tagged mm-wave BS remains LOS. Therefore, the MU will remain associated with the tagged mm-wave BS.

2. The second scenario: HO occurs. After MU displacement and regardless of whether the tagged mm-wave BS is still LOS or not, another candidate mm-wave BS becomes visible "LOS" and closer to the MU than the tagged mm-wave BS. Therefore, HO occurs, and the MU will switch to this mm-wave BS.

3. The third scenario: MU is in an outage. After MU displacement, the propagation path between the MU and the tagged mm-wave BS will be blocked by a blockage, and there will be no other LOS mm-wave BS visible to the MU. As a result, the MU will switch to the outage state. This scenario will be neglected in our analysis, and we assume that there is always at least one mm-wave BS visible to the MU. Therefore, the MU will not switch to the outage state.

4.3 HO Probability Analysis

In this analysis, we consider a mm-wave cellular network with a single tier of mm-wave BSs, whose locations are distributed according to a PPP. This analysis is restricted to $\mathbb{R}^2$ space, and the height of MU, blockages and mm-wave BSs are ignored and left to future work. The NLOS events of multiple mm-wave BSs may be correlated based on the location of dynamic blockages. For example, a blockage is located closer to the MU may simultaneously block more than one mm-wave BS. On the other hand, a blockage is located farther away from the MU may block only one mm-wave BS. However, in this analysis, we assume an independent NLOS events of all the mm-wave BS-MU links and leave the correlation analysis for future work.

We assume that HO occurs only if there is another LOS mm-wave BS that became closer to the MU after a displacement of d. There will be two scenarios that need to be considered, as follows:

Scenario 1:

After MU's displacement from the initial location, P_1, to the new location, P_2, the propagation path between the MU and the tagged mm-wave BS remains LOS, and no blockages interrupt the propagation path. In this scenario, the HO occurs only if there is at least one mm-wave BS, closer than the tagged mm-wave BS, as illustrated in figure (4.1).

Scenario 2:

After MU's displacement from the initial location, P_1, to the new location, P_2, the propagation path between the MU and the tagged mm-wave BS becomes blocked by at least one blockage. In this scenario, the HO occurs as long as another LOS mm-wave BS is LOS, located anywhere in the coverage area, as illustrated in figure (4.2).

In the first scenario, the HO occurs only if there is at least one candidate mm-wave BS_c becomes LOS to the MU from the new location,$P2$, inside the circle of radius, R, centered at P_2. Since the MU is associated to the tagged mm-wave, BS_t, which means that all other BS_c inside the circle of radius, r, are blocked. Therefore, HO probability in this scenario, $\mathbb{P}_{S1}[HO]$, is given by:

$$\mathbb{P}_{S1}[HO] = \mathbb{P}[S_1 \cap HO] = \mathbb{P}[S_1] \times \mathbb{P}[HO|S_1] \tag{4.1}$$

where, $\mathbb{P}[S_1] = \mathbb{P}[E_1|E_2]$, which is the conditional probability of the following events:

E_1: is the event that the link between the BS_t and the MU at location $P2$ is LOS.

E_2: is the event that the link between the BS_t and the MU at location $P1$ is LOS.

and $\mathbb{P}[HO|S_1] = \mathbb{P}[E_3|E_4]$, is the conditional probability of the following events:

E_3: is the event that there is at least one BS_c LOS to the MU at location $P2$, inside the circle of radius, R, centered at $P2$.

E_4: is the event that all BS_c are NLOS to the MU at location $P1$, inside the circle of radius, r, centered at the origin.

Therefore, the HO probability of the first scenario is given by:

$$\mathbb{P}_{S1}[HO] = \mathbb{P}[E_1|E_2] \times \mathbb{P}[E_3|E_4] \tag{4.2}$$

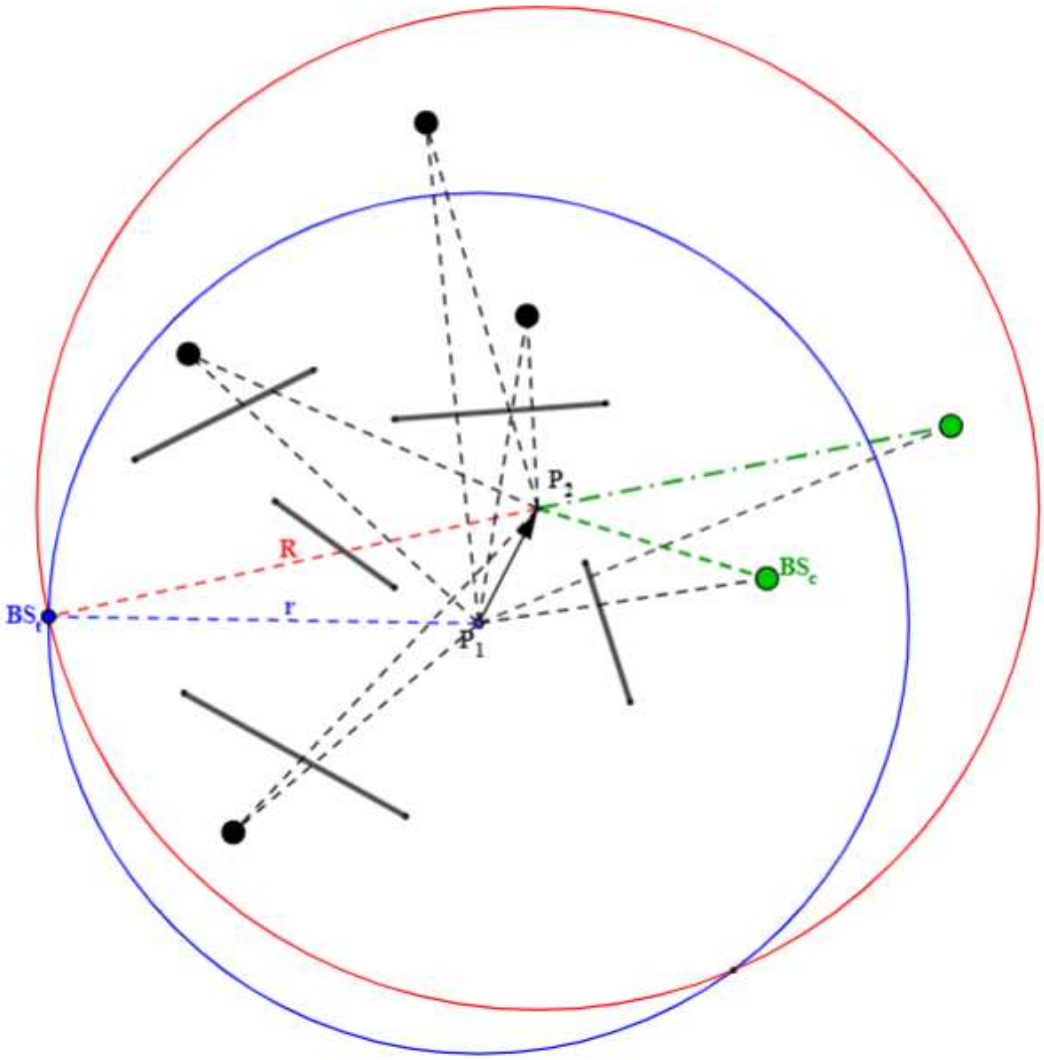

Figure 4.2: The second scenario where the link between the tagged mm-wave BS and the MU from the new location, P2, is NLOS.

In the second scenario, the link between the tagged mm-wave BS and the MU from the new location,$P2$, is NLOS and blocked by at least one blockage, as illustrated in figure (4.2). In this case, the HO only occurs if there at least one BS_c becomes visible and has a LOS propagation path to the MU at the new location,$P2$, and located within the transmission range of the MU. Therefore, HO probability in this scenario, $\mathbb{P}_{S2}[HO]$, is given by:

$$\mathbb{P}_{S2}[HO] = \mathbb{P}[S_2 \cap HO] = \mathbb{P}[S_2] \times \mathbb{P}[HO|S_2] \tag{4.3}$$

Where, $\mathbb{P}[S_2] = \mathbb{P}[E_5|E_2]$, is the conditional probability of the following event:
E_5: is the event that the link between the BS_t and the MU at location $P2$ is NLOS, where $\mathbb{P}[E_5|E_2]$ is given by:

$$\mathbb{P}[E_5|E_2] = 1 - \mathbb{P}[E_1|E_2] \tag{4.4}$$

and, $\mathbb{P}[HO|S_2] = \mathbb{P}[E_6|E_4]$, is the conditional probability of the following event:
E_6: is the event that there is at least one BS_c LOS to the MU at location $P2$, located within the transmission range of the MU. Since we neglected the outage scenario in our analysis, and we assumed there is always at least one BS_c visible to the MU. Therefore, when the propagation path R, between the MU at the new location P_2 and the BS_t, becomes NLOS, the MU will associate to a new mm-wave BS_c, and HO will occur. Hence, the conditional probability, $\mathbb{P}[E6|E4]$ is given by:

$$\mathbb{P}[E6|E4] = 1 \tag{4.5}$$

Equation (4.5) reduces equation (4.3) to:

$$\mathbb{P}_{S2}[HO] = 1 - \mathbb{P}[E_1|E_2] \tag{4.6}$$

Using the theorem of total probability we get the total HO probability as follows:

$$\mathbb{P}_t[HO] = \mathbb{P}_{S1}[HO] + \mathbb{P}_{S2}[HO] \tag{4.7}$$

Substituting equation (4.2) and equation (4.6) in equation (4.7) we get the total HO probability, and it is given by:

$$\mathbb{P}_t[HO] = \mathbb{P}[E_1|E_2] \times (\mathbb{P}[E_3|E_4] - 1) + 1 \tag{4.8}$$

It turned out that the number of blockages, K, over a connection path between the MU and the tagged mm-wave BS, has a Poisson distribution with mean (μ_b) l [24]. Where l is the distance between the MU and the tagged mm-wave BS, and μ_b is given by:

$$\mu_b = \frac{2\lambda_b}{\pi} E[L] \tag{4.9}$$

Where, λ_b, is the density of blockages and $E[L]$ is the average blockage length. The probability that the link between the MU and the mm-wave BS will be LOS is given by:

$$\mathbb{P}[LOS|l] = exp(-\mu_b l) \tag{4.10}$$

Otherwise, the link will be NLOS, which is given by:

$$\mathbb{P}[NLOS|l] = 1 - \mathbb{P}[LOS|l] = 1 - exp(-\mu_b l) \tag{4.11}$$

Figure 4.3 shows the probability that the link between the mm-wave BS and MU is LOS versus the distance with different blockages lengths, $E[L]$= 5, 10, 15 and 20, and blockages density is λ_b=1×10^{-3} mm-wave BS/m^2. In equation (4.10), the probability that the link between the mm-wave BS and MU is LOS depends mainly on the distance, $\boldsymbol{l}$, between the MU and mm-wave BS.

- **Analysis of LOS probability of the link between mm-wave BS_t and the MU, at P_2, given that it is LOS at P_1 :**

This subsection analyses and simplifies the conditional LOS probability, $\mathbb{P}[E_1|E_2]$, of the link, R, between the tagged mm-wave BS, BS_t, and the MU after a displacement of d, at P_2, given that it is LOS at the initial location, P_1.

Similar to [24], consider a set of M_{L,θ_b} representing the number of blockages whose lengths equal to L with an orientation of θ_b, that is a subset of M blockages whose lengths between $(L, L + dL)$, and orientations (θ_b, θ_b+$d\theta_b$). Since each blockage has an independent length and orientation, and using random splitting property of PPP, M_{L,θ_b} is

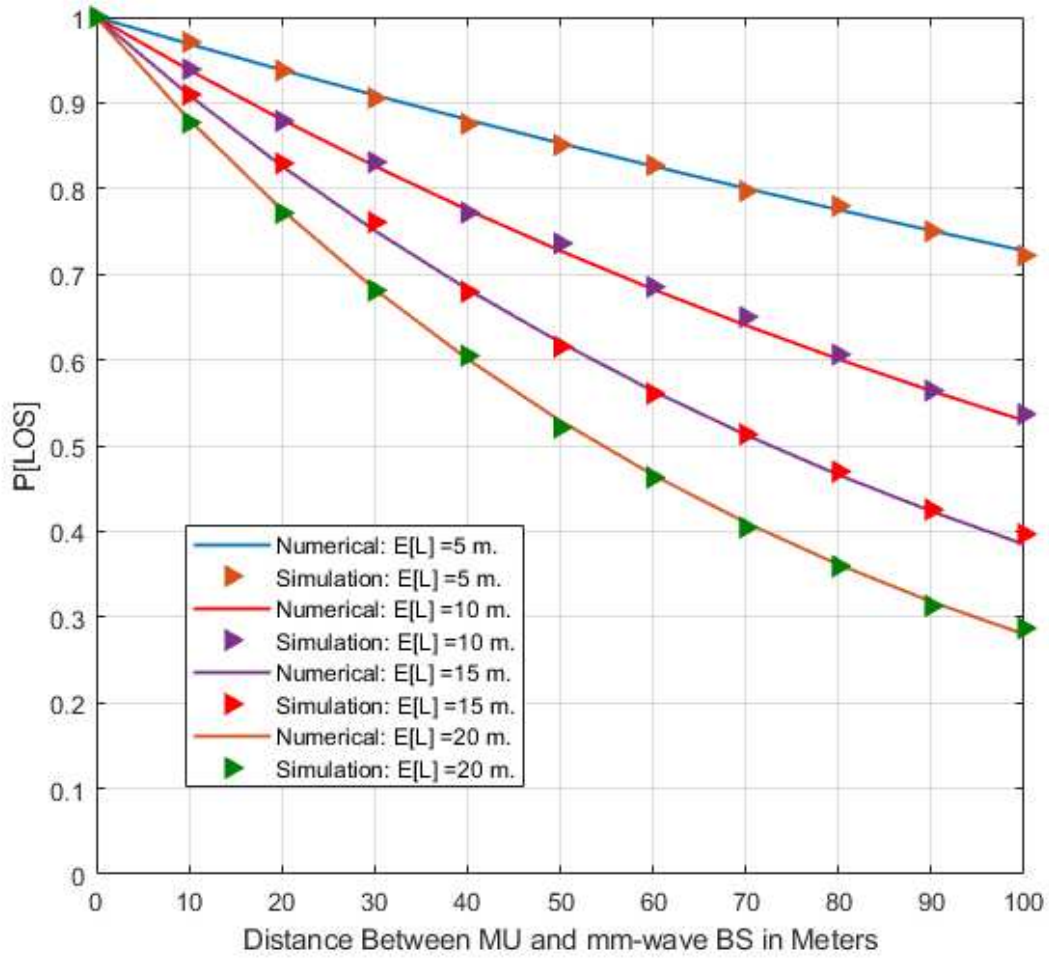

Figure 4.3: Probability that the link between the mm-wave BS and MU is LOS versus the distance with different blockage lengths. Blockages density λ_b=1 $\times$ 10^{-3}. Average blockage lengths: $E\,[L]$=5, 10, 15 and 20.

a PPP with density $\lambda_{b_{(L,\theta_b)}} = \lambda_b f_L(L) dL f_{\theta_b}(\theta_b) d\theta_b$. Because of the independence of lengths and orientations of the blockages. Hence, M is independent for each L and θ_b, and thanks to the superposition property of independent Poisson processes, M is Poisson distributed with parameter $E[M]$.

$$E[M] = \sum_{L,\theta_b} \mathbb{E}[M_{L,\theta_b}] \tag{4.12}$$

Given that the propagation path, r, between the MU and the tagged mm-wave BS at the initial location, P_1, do not intersect with any blockage, that means no blockages whose centers lie inside the parallelogram, $BCEF$, with a length of r and width of $Lsin(\theta_b)$. Therefore, the probability, $\mathbb{P}[E_1|E_2]$, that the link between BS_t and MU at $P2$,R, is LOS, given that the link between BS_t and MU at $P1$, r, is LOS as well, is given by:

$$\mathbb{P}[E_1|E_2] = \frac{\mathbb{P}[E_1 \cap E_2]}{\mathbb{P}[E_2]} \tag{4.13}$$

Since it was given that the link between BS_t and MU at $P1$ is LOS which means that no blockages whose centers lie in the parallelogram, $BCEF$ as illustrated in 4.4. Therefore, the event of having no blockages in the parallelogram, $BCEF$, is equivalent to the event of having no blockages in the triangle, BCJ. On the other hand, there is no overlapping between the parallelogram, $ABJD$, and the triangle, BCJ, which means that the two events are independent. Therefore, $\mathbb{P}[E_1 \cap E_2]$ is given by:

$$\mathbb{P}[E_1 \cap E_2] = \mathbb{P}[E_7] \times \mathbb{P}[E_2] \tag{4.14}$$

Where, E_7, is the event that no blockages whose centers fall inside the parallelogram, $ABJD$. Substituting equation (4.14) in equation (4.13):

$$\mathbb{P}[E_1|E_2] = \mathbb{P}[E_7] \tag{4.15}$$

Note that the events $E1$ and $E2$ are independent when there is no overlapping area between the two links, r and R, as illustrated in figure (4.5). Therefore, the events $E1$

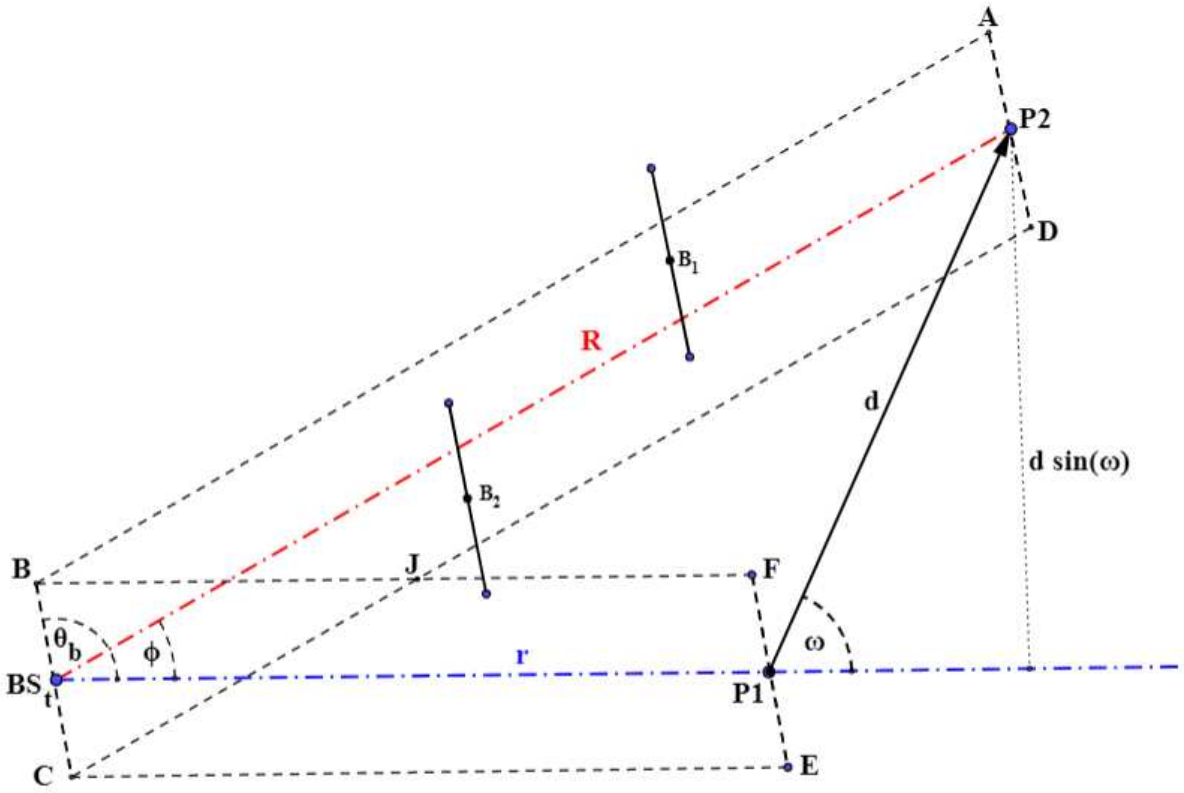

Figure 4.4: Relationship between the link, R, and the link, r. There is overlapping area when, $\theta_b : (\phi \leq \theta_b \leqslant \pi)$

and $E2$ are dependent only when $\theta_b = (0 \leq \theta_b \leqslant \phi)$.

Where, ϕ, is given by:

$$\phi = sin^{-1}\left[\frac{dsin(\omega)}{R}\right] \tag{4.16}$$

Now, we need to find out the distribution of the number of blockages that could fall inside the parallelogram, A_{ABJD}, which is a subset of the area A. Since the number of blockages, N_{L,θ_b}, whose centers fall in an area, A, for a given blockage length, L, and blockage orientation, θ_b, follows PPP and uniformly distributed in A, therefore, the probability, P, that any blockage whose center could lie in the parallelogram, A_{ABJD}, is given by:

$$P = \frac{Area\ of\ ABJD}{Total\ area\ A} \tag{4.17}$$

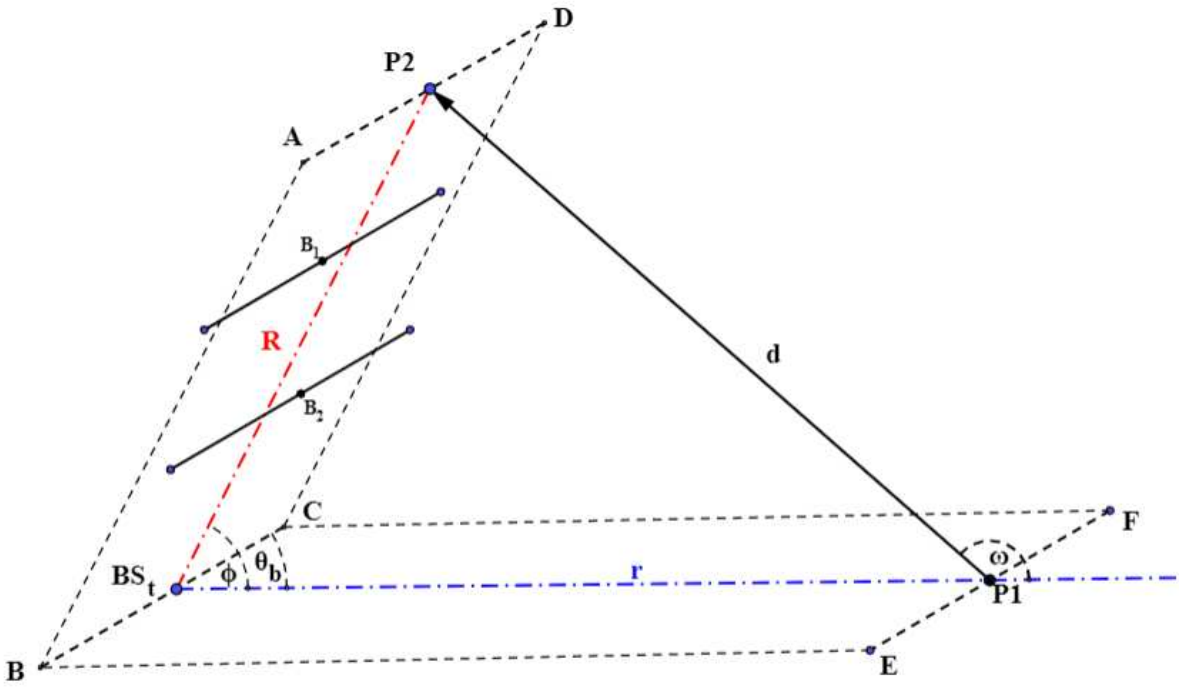

Figure 4.5: Relationship between the link, R, and the link, r. No overlapping area when, $\theta_b : (0 \leq \theta_b \leqslant \phi)$.

Any blockage whose center lies inside the parallelogram A_{ABJD} must intersects with the link R.

The probability that the number of blockages whose centers lie in the parallelogram A_{ABJD} is m, $\mathbb{P}[M_{L,\theta_b} = m]$, can be calculated as follows:

$$\mathbb{P}[M_{L,\theta_b} = m] = \frac{exp(-\lambda_b A_{ABJD} P)(\lambda_b A_{ABJD} P)^m}{m!} \tag{4.18}$$

Where, M_{L,θ_b} is a Poisson random variable with parameter:

$$E[M_{L,\theta_b}] = \lambda_b A_{ABJD}. \tag{4.19}$$

and the area of the parallelogram, A_{ABJD}, is given by:

$$A_{ABJD} = A_{ABCD} - A_{BCJ} = [RLsin(\theta_b - \phi)] - [\frac{L^2 sin(\theta_b - \phi)sin(\theta_b)}{2sin(\phi)}] \tag{4.20}$$

Since the length, L, and the orientation, θ_b, of each line segment is independent from all

other line segments, therefore, M_{L,θ_b} are independent for each L and θ_b. Thanks to the superposition property of independent PPP, the expected number of blockages lie in the parallelogram ABJD for any length, $L\epsilon(L_{min}, L_{max})$, and any orientation, $\theta_b\epsilon(\theta_{b_{min}}, \theta_{b_{max}})$ is given by:

$$E[M] = \sum_{L,\theta_b} \mathbb{E}[M_{L,\theta_b}] = \int_{\theta_{b_{min}}}^{\theta_{b_{max}}} \int_{L_{min}}^{L_{max}} f_{\theta_b}(\theta_b) f_L(L) \lambda_b A_{ABJD} dL d\theta_b \tag{4.21}$$

Therefore, the probability that the propagation path, R, for the MU at P_2 is LOS,given that the propagation path, r, to the MU at P_1 is also LOS is given by:

$$\mathbb{P}[E1|E2] = \mathbb{P}[M = 0] = exp(-E[M]) \tag{4.22}$$

Note that when the blockage has an orientation distributed uniformly, θ_b ϵ (0,π), the probability that no blockages lie in the propagation path is given by:

$$\mathbb{P}[E1|E2] = \mathbb{P}[M = 0] = (\frac{\phi}{\pi}) \times exp(-E[M1]) + (\frac{\pi - \phi}{\pi}) \times exp(-E[M2]) \tag{4.23}$$

Where (4.23) follows the theorem of total probability and, $E[M1]$ and $E[M2]$ are given by:

$$E[M1] = \int_0^{\phi} \int_{L_{min}}^{L_{max}} \frac{\lambda_b A_{ABCD}}{\phi(L_{max} - L_{min})} dL d\theta_b \tag{4.24}$$

$$E[M2] = \int_{\phi}^{\pi} \int_{L_{min}}^{L_{max}} \frac{\lambda_b A_{ABJD}}{(\pi - \phi)(L_{max} - L_{min})} dL d\theta_b \tag{4.25}$$

Where,

A_{ABJD}: is the area of the parallelogram ABJD, as illustrated in figure (4.4).

A_{ABCD}: is the area of the parallelogram ABCD, as illustrated in figure (4.5).

In order to validate the theoretical analysis, a Monte-Carlo simulation is carried out. The outcomes show that numerical and simulation results are in a good matching, as shown in figure(4.6) and figure(4.7). It is assumed that the distance, r, is 40m, and the

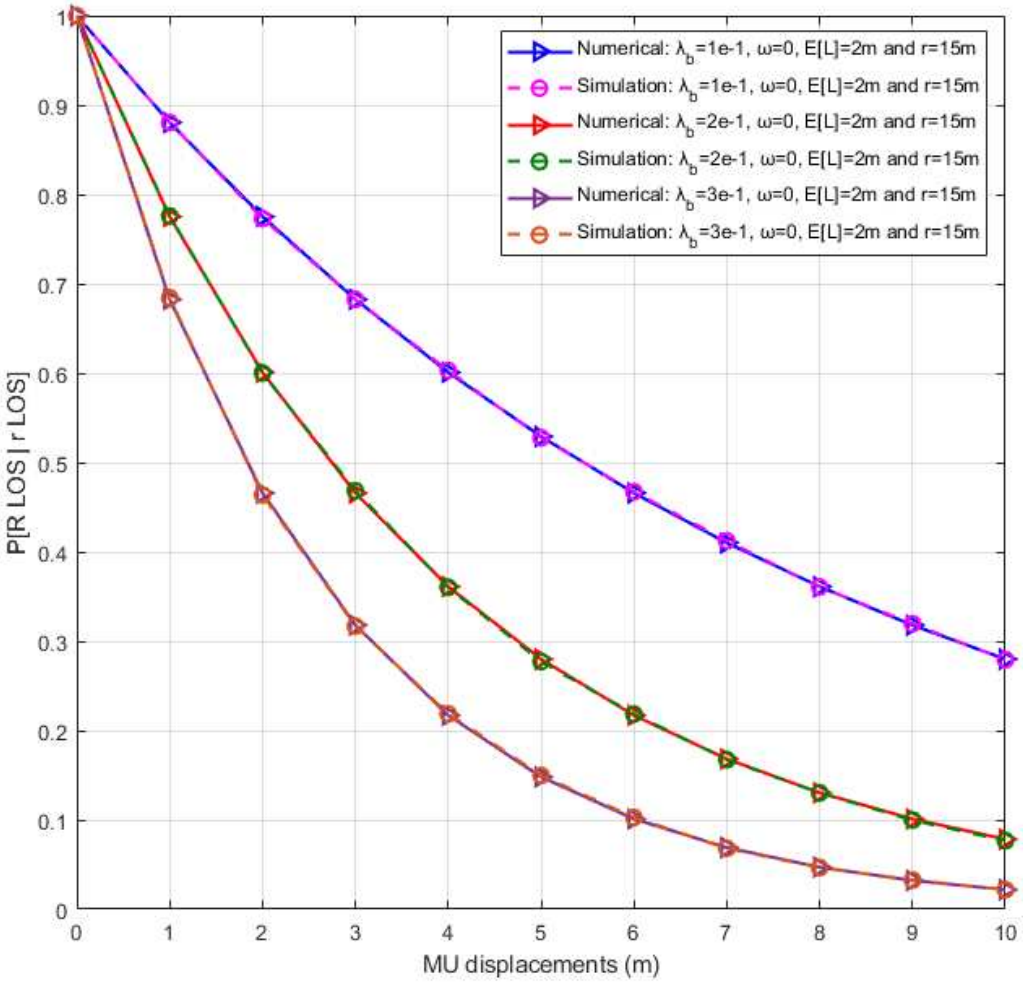

Figure 4.6: P[R LOS—r LOS] with different blockage intensities.

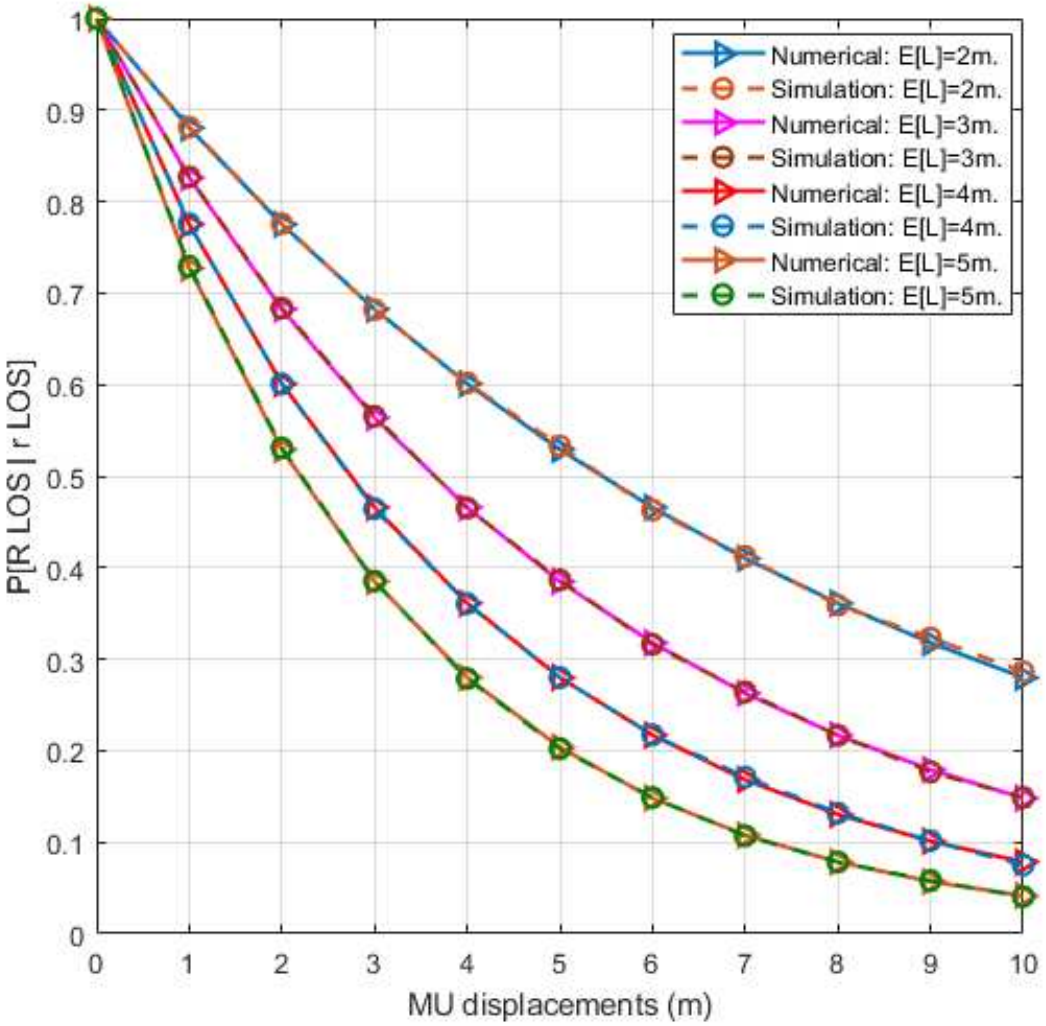

Figure 4.7:
P[R LOS—r LOS] with different blockage lengths.

MU makes a displacement, d, varying from 0 to 10m with steps of 1m, at angle $\omega = 0$ and $\frac{\pi}{2}$. It can be noticed that when the MU is moving at a minimal distance, the propagation path, R, is with a high probability of being LOS. On the other hand, as the MU moves at a higher distance, the probability that the propagation path, R, is with a lower probability of being LOS. Note that when the MU is moving in a radial direction with respect to the connection direction, the propagation path, R, between the MU, at the new location P_2, and the tagged mm-wave BS with a higher probability of being LOS. On the other hand, when the MU is moving in a perpendicular direction with respect to the connection direction, the propagation path, R, is less likely to be LOS.

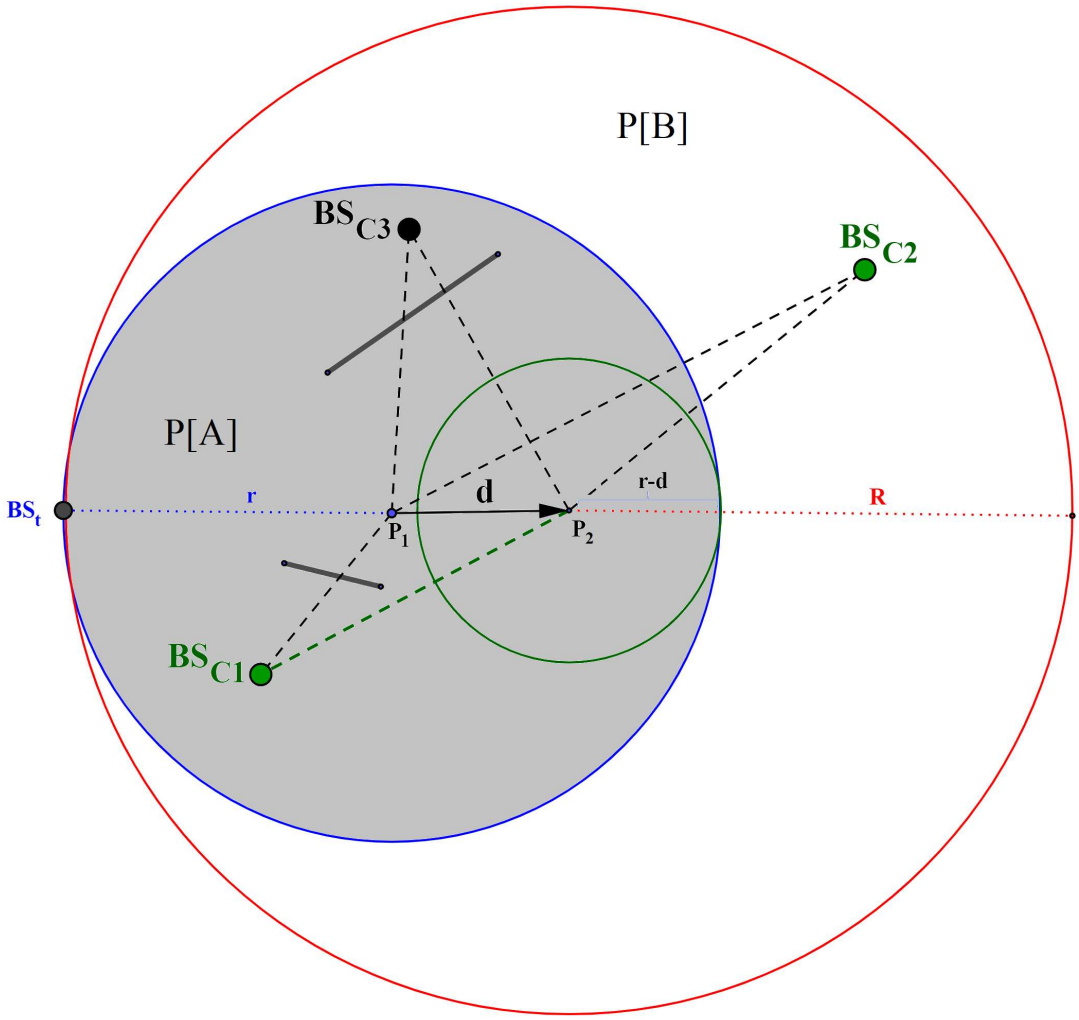

Figure 4.8: Probability at least 1 BSc is LOS from P2 given that it is NLOS from P1 inside the circle with radius R.

Recall that $\mathbb{P}[E_3|E_4]$ is the probability at least one candidate BS is LOS to the MU

at location P_2 given that it is NLOS from P_1, inside the circle with radius R, which can be simplified as follows:

$$\mathbb{P}[E_3|E_4] = 1 \; - \; \mathbb{P}[A \cap B] \tag{4.26}$$

Where:

A: is the event that all BS_c are blocked and they have a NLOS propagation path to the MU at the new location, P_2, lie in the common area, A_c, of the two circles with radius r centered at P_1, and R centered at P_2, given that it was with a NLOS propagation path to the MU at the initial location P_1.

B: is the event that all BS_c are blocked and they have a NLOS propagation path to the MU at the new location, P_2, lies in the excess area, inside the circle with radius R centered at P_2, and outside the circle with radius r centered at P_1. In this case, as illustrated in figure 4.8, the MU will associate to any BS_c that lies outside the circle with radius r centered at P_1 and inside the circle with radius R centered at P_2, only if there is no other BS_c, with LOS propagation path to the MU at the new location P_2, lies in the common area, A_c, of the two circles centered at P_1 with radius r and P_2 with radius R, respectively.

Since there is no overlapping areas, we assume that the two events, A and B, are independent. Therefore, equation (4.26) is given by:

$$\mathbb{P}[A \cap B] = \mathbb{P}[A] \times \mathbb{P}[B] \tag{4.27}$$

- **Analysis of the probability all candidate mm-wave BS are NLOS to the MU at the new location, given that they are NLOS from the initial location, in the common area:**

Seeking for simplicity, we will consider one BS_c in the following steps of our analysis, after that we will generalize the analysis to nBS_c.

Let us define the following events, as shown in figure (4.9):

EV1: is the event of no blockages lie in the area of ABDE.

EV2: is the event of no blockages lie in the area of BCD.

EV3: is the event of at least one blockage lies in the area of BCGF.

EV4: is the event of at least one blockage lies in the area of DCGF.

$$\mathbb{P}[One\ BS_c\ LOS\ in\ A_c\ to\ P_2|NLOS\ to\ P_1] = \mathbb{P}[EV1] \times \mathbb{P}[EV2|EV3] \tag{4.28}$$

$$\mathbb{P}[One\ BS_c\ LOS\ in\ A_c\ to\ P_2|NLOS\ to\ P_1] = \mathbb{P}[EV1] \times \frac{\mathbb{P}[EV2 \cap EV3]}{\mathbb{P}[EV3]} \tag{4.29}$$

$\mathbb{P}[EV2 \cap EV3]$ is the probability of the two events of no blockage lies in the area BCD given that at least one blockage lies in the area BCGF. In other words, the probability of no blockages whose centers lie the area BCD, given that at least one blockage whose center lies in the area BCGF. Note that $\mathbb{P}[EV2 \cap EV3]$ is equivalent to $\mathbb{P}[EV2 \cap EV4]$. The two events, EV2 and EV4, are independent since there is no overlapping area between the two areas, BCD and DCGF. Therefore,

$$\mathbb{P}[One\ BS_c\ LOS\ in\ A_c\ to\ P_2|NLOS\ to\ P_1] = \mathbb{P}[EV2] \times \mathbb{P}[EV4] \tag{4.30}$$

Substituting equation (4.30) in equation (4.28):

$$\mathbb{P}[One\ BS_c\ LOS\ in\ A_c\ to\ P_2|NLOS\ to\ P_1] = \frac{\mathbb{P}[EV1] \times \mathbb{P}[EV2] \times \mathbb{P}[EV4]}{\mathbb{P}[EV3]} \tag{4.31}$$

Since the the blockages are distributed according to PPP, and given the density of blockages λ_b, the number of the blockages lies in area A is a Poisson random variable, with mean $A\lambda_b$. Therefore, equation (4.31) can be represented as follows:

$$\mathbb{P}[One\ BS_c\ LOS\ in\ A_c\ to\ P_2|NLOS\ to\ P_1] = \frac{exp(-\lambda_b A_h)\ exp(-\lambda_b A_{g,h})\ (1 - exp(-\lambda_b A_g))}{1 - exp(-\lambda_b A_g + A_{g,h})} \tag{4.32}$$

Where:

A_h: is the expected area of the parallelogram ABDE.

A_g: is the expected area of the parallelogram CDFG.

$A_{g,h}$: is the expected area of the parallelogram BCD.

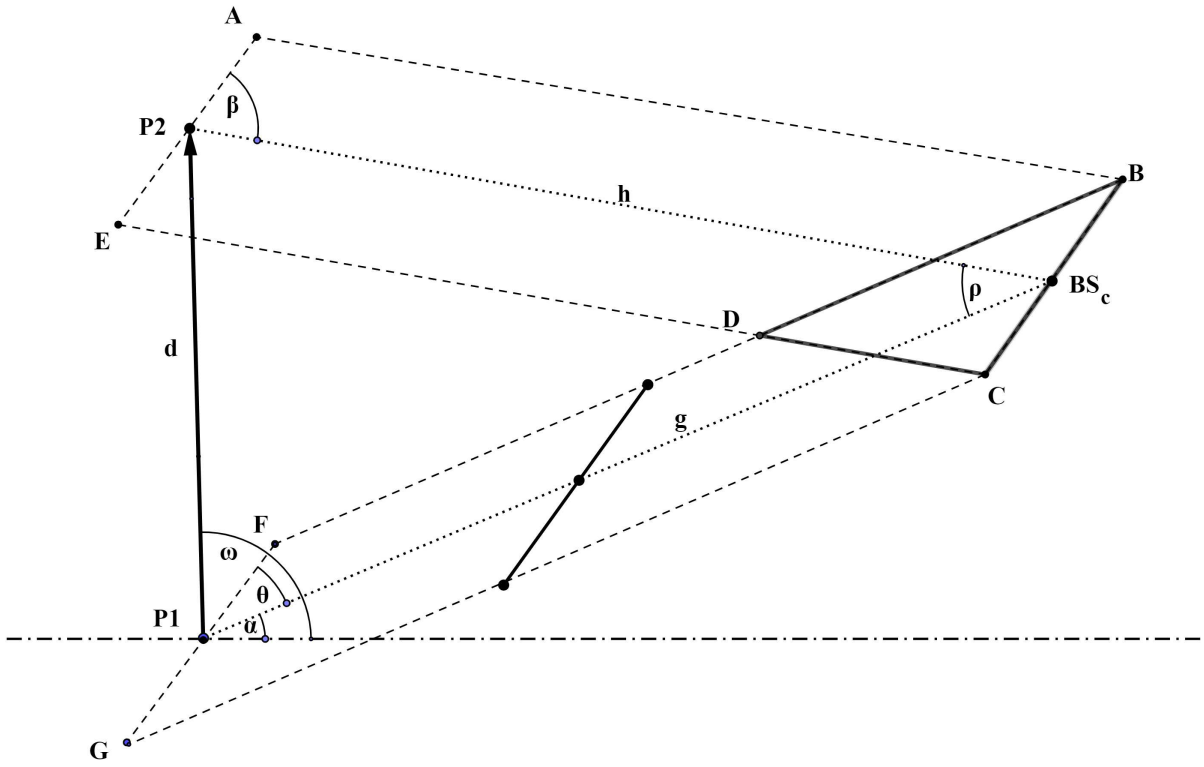

Figure 4.9: Probability BSc is LOS from P2 given that it is blocked from P1.

When the MU located anywhere in the common area, equation (4.32) can be further simplified as follows:

$$\mathbb{P}[One\ BS_c\ LOS\ in\ A_c\ to\ P_2|NLOS\ to\ P_1] = \int_l f_{L_1}(l_1)\frac{exp(-\lambda_b(A_h + A_{g,h}))(1 - exp(A_g))}{1 - exp(-\lambda_b(A_g + A_{g,h}))}dl_1 \tag{4.33}$$

Where $f_{l_1}(L_1)$ is the probability density function of the distance, $\boldsymbol{l}$, between the MU and BS_c at P_2, and it is given as:

$$f_{L_1}(l_1) = \begin{cases} \frac{d}{dl_1}\frac{A_{l_1}}{A_{r-d}}\ , & l_1 = [0, r-d] \\ \frac{d}{dl_1}\frac{A_{C_{R,l_1}} - A_{r-d}}{A_{C_{R,r}} - A_{r-d}}\ , & l_1 = [r-d, R] \end{cases} \tag{4.34}$$

Where:

A_{l_1}: is the area of the circle of radius l, centered at P_2.

A_{r-d}: is the area of the circle of radius r-d, centered at P_2.

$A_{C_{R,l}}$: is the common area between two circles of radius R centered at P_2, and radius l centered at same place, P_2.

$A_{C_{R,r}}$: is the common area between two circles of radius R centered at P_2, and r centered at P_1.

l_1: is the distance between the MU at location, P_2, and the mm-wave BS_c located in the common area, $A_{C_{R,r}}$.

$\mathbb{P}[One\ BS_c\ NLOS\ in\ A_c\ to\ P_2|NLOS\ to\ P_1]$ is the probability of one mm-wave BS_c NLOS from P_2 given that it is NLOS from P_1, and it is given by:

$$\mathbb{P}[1\ BS_c\ NLOS\ in\ A_c\ to\ P_2|NLOS\ to\ P_1] = 1 - \mathbb{P}[One\ BS_c\ LOS\ in\ A_c\ to\ P_2|NLOS\ to\ P_1] \tag{4.35}$$

Substituting equation (4.33) in equation (4.35):

$$\mathbb{P}[1\ BS_c\ NLOS\ in\ A_{C_{R,r}}\ to\ P_2|NLOS\ to\ P_1] = 1 - \int_{l_1} f_{L_1}(l_1)\frac{e^{-\lambda_b(A_h + A_{g,h})}(1 - e^{(A_g)})}{1 - e^{-\lambda_b(A_g + A_{g,h})}}dl_1 \tag{4.36}$$

The probability that the expected number of candidate mm-wave BS_c, $\mathbb{P}[N = n_{BS_c}; A_{C_{R,r}}]$, falling in the common area between the circle of radius r, and the circle of radius R, is distributed according to Poisson law with parameter $\lambda_{BS} A_{C_{R,r}}$, i.e.

$$\mathbb{P}[N = n_{BS_c}; A_{C_{R,r}}] = \frac{[\lambda_{BS} A_{C_{R,r}}]^{n_{BS_c}}}{n_{BS_c}!} exp(-\lambda_{BS} A_{C_{R,r}}) \tag{4.37}$$

Assuming uncorrelated and independent blockage events of all the mm-wave BS-MU links. Therefore, the probability that n BS_c are blocked in the common area, $\mathbb{P}[A|n_{BS_c}]$, is given by:

$$\mathbb{P}[n\ BS_c\ NLOS\ in\ A_{C_{R,r}}\ to\ P_2|NLOS\ to\ P_1] = \mathbb{P}[1\ BS_c\ NLOS\ in\ A_{C_{R,r}}\ to\ P_2|NLOS\ to\ P_1]^{n_{BS_c}} \tag{4.38}$$

Substituting equation (4.36) in equation (4.38):

$$\mathbb{P}[n\ BS_c\ NLOS\ in\ A_{C_{R,r}}\ to\ P_2|NLOS\ to\ P_1] = \left[1 - \int_{l_1} f_{L_1}(l_1) \frac{e^{-\lambda_b(A_h + A_{g,h})}(1 - e^{(A_g)})}{1 - e^{-\lambda_b(A_g + A_{g,h})}} dl_1\right]^{n_{BS_c}} \tag{4.39}$$

Now, we need to generalize our analysis for any number of BS_c fall in the common area $A_{C_{R,r}}$. Therefore, $\mathbb{P}[A|n\ BS_c]$, is given by:

$$\mathbb{P}[A|n\ BS_c] = \left[\frac{[\lambda_{BS} A_{C_{R,r}}]^{n_{BS_c}}}{n_{BS_c}!} exp(-\lambda_{BS} A_{C_{R,r}})\right] \left[1 - \int_{l_1} f_{L_1}(l_1) \frac{e^{-\lambda_b(A_h + A_{g,h})}(1 - e^{(A_g)})}{1 - e^{-\lambda_b(A_g + A_{g,h})}} dl_1\right]^{n_{BS_c}} \tag{4.40}$$

For n_{BS_c} distributed over the interval [0, ∞], the probability, $\mathbb{P}[A]$, is given by:

$$\mathbb{P}[A] = \sum_{n=0}^{\infty} \left[\frac{[\lambda_{BS} A_{C_{R,r}}]^{n_{BS_c}}}{n_{BS_c}!} exp(-\lambda_{BS} A_{C_{R,r}})\right] \left[1 - \int_{l_1} f_{L_1}(l_1) \frac{e^{-\lambda_b(A_h + A_{g,h})}(1 - e^{(A_g)})}{1 - e^{-\lambda_b(A_g + A_{g,h})}} dl_1\right]^{n_{BS_c}} \tag{4.41}$$

Equation (4.41) can be further simplified as follows:

$$\mathbb{P}[A] = exp\left[-\lambda_{BS} A_{C_{R,r}} \int_{l_1} f_{L_1}(l_1) \frac{e^{-\lambda_b(A_h+A_{g,h})}(1-e^{(A_g)})}{1-e^{-\lambda_b(A_g+A_{g,h})}} dl_1\right] \tag{4.42}$$

- **Analysis of the probability all candidate mm-wave BS are NLOS to the MU at the new location, in the excess area:**

Similarly, we need to calculate,$\mathbb{P}$[B], which is the probability that all mm-wave BS_c are blocked with NLOS propagation path to the MU at the new location, P_2, in the excess area, outside the circle of radius r, and inside the circle of radius R.

Denote A_c the common area between the two circles with radius of R and r, respectively, and denote $A_R \setminus A_c$ excess area resulted from MU displacement, from the origin at (P_1) to the new location (P_2), outside the circle with radius r and inside the circle with radius R, as shown in figure (4.10).

In this scenario, we need to calculate the probability that all mm-wave BS_c are blocked with NLOS propagation path to the MU at P_2. We will begin the analysis for one mm-wave BS_c. The probability that mm-wave BS_c is blocked, (i,e,. the path between this mm-wave BS_c and the MU is NLOS), is given by:

$$\mathbb{P}[BS_c \; is \; blocked] = 1 \; - \; \int_{l_2 \; min}^{l_2 \; max} f_{L_2}(l_2) \; \mathbb{P}[LOS] \; dl_2 \tag{4.43}$$

Where:

l_2: is the distance between the MU at location, P_2, and the mm-wave BS_c located in the excess area, $A_{R\setminus R\cap r}$.

$f_{L_2}(l_2)$: is the probability distribution function of l_2.

$l_{2\ min}$= r - d.

$l_{2\ max}$= R.

The probability density function of l_2, $F_{L_2}(l_2)$, can be calculated by taking the derivative of the cumulative distribution function of l_2, $F_{L_2}(l_2)$, as follows:

$$f_{L_2}(l_2) = \frac{d}{dl} F_{L_2}(l_2) \tag{4.44}$$

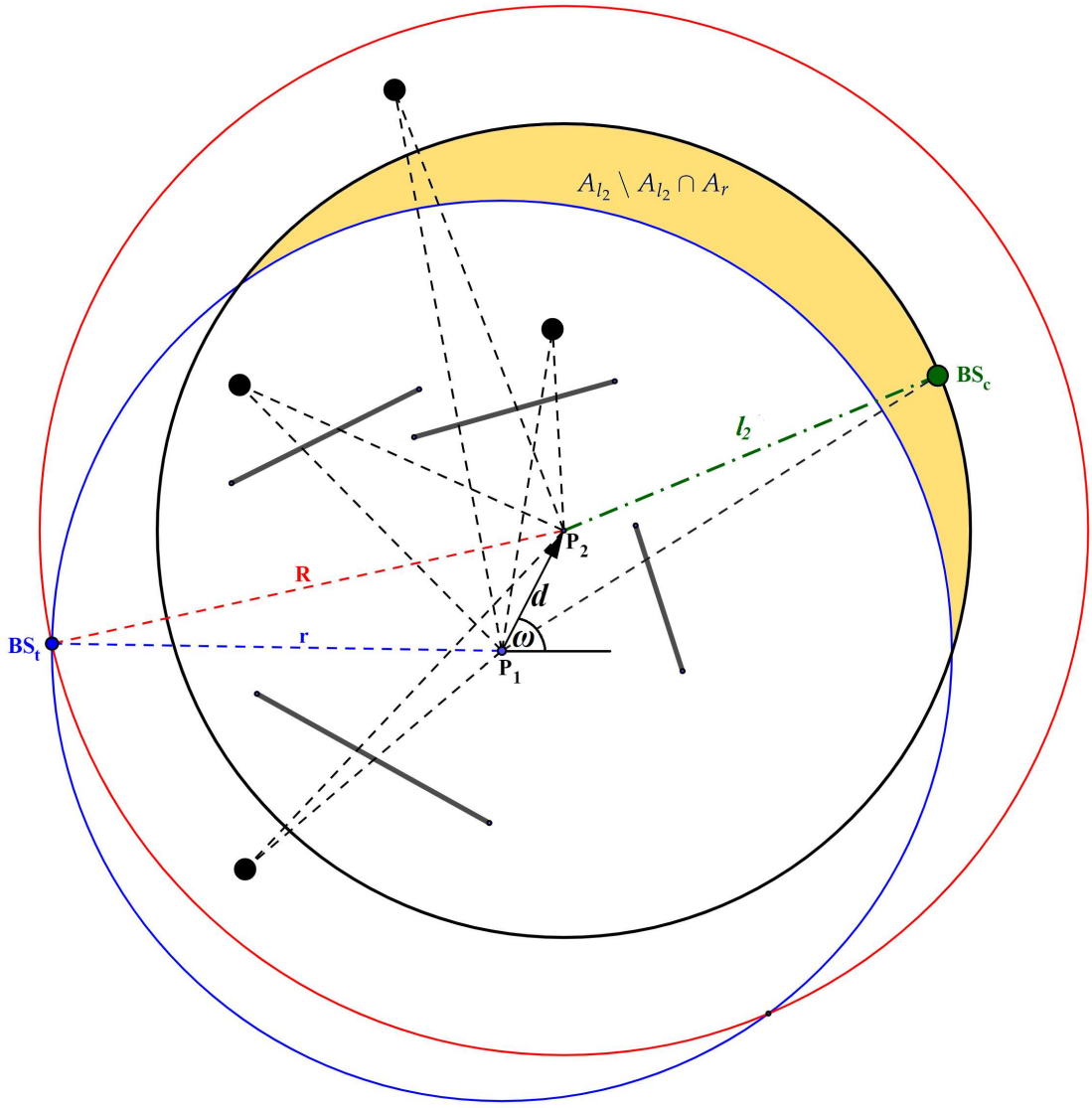

Figure 4.10: System model of $P[B]$ where the MU is moving in a distance of $\boldsymbol{d}$, and angle of ω.

The cumulative distribution function, $F_{L_2}(l_2)$, can be calculated as follows:

$$F_{L_2}(l_2) = \frac{A_{l_2} \setminus A_{l_2} \cap A_r}{A_R \setminus A_R \cap A_r} \tag{4.45}$$

Where, $A_{l_2} \setminus A_{l_2} \cap A_r$ is the common area between the two circles with radius r and l. It can be found using some basic trigonometry, and is given by:

$$A\left(l_2\right) \cap A\left(r\right) = l_2^2 \; cos^{-1}(\frac{l_2^2 + d^2 - r^2}{2dl_2}) + r^2 \; cos^{-1}(\frac{r^2 + d^2 - l_2^2}{2dr}) - a(l_2) \tag{4.46}$$

Where $a(l_2)$ is given by:

$$a(l_2) = \frac{1}{2}\sqrt{(l_2 + r - d)(l_2 + r + d)(d + l_2 - r)(d - l_2 + r)} \tag{4.47}$$

Therefore, the excess area outside the circle with radius r and inside the circle with radius l, denoted by $A_{l_2} \setminus A_{l_2} \cap A_r$, is given by:

$$A_{l_2} \setminus A_{l_2} \cap A_r = \pi l_2^2 - \left[l_2^2 \; cos^{-1}(\frac{l_2^2 + d^2 - r^2}{2dl_2}) + r^2 \; cos^{-1}(\frac{r^2 + d^2 - l_2^2}{2dr}) - a(l) \right] \tag{4.48}$$

The excess area outside the circle with radius r, and inside the circle with radius R, $A_R \setminus A_R \cap A_r$, is given by:

$$A_R \setminus A_R \cap A_r = \pi R^2 - R^2 \left[\omega - \sin^{-1}\left(\frac{d \sin \omega}{R} \right) \right] + rd \; sin \; \omega - r^2 \left(\pi - \omega \right) \tag{4.49}$$

Substituting equation (4.48) and equation (4.49) in equation (4.45) we get $F_{L_2}(l_2)$:

$$F_{L_2}(l_2) = \frac{\pi l_2^2 - \left[l_2^2 \; cos^{-1}(\frac{l_2^2 + d^2 - r^2}{2dl_2}) + r^2 \; cos^{-1}(\frac{r^2 + d^2 - l_2^2}{2dr}) - a(l_2) \right]}{\pi R^2 - R^2 \left[\omega - \sin^{-1}\left(\frac{d \sin \omega}{R} \right) \right] + rd \; sin \; \omega - r^2 \left(\pi - \omega \right)} \tag{4.50}$$

By taking the derivative, we get $F_{L_2}(l_2)$:

$$f_{L_2}(l_2) = \frac{a_1(l_2) - a_2(l_2) - a_3(l_2) - a_4(l_2) + a_5(l_2)}{\pi R^2 - R^2 \left[\omega - \sin^{-1}\left(\frac{d \sin \omega}{R} \right) \right] + rd \; sin \; \omega - r^2 \left(\pi - \omega \right)} \tag{4.51}$$

where:

$a_1(l_2)$=$2\pi l_2$

$$a_2(l) = 2l_2\ cos^{-1}[\tfrac{(l_2^2+d^2-r^2)}{(2dl_2)}]$$

$$a_3(l_2) = \frac{l_2^2(\frac{1}{d}\frac{d^2-r^2+l_2^2}{2dl_2^2})}{\sqrt{1-\frac{(d^2-r^2+l_2^2)^2}{4d^2l_2^2}}}$$

$$a_4(l_2) = \frac{rl_2}{d\sqrt{1-\frac{(r^2+d^2-l_2^2)^2}{4d^2r^2}}}$$

$$a_5(l_2) = \frac{l_2(d^2+r^2-l_2^2)}{\sqrt{-(-d-r-l_2)(d-r-l_2)(d+l_2-r)(d-l_2+r)}}$$

Note that the probability a candidate mm-wave BS falling in A_R is blocked from the new location P_2, is given in equation (4.43) and can be rewritten as follows:

$$\mathbb{P}[1\ BS_c\ in\ A_{R\setminus R\cap r}\ is\ blocked] = 1\ -\ \int_{r-d}^{R} f_{L_2}(l_2)\ exp(-\frac{2\lambda_b}{\pi}E[L].\ l_2)\ dl_2 \tag{4.52}$$

The probability that the expected number of candidate mm-wave BS_c, $\mathbb{P}[N = n_{BS_c}; A_{R\setminus R\cap r}]$, falling outside the circle of radius r, and inside the circle of radius R, is distributed according to Poisson law with parameter $\lambda_{BS}A_{R\setminus R\cap r}$, i.e.

$$\mathbb{P}[N = n_{BS_c}; A_{R\setminus R\cap r}] = \frac{[\lambda_{BS}A_{R\setminus R\cap r}]^{n_{BS_c}}}{n_{BS_c}!}exp(-\lambda_{BS}A_{R\setminus R\cap r}) \tag{4.53}$$

Assuming uncorrelated and independent blockage events of all the mm-wave BS-MU links. Therefore, the probability that $n\ BS_c$ are blocked in the excess area, is given by:

$$\mathbb{P}[n\ BS_c\ in\ A_{R\setminus R\cap r}\ are\ blocked] = \mathbb{P}[1\ BS_c\ in\ A_{R\setminus R\cap r}\ is\ blocked]^{n_{BS_c}} \tag{4.54}$$

Substituting equation (4.52) in equation (4.54):

$$\mathbb{P}[n\ BS_c\ in\ A_{R\setminus R\cap r}\ are\ blocked] = \left[1\ -\ \int_{r-d}^{R} f_{L_2}(l_2)\ exp(-\frac{2\lambda_b}{\pi}E[L].\ l_2)\ dl_2\right]^{n_{BS_c}} \tag{4.55}$$

Now, we need to generalize our analysis for any number of BS_c fall in the excess area $A_{R\setminus R\cap r}$. Therefore, $\mathbb{P}[B|n\ BS_c]$, is given by:

$$\mathbb{P}[B|n\ BS_c] = \left[\frac{[\lambda_{BS}A_{R\setminus R\cap r}]^{n_{BS_c}}}{n_{BS_c}!}exp(-\lambda_{BS}A_{R\setminus R\cap r})\right]\left[1-\int_{r-d}^{R} f_{L_2}(l_2)\ exp(-\frac{2\lambda_b}{\pi}E[L].\ l_2)\ dl_2\right]^{n_{BS_c}} \tag{4.56}$$

For n_{BS_c} distributed over the interval $[0,\ \infty]$, the probability, $\mathbb{P}[B]$, is given by:

$$\mathbb{P}[B] = \sum_{n_{BS_c}=0}^{\infty}\left[\frac{[\lambda_{BS}A_{R\setminus R\cap r}]^{n_{BS_c}}}{n_{BS_c}!}exp(-\lambda_{BS}A_{R\setminus R\cap r})\right]\left[1-\int_{r-d}^{R} f_{L_2}(l_2)\ exp(-\frac{2\lambda_b}{\pi}E[L].\ l_2)\ dl_2\right]^{n_{BS_c}} \tag{4.57}$$

Equation (4.57) can be further simplified as follows:

$$\mathbb{P}[B] = exp\left[-\lambda_{BS}A_{R\setminus R\cap r}\int_{r-d}^{R} f_{L_2}(l_2)\ exp(-\frac{2\lambda_b}{\pi}E[L].\ l_2)\ dl_2\right] \tag{4.58}$$

Substituting (4.42) and equation (4.58) in equation (4.27) we get the conditional probability that all mm-wave BS_c are blocked for the MU at the new location, P_2, given that all of them are also blocked or further than r for the MU at location, P_1, as follows:

$$\mathbb{P}[A\cap B] = \mathbb{P}[A]\times\mathbb{P}[B] \tag{4.59}$$

$$\begin{aligned}\mathbb{P}[A\cap B] = exp\left[-\lambda_{BS}A_{C_{R,r}}\int_{l_1} f_{L_1}(l_1)\frac{e^{-\lambda_b(A_h+A_{g,h})}(1-e^{(A_g)})}{1-e^{-\lambda_b(A_g+A_{g,h})}}dl_1\right] \\ \times exp\left[-\lambda_{BS}A_{R\setminus R\cap r}\int_{r-d}^{R} f_{L_2}(l_2)\ e^{(-\frac{2\lambda_b}{\pi}E[L].\ l_2)}\ dl_2\right]\end{aligned} \tag{4.60}$$

Substitute equation (4.60) in equation (4.26), we get the probability at least one candidate BS is LOS to the MU at location P_2 given that all of them are NLOS from P_1, inside the circle with radius R, which can be simplified as follows:

$$\mathbb{P}[E_3|E_4] = 1 \; - \; exp\Bigg[-\lambda_{BS} A_{C_{R,r}} \int_{l_1} f_{L_1}(l_1) \frac{e^{-\lambda_b(A_h+A_{g,h})}(1-e^{(A_g)})}{1-e^{-\lambda_b(A_g+A_{g,h})}} dl_1\Bigg] \\ \times exp\Bigg[-\lambda_{BS} A_{R\setminus R\cap r} \int_{r-d}^{R} f_{L_2}(l_2)\; e^{(-\frac{2\lambda_b}{\pi} E[L].\; l_2)}\; dl_2\Bigg] \tag{4.61}$$

Substituting equation (4.23) and equation (4.61) in equation (4.8), we get the total HO probability for a MU moving a distance of d with a direction of ω relative to the connection direction, as follows:

$$\mathbb{P}_t[HO] = 1 - \Bigg[(\frac{\phi}{\pi}) \times exp(-E[M1]) + (\frac{\pi-\phi}{\pi}) \times exp(-E[M2])\Bigg] \\ \times exp\Bigg[-\lambda_{BS} A_{C_{R,r}} \int_{l_1} f_{L_1}(l_1) \frac{e^{-\lambda_b(A_h+A_{g,h})}(1-e^{(A_g)})}{1-e^{-\lambda_b(A_g+A_{g,h})}} dl_1\Bigg] \\ \times exp\Bigg[-\lambda_{BS} A_{R\setminus R\cap r} \int_{r-d}^{R} f_{L_2}(l_2)\; e^{(-\frac{2\lambda_b}{\pi} E[L].\; l_2)}\; dl_2\Bigg] \tag{4.62}$$

which can be computed numerically.

4.4 Performance Evaluation and Discussion:

The results in figure (4.11), figure (4.12) and figure (4.13), show the impact of multiple static blockages on HO probability in different scenarios in mm-wave cellular network. We compared our analysis with the case no blockages are incorporated into the system. We assume that the distance between the MU and tagged mm-wave BS, in the initial position P_1, is r=15m. The MU makes a displacement of, $\boldsymbol{d}$, in different directions of ω. The first result in figure (4.11), we assume the MU makes displacements in a radial direction with respect to the connection direction, i,e. ω=0, the average length of the blockages is $E[L]$ = 3m to 6m. In both cases, with and without blockages, it can be noted that, as the MU makes higher displacement, the HO probability also gets higher. However, in the case where blockages are incorporated into the system, the HO probability is higher than that of no blockages incorporated into the system. That depends mainly on the blockage length. As the blockage length gets longer, the probability of HO gets higher. The second result shows the HO probability with MU displacement in different densities of blockages. It can be observed that the HO probability is higher as the density of the blockages gets higher. The third result shows the HO probability with different angles of the direction of the MU. It can be observed that the MU has the lowest HO probability when the MU

moves in a direction toward the tagged mm-wave BS, while the highest HO probability is when the MU moves in a perpendicular direction with respect to the connection direction. Since the propagation path between the MU at the initial location and the tagged mm-wave BS is given to be LOS, the HO probability gets to the lowest value when the MU is moving in a radial direction with respect to the connection direction. In all scenarios, the HO might happen even when the MU moves towards the tagged mm-wave BS. It might have another mm-wave BS closer than the tagged mm-wave BS to the MU but blocked by a blockage, and it becomes visible to the MU after a displacement in a certain distance and direction. Therefore, the HO may occur when the MU makes a displacement under any circumstances as long as blockages' presence could block the LOS propagation path between the MU and the BS_t. It might cause the ping-pong effect, especially for short blockage lengths, which needs to be considered in designing an efficient HO scheme.

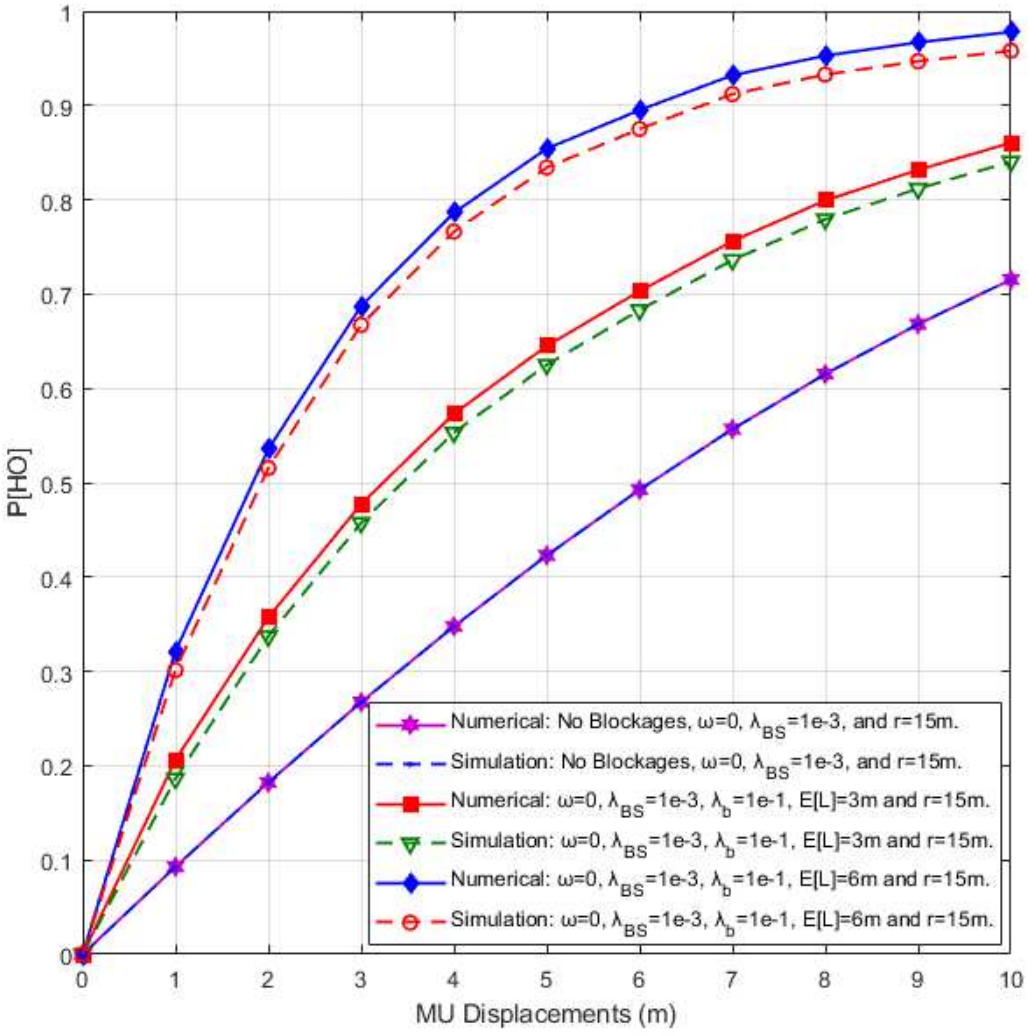

Figure 4.11: HO probability with different blockages' lengths.

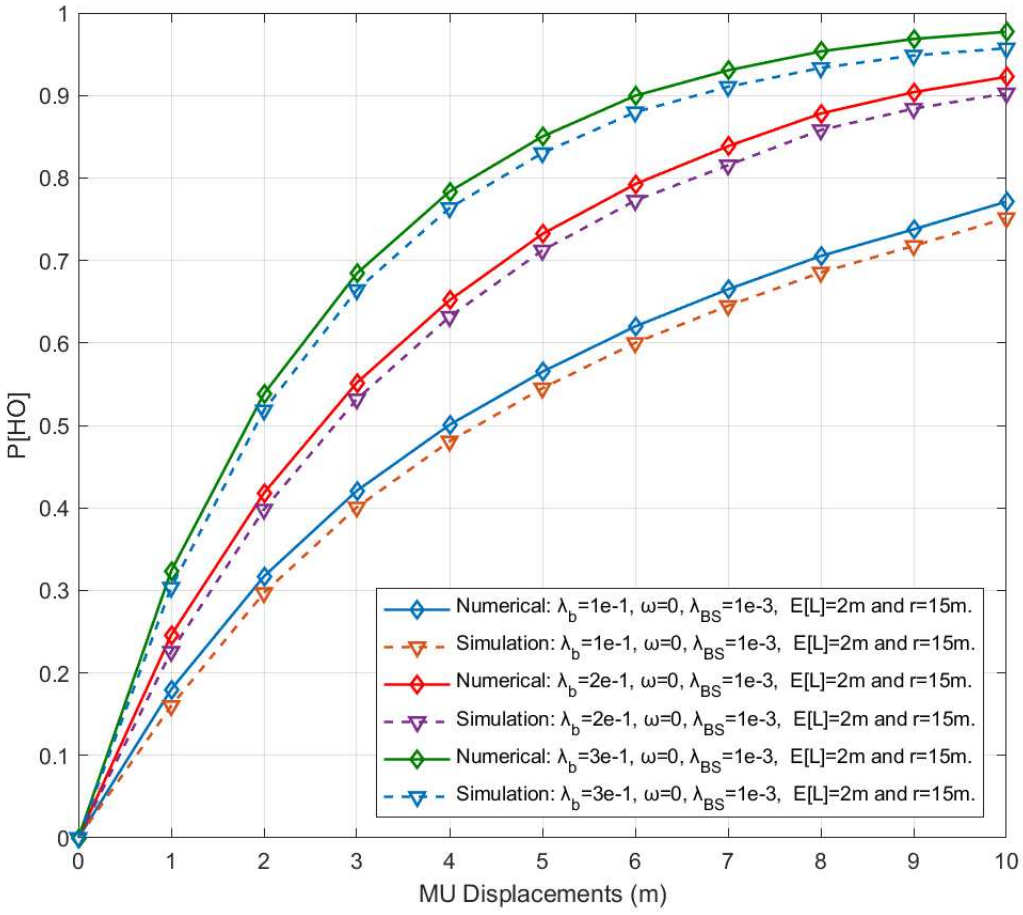

Figure 4.12: HO probability with different blockages' densities.

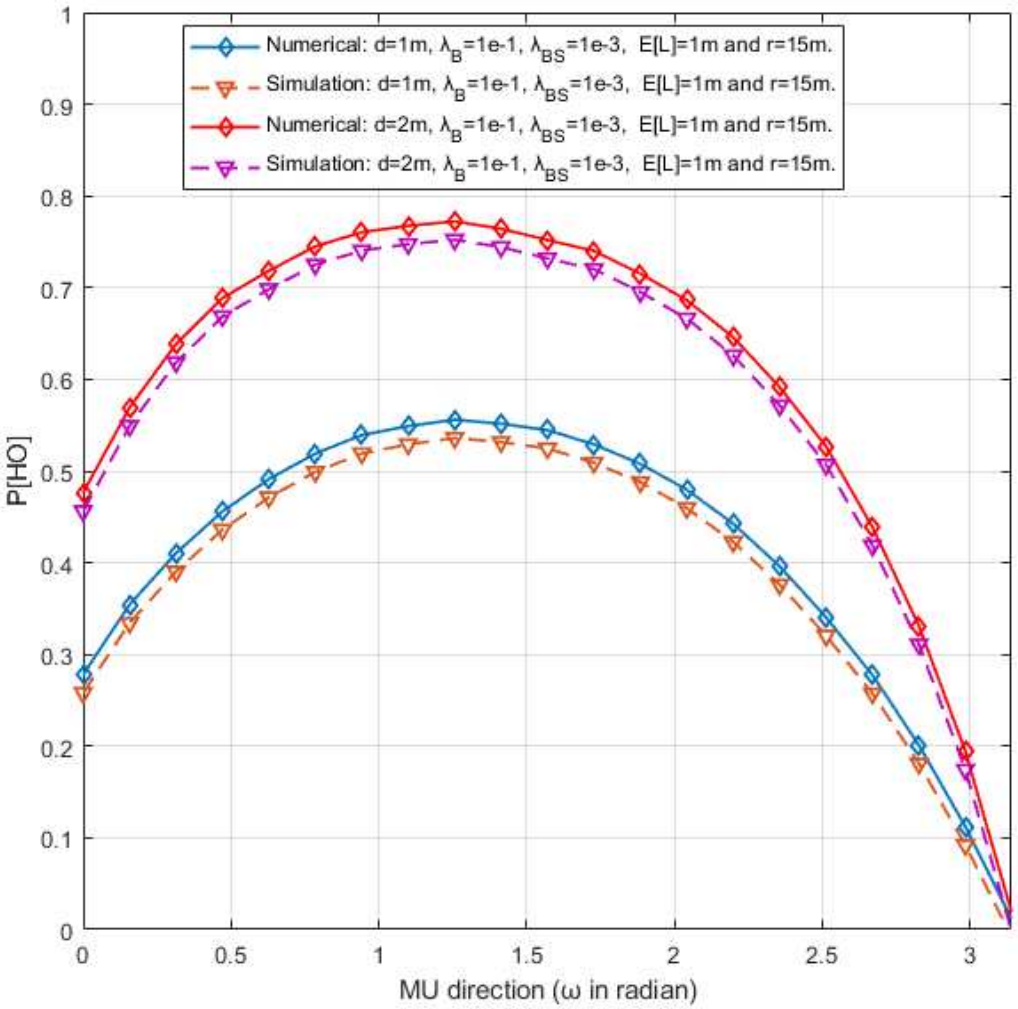

Figure 4.13: HO probability with different directions of MU (ω).

Chapter 5
Impact of Self and Dynamic-Blockage on HO and Blocking Probability

5.1 Impact of Self-Blockage on HO Probability

5.1.1 Introduction

This subsection analyzes the impact of self-blockage on HO probability for a MU with mobility in a 5G mm-wave cellular network. Self-blockage is defined as a blockage that could happen for the MU device resulting from MU's own body, and consequently, the MU may lose the LOS accessibility to the tagged mm-wave BS. As a result, MU may do frequent HOs, impacting the system's overall performance.

5.1.2 Assumptions and System Model

In this section we present a mathematical analysis for the self-blockage impact on MU based on the following assumptions:

1. Self-blockage zone and signal model:

   Self-blockage zone is modelled as a sector of a disc centred at the origin and has a radius of, R, S(O, R). The sector is making an angle of, θ, towards the MU's body, as shown in figure (5.1). We also assume that the direction of the center of the blocking angle is with respect to the displacement direction of the MU. Since the human body causes a severe attenuation to the mm-wave signal, [7, 43], we assume that the MU's body blocks any signal from any mm-wave BS that lies in the blocking zone. Consequently, all mm-wave BSs that lie in the blocking zone are considered blocked. Furthermore, we incorporate the blocking angle change such that the blocking zone is not covering the tagged mm-wave BS.

2. Mm-wave BSs distribution and MU mobility:

   We assume that the mm-wave BSs are modelled according to PPP and distributed uniformly in the 2-D plane. All mm-wave BSs transmit the same transmission power. Therefore, the MU associates with the closest LOS mm-wave BS. The MU is making a displacement of, d, per time unit speed from the initial location at $P1$, (at the origin), towards a new location at $P2$.

3. HO probability:

   When the MU makes a displacement from the inial location, $P1$, to the new location, $P2$, the distance to the tagged mm-wave BS will change accordingly. HO will only occur if there is any other mm-wave BS than the tagged mm-wave BS becomes

LOS and closer to the MU after the displacement. Therefore, any mm-wave BS becomes visible to the MU out of the circle with radius, r, and inside the circle with radius, R, but not in the self-blockage zone, will be a candidate mm-wave BS. Consequently, a HO will occur to it.

4. We neglect the impact of the other types of blockages in this analysis.

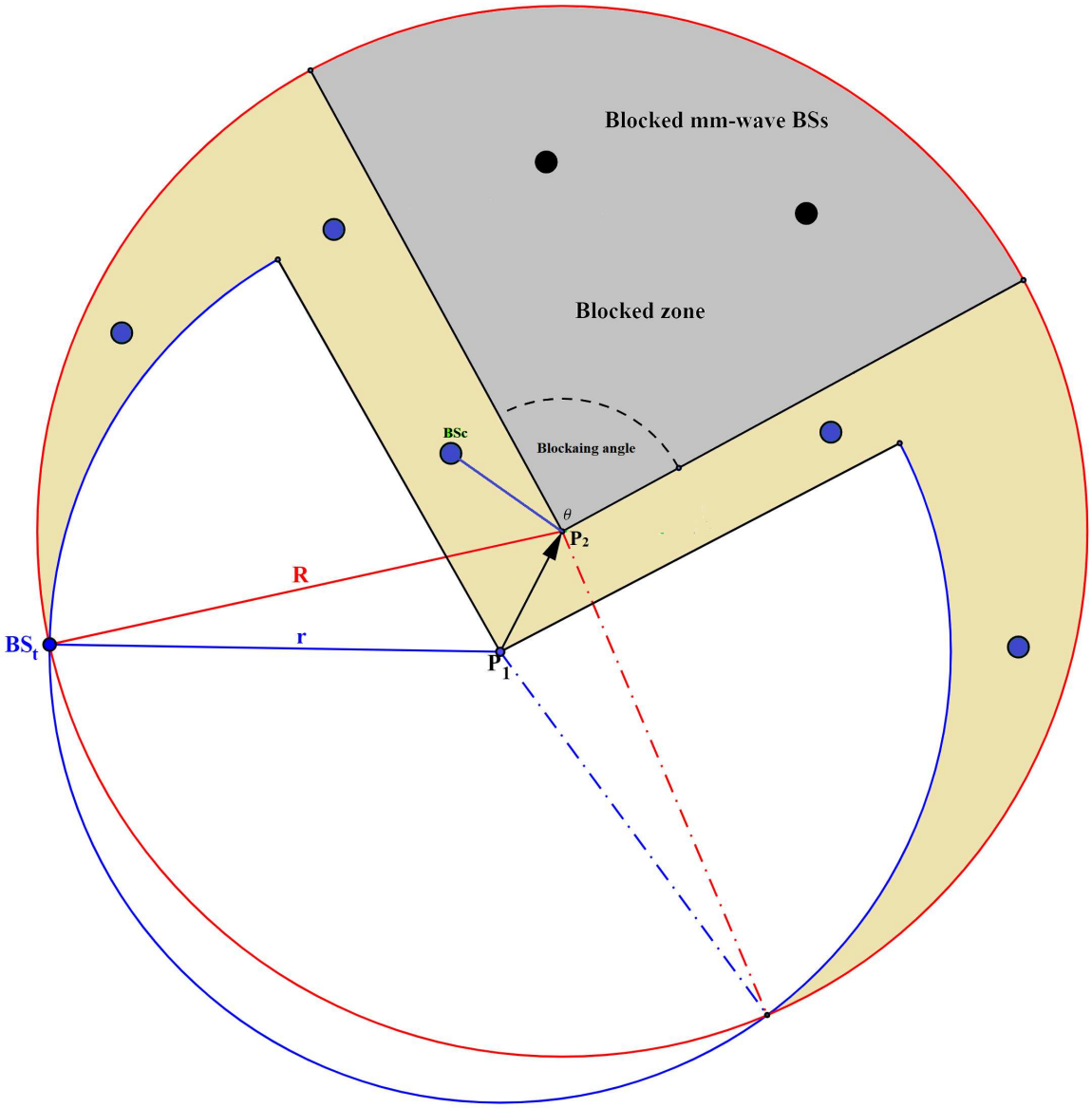

Figure 5.1: Self-blockage system model.

Let, A, denotes the excess visible area as illustrated in figure 5.1 with the yellow color, which can be calculated as follows:

$$A = A_R - A_C + A_{S1} - A_{S2} \tag{5.1}$$

Where:

A_R: is area of the circle with radius R.

$$A_R = \pi R^2 \tag{5.2}$$

A_C: is the common area between the two circles of radius r and R, respectively.

$$A_C = R^2 \left[\omega - \sin^{-1}\left(\frac{d\sin(\omega)}{R}\right)\right] + rdsin(\omega) - r^2(\pi - \omega) \tag{5.3}$$

A_{S1}: is the area of the sector generated from the self-blockage when the MU is at the initial location, at $P1$.

$$A_{S1} = \frac{\theta}{2} r^2 \tag{5.4}$$

A_{S2}: is the area of the sector generated from the self-blockage when the MU is at the new location, at $P2$.

$$A_{S2} = \frac{\theta}{2} R^2 \tag{5.5}$$

Where, R, is given in equation (3).

The visible excess area (A) is obtained by substituting (5.5), (5.4), (5.3) and (5.2) in (5.1):

$$A = \pi R^2 - [R^2 \left[\omega - \sin^{-1}\left(\frac{d\sin(\omega)}{R}\right)\right] + rdsin(\omega) - r^2(\pi - \omega)] + \frac{\theta}{2} r^2 - \frac{\theta}{2} R^2 \tag{5.6}$$

The probability of HO for a MU moving at speed of d per time unit and an angle of ω with respect to the connection direction, and considering blocking angle of θ, is given by:

$$\mathbb{P}[HO|r, w, \theta] = 1 - exp(-\lambda A) \tag{5.7}$$

$$\mathbb{P}[HO|r, w, \theta] = 1 - exp(-\lambda(A_R - A_C + A_{S1} - A_{S2})) \tag{5.8}$$

When the blocking angle is assumed to be distributed on $\theta \in [0, \pi)$, the HO probability is given by:

$$\mathbb{P}[HO|r, w] = 1 - \int_0^{\pi} f_\theta(\theta) exp(-\lambda(A_R - A_C + A_{S1} - A_{S2}))d\theta \tag{5.9}$$

Where: $f_\theta(\theta)$ is probability distribution function of the angle $\theta\epsilon[0, \theta_{max})$ and it is given by: $f_\theta(\theta)=\frac{1}{\theta_{max}}$

Furthermore, when the MU is moving in a uniform direction such that the tagged mm-wave BS is not lying in the blocking zone and the direction of the center of the blocking angle is identical to that of the direction of the displacement of the MU. Therefore, the HO rate is given by:

$$\mathbb{P}[HO|r] = 1 - \int_0^{\pi} \int_0^{\pi - \frac{\theta}{2}} f_\theta(\theta) f_\omega(\omega) exp(-\lambda(A_R - A_C + A_{S1} - A_{S2}))d\omega d\theta \tag{5.10}$$

Where: $f_\omega(\omega)$ is probability distribution function of the angle $\omega\epsilon[0, \pi - \frac{\theta}{2})$ and it is given by: $f_\omega(\omega)= \frac{1}{(\pi - \frac{\theta}{2})}$. Note that because of the symmetry, the HO probability for a MU making a displacement with a direction of $(2\pi - \omega)$ is the same as that for a MU making a displacement with a direction of (ω).

5.1.3 Results and Discussion

The results in figures (5.2) and (5.3) show the self blockage impact on the HO probability for a MU moves in a speed of d per time unit in a direction of ω. In figure (5.2) we assume that the MU is moving in a radial direction with respect to the connection direction, while in figure (5.3) we assume that the MU is moving in a perpendicular direction with respect to the connection direction. It can be noticed that the self blockage has an impact on HO probability, especially when the MU is moving in a radial direction. As the direction of the MU becomes closer to the tagged mm-wave BS as the difference of the HO probability getting lower.

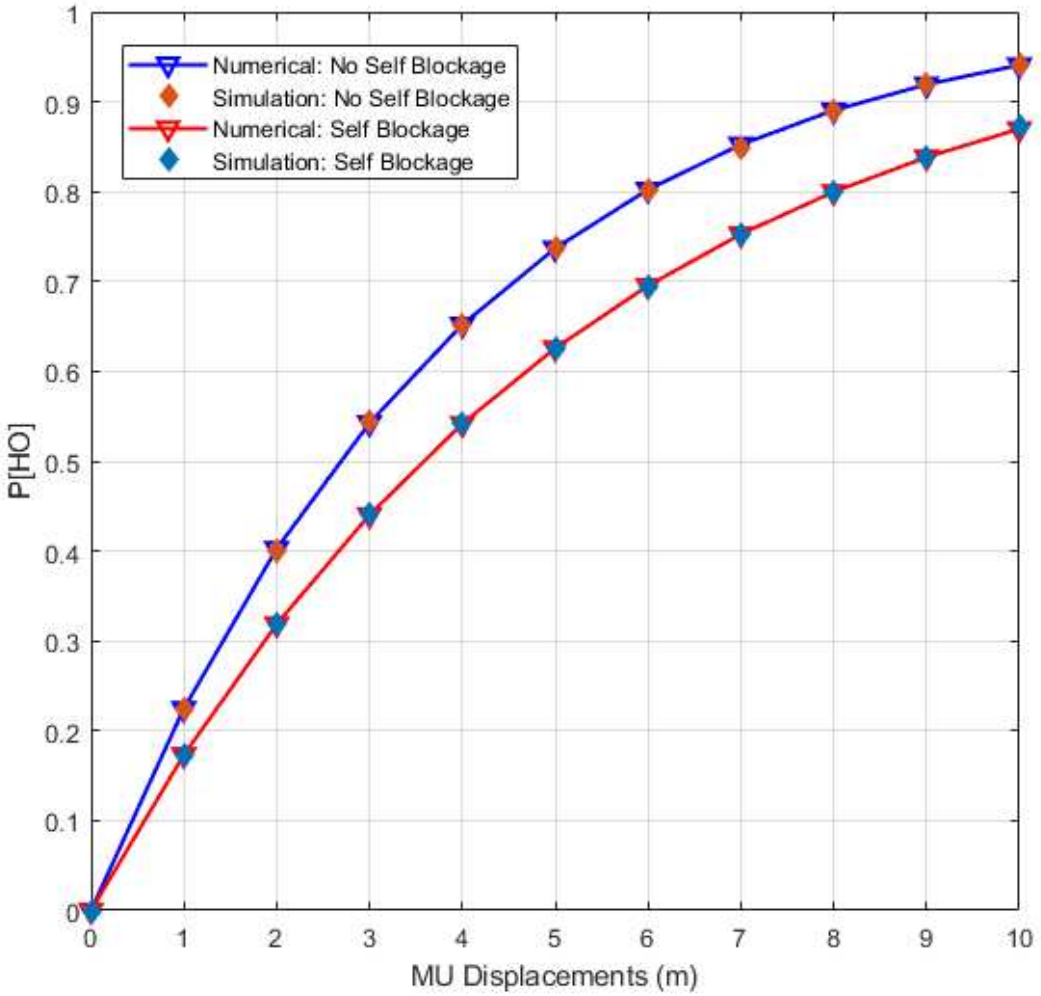

Figure 5.2: Self blockage impact on HO probability for a MU moving in a radial direction.

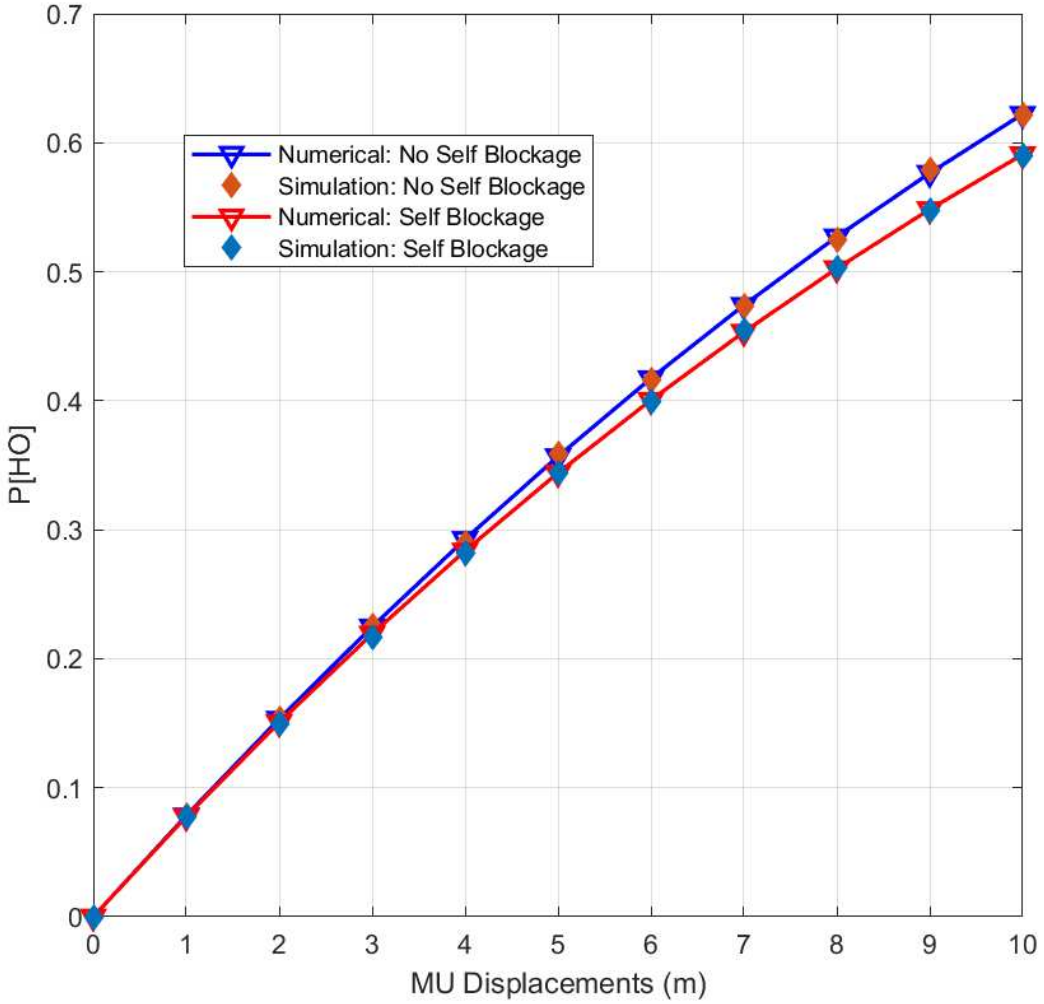

Figure 5.3: Self blockage impact on HO probability for a MU is moving in a perpendicular direction.

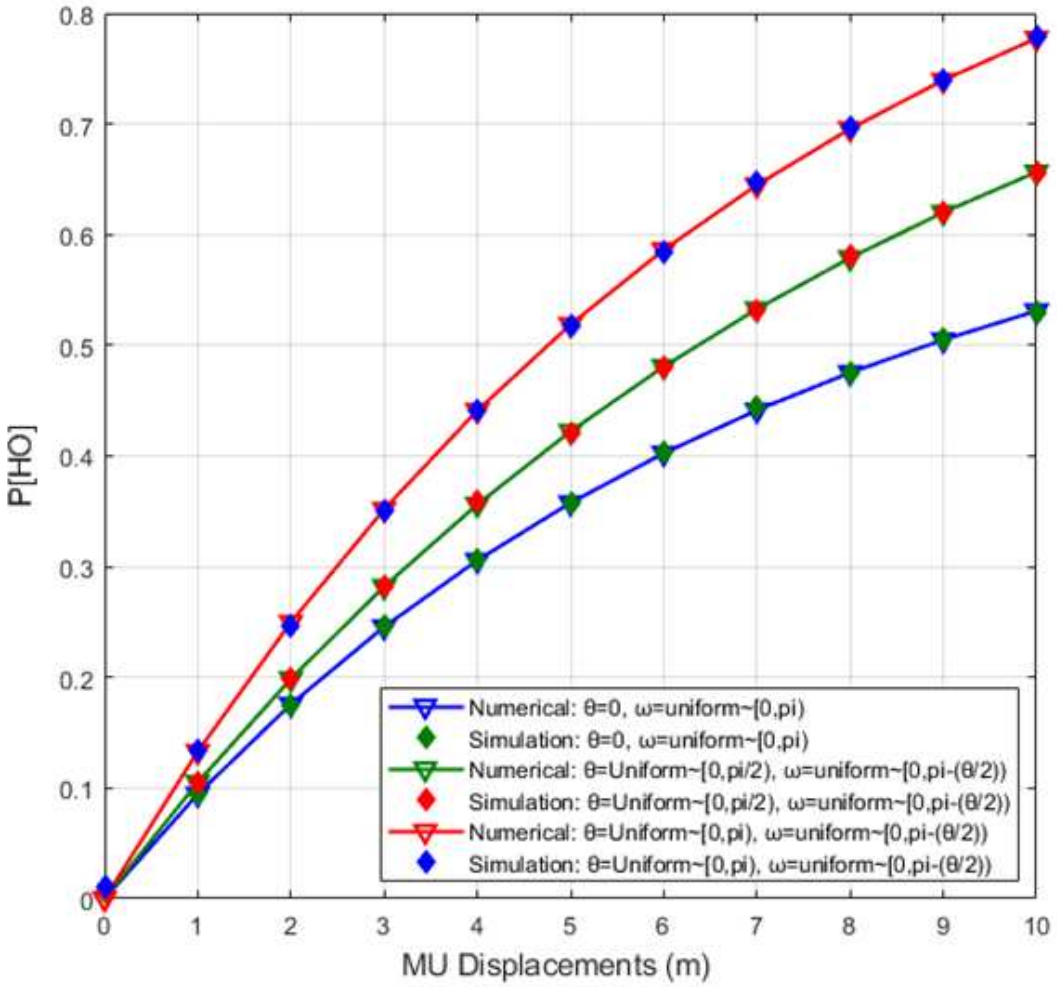

Figure 5.4: Self blockage impact on HO probability for a MU is moving in a uniform direction and different uniform distributions of the blocking angle.

On the other hand, figure (5.4) shows the result of self blockage impact on HO probability for a MU moving in a uniform direction with respect to the connection direction. In this particular result we assume that the blocking angle, θ has a uniform distribution, $\theta\epsilon[0, \pi)$. Therefore, to keep the tagged mm-wave BS LOS, we assume that the MU is moving in a uniform direction such that the maximum angle of ω is distributed in the range of $\omega\epsilon[0, \pi - \frac{\theta}{2})$. As illustrated in figure (5.4), as the blocking angle θ increases as the HO rate increases as well.

5.2 Impact of Dynamic Blockage on Blocking Probability

5.2.1 Introduction

This subsection aims to analyze the impact of dynamic blockages on blocking probability for a MU with mobility in 5G mm-wave cellular network, and to evaluate the overall performance of mm-wave cellular network. The quality of the connections in mm-wave systems depends mainly on the presence of the LOS link between the mm-wave BS and the MU with the presence of dynamic objects, such as human bodies, vehicles, etc. As a result, the continuity of the connections without interruptions due to dynamic blockages is diminishing.

Understanding blockages' impact on the system performance is particularly crucial for establishing reliable connections between the system entities. Therefore, there is a need to understand the effect of dynamic blockages on the performance of the system in mm-wave cellular network.

5.2.2 System Model and Problem Formulation

Consider a MU moves at a constant velocity of V_M per time unit, from position P_1 to P_2, with a direction of ω and consider dynamic blockages in the region distributed in the disc B(o,R) according to a homogeneous PPP with density λ_b, make displacements with a constant distance of V_B per time unit, in a random direction at angle of θ_b relative to the positive x-axis, as show in figure (5.5). The 2D distance between the BS_t to the MU at P_1 is r and the 2D distance between the BS_t to MU at P_2 is R, and the LOS link makes

an angle φ from the positive x−axis in the $\mathbb{R}^2$ plane, where θ_b is distributed uniformly in $[0,\ 2\pi]$.

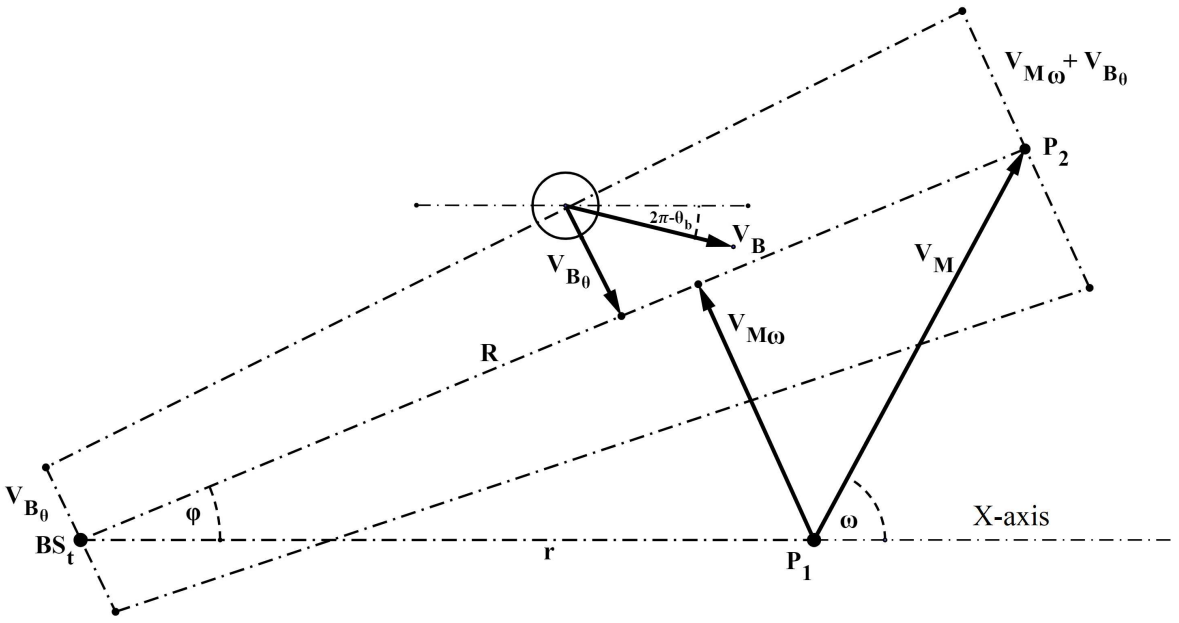

Figure 5.5: System model of dynamic blockage.

The arrival process of the blockages crossing the BS-MU link is Poisson with intensity α. The blockage duration is independent of the blockages arrival process and is exponentially distributed with mean $\frac{1}{\mu}$. Therefore, the blocking event follows an exponential on-off process with α and μ being the blocking and unblocking rates, respectively.

The probability of blockage $\mathbb{P}_d$ of the $BS_t - P_2$ link due to dynamic blockages can therefore be expressed as follows:

$$\mathbb{P}_d = \frac{\frac{1}{\mu}}{\frac{1}{\alpha} + \frac{1}{\mu}} = \frac{\alpha}{\alpha + \mu} \tag{5.11}$$

The component of the MU's displacement of time unit perpendicular to the $BS_t - P_2$ link is $V_{M_\omega} = r\ sin(\varphi)$, where, $\varphi = tan^{-1}\left[\frac{d\ sin(\omega)}{r\ +\ d\ cos(\omega)}\right]$, and the component of the blockage's displacement of time unit perpendicular to the $BS_t - P_2$ link is $V_{B_\theta} = V_B\ cos((\frac{\pi}{2}) - (\varphi + \theta_b)) = V_B\ sin(\varphi - \theta_b)$.

Considering a polygon area that has a width in one side of $V_{B_\theta}\Delta t$ and the other side

is $(V_{M_\omega} + V_{B_\theta})\Delta t$. The blockages in this area will block the LOS link over the interval of time Δt. Note that there are two areas of the two sides of the link. Therefore, the average frequency of blockageA_v in the two sides is given by:

$$A_v = \lambda_b R(V_{M_\omega} + 2\ V_{B_\theta})\Delta t \tag{5.12}$$

Where R is the distance between the BS_t and the MU at location P_2, and it is given by:

$$R = \sqrt{r^2 + V_M^2 + 2\ V_M\ r\ cos(\omega)} \tag{5.13}$$

Thus, the frequency of blockage per unit time A_{v_t} is given by:

$$A_{v_t} = \lambda_b\ R\ (V_{M_\omega} + 2\ V_{B_\theta}) \tag{5.14}$$

$$A_{v_t} = \lambda_b R\ \ (r\ sin(\varphi) + 2\ V_B\ sin(\varphi - \theta_b)) \tag{5.15}$$

Taking an average over the uniform distribution of θ_b (uniform over $[0,\ 2\pi]$), we get the blockage rate α as follows:

$$\alpha = \lambda_b\ R\ \int_{\varphi-\pi}^{\varphi} \ (r\ sin(\varphi)\ + 2\ V_B\ sin(\varphi - \theta_b))\ d\theta_b \tag{5.16}$$

$$\alpha = \lambda_b\ R\ (\pi r sin(\varphi) + 4\ V_B) \tag{5.17}$$

Substituting equation (5.17) in equation (5.11), we get the probability of blockage due to dynamic blockages:

$$\mathbb{P}_d = \frac{\lambda_b\ R\ (\pi r sin(\varphi) + 4\ V_B)}{\lambda_b\ R\ (\pi r sin(\varphi) + 4\ V_B) + \mu} \tag{5.18}$$

$$\mathbb{P}_d = 1 - \frac{\mu}{\mu + \lambda_b \; R \; (\pi r sin(\varphi) + 4 \; V_B)} \tag{5.19}$$

5.2.3 Results and Discussion

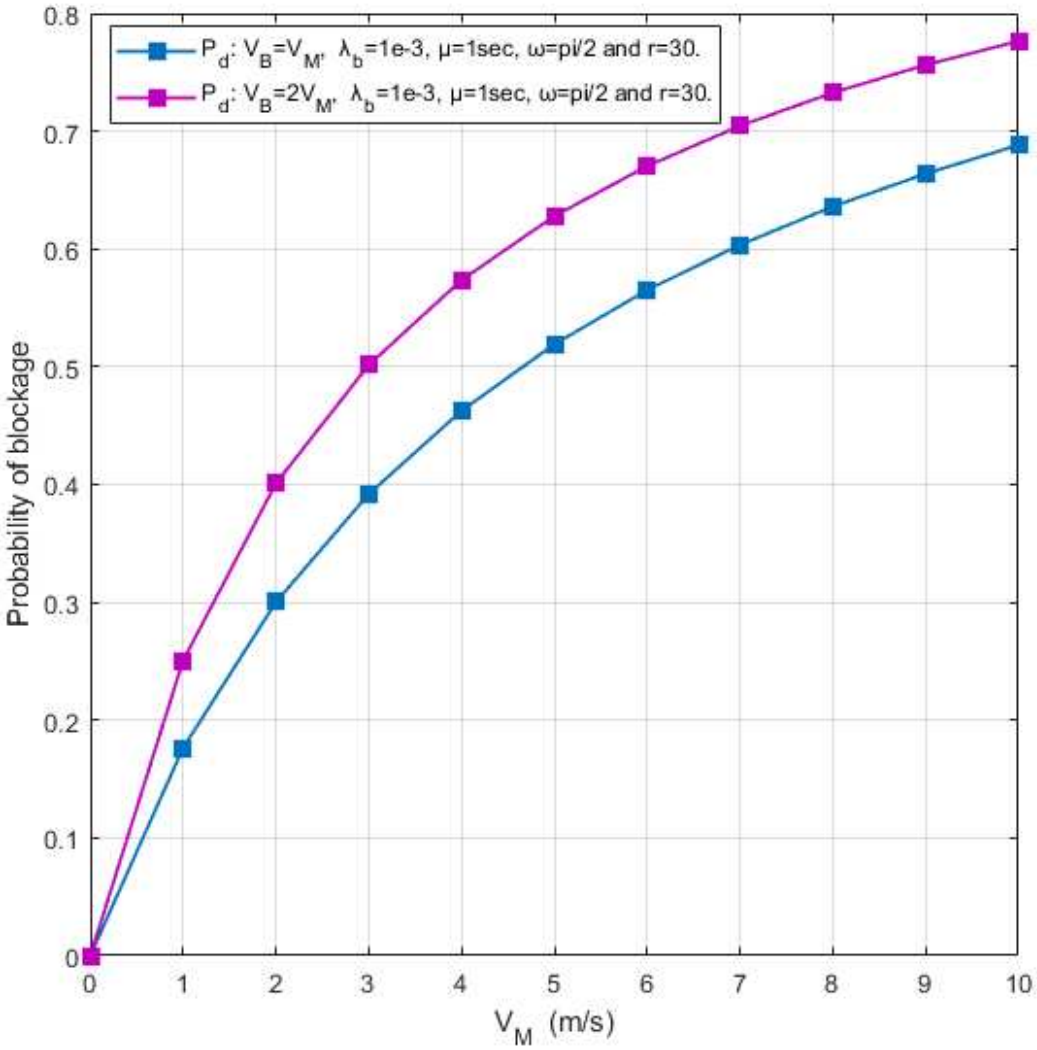

Figure 5.6: Probability of blockage, $\mathbb{P}_d$, with different blockages' speed.

In this Section, we evaluate the impact of mobile blockages such as human bodies and vehicles on the direct LOS mm-wave BS-MU link. We consider the link available if any dynamic blockage does not permanently block it. Otherwise, it is considered blocked. We evaluate the impact of blockage speed and density on the blocking probability of the direct

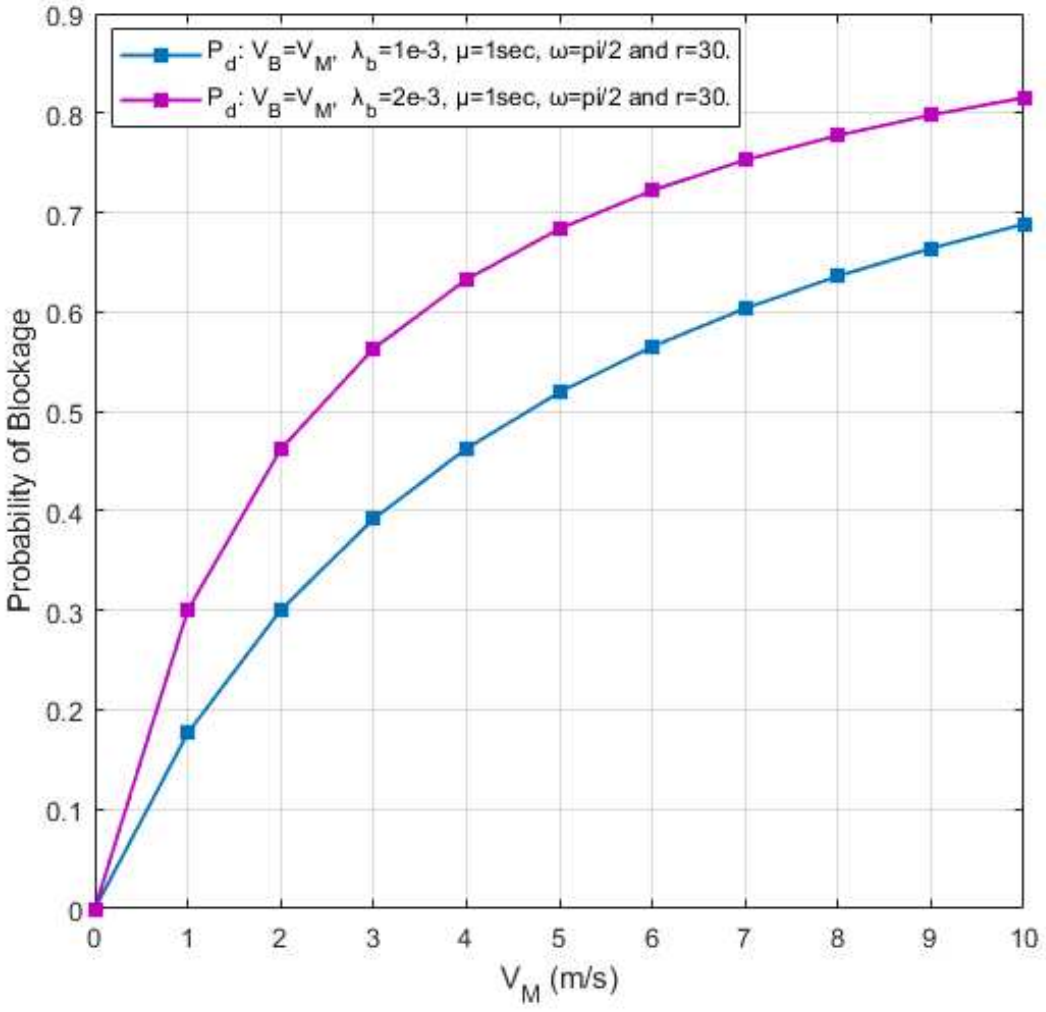

Figure 5.7: Probability of blockage, $\mathbb{P}_d$, with different density of blockages.

LOS mm-wave BS-MU link. We compare the blocking probability results with different velocities of dynamic blockages and MU. The result in figure (5.6) shows the blocking probability, $\mathbb{P}_d$, with different velocities of the blockages. It can be noticed clearly that the blocking probability gets higher when the blockages are moving at a higher velocity. That can be interpreted as, The higher speed of blockages, the higher likelihood of having the link between the mm-wave BS and the MU blocked. The result in figure (5.7) shows the impact of the density of blockages on the blocking probability of the link between the mm-wave BS and the MU. The higher density of dynamic blockages results in a higher blocking probability of the link between the mm-wave BS and the MU.

In conclusion, dynamic blockages have a remarkable impact on the LOS link between the mm-wave BS and the MU. That results in a higher probability of blocking the LOS link for a period of time while the blockage crosses the link, which could cause an increase of the HO probability and the ping-pong effect. Therefore, the impact of dynamic blockages needs to be considered carefully in designing the mm-wave cellular systems.

Chapter 6
Impact of Blockages on Resource Allocation in Mm-Wave Cellular Systems

6.1 Introduction

The use of mm-wave bands has been identified as a promising candidate for the 5^{th} generation of wireless cellular systems to ensure the best efforts of delivering peak and high data rates and to meet the massive demand of the future capacity. Challenge facing mm-wave cellular systems could cause significant degradation of system performance due to interruptions by blockages, such as human bodies or vehicles. Service disconnection resulting from blockage interruptions could cause frequent HOs for the MU in a short time. However, the propagation characteristics in the mm-wave band are more challenging than in traditional cellular networks. In urban mm-wave cellular networks, especially when the cell size becomes relatively small, the HO procedure has a significant impact on system performance, and because of the blockage interruptions, the MU may switch from a given cell to any adjacent cell multiple times during the lifetime of a particular call or data session. Therefore, from the network perspective, the service provider must consider the rate at which ongoing calls arrive from neighboring cells and the arrival rate of new calls. The probability of initiating calls and the probability of forced termination of ongoing calls are the primary criteria for the performance of the cellular network.

One of the most important concerns for an MU is that service is not to be terminated during an ongoing call, and priority is to be given to HO requests than the originating calls. Several traffic models have been proposed based on different assumptions for an MU with mobility in order to find out the arrival rate of originating calls and HO calls. In 5G mm-wave cellular systems, the blockage impact must be considered in designing such models. However, we focus our attention on the HO schemes in single traffic systems where the priority is given to HO requests by assigning K channels exclusively for HO calls among the M channels in a cell. In this case, K is the number of reserved channels [44]. Severe path attenuation and vulnerability to LOS blockage in mm-wave cellular systems result in a much more unpredictable number of HOs than in traditional cellular systems. In addition to that, the small cell size in mm-wave cellular systems contributes to increasing the HO rate, especially for users with high speed of mobility. As a result, the number, K, of channels assigned exclusively for HO calls among the M channels needs to be adjusted accordingly and adopted according to some metrics, such as blockages size,

the speed, and direction of blockages, etc. That is to maintain the QoS requirement.

In this chapter, we address the problem of HO requests in mm-wave cellular systems. We apply a classical HO scheme based on the HO priority strategy in the mm-wave cellular system. That shows how blockages affect resource allocation in the mm-wave cellular system. We show how adjusting the number of reserved channels, K, that are reserved solely for the HO requests can minimize the blocking probability of HO requests and satisfy the minimum requirements of QoS of the system overall.

6.2 System Model and Problem Formulation

We consider the HO priority scheme, similar to [45] and [46], where the priority is given to HO requests by assigning K channels exclusively for HO calls among the M available channels in the cell. In this scheme, we adjust the number of reserved channels, K, for HO requests according to some metrics associated with blocking probability studied in previous chapters. Metrics such as density and size of blockages, blockage duration, the MU speed, etc. We consider the performance model of a single cell in an mm-wave cellular wireless communication network, where an MU moves across the cell boundary. The channel in the old mm-wave BS is released, and an idle channel is required in the new mm-wave BS. In some soft HO systems, an MU may establish more than one radio link at the same time. Thus, within the overlay area of cells, an MU can connect to multiple BSs simultaneously. As a result, more free channels are required for HO calls in each cell. One of the most important MU's concerns is that service not be terminated during an ongoing call or data session. Therefore, we aim to prioritize HO requests over the originating requests. For this propose, we consider the approach that guarantees the availability of a free channel when a HO call arrives by dedicating an adjustable number, K, of channels in each cell exclusively for HO calls as shown in figure (6.1).

6.3 Performance Analysis of HO Scheme

In order to analyze the performance of the HO scheme, the QoS measures that we are interested in are:

P_{Nb}: the steady state probability of blocking a new calls; and

P_{Hb}: the steady state probability of blocking a HO calls.

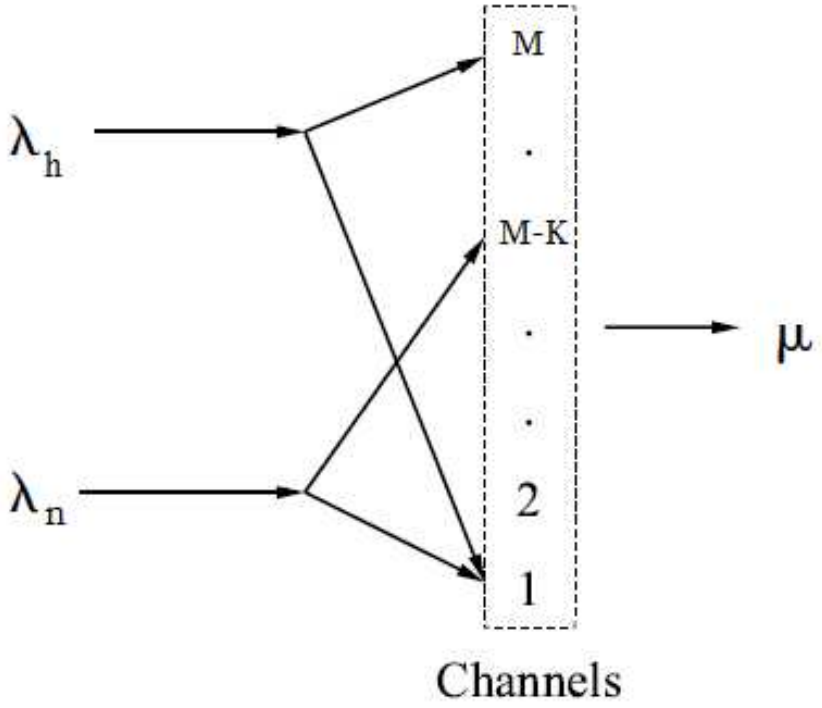

Figure 6.1: System model with priority for HO call.

Consider an mm-wave cellular system with many cells, each having M channels, and at any given time unit some of them will be in use. We assume a homogeneous system, and all cells are identical, and we focus our attention on a single cell. We assume only two sources of new calls arriving into the cell: either a call that was accepted in previous time by the network and that is now being handed over from a neighbour cell, or a new call that has just been accepted by the cell.

Assume that the arrival process of new calls in a cell is Poisson with rate of λ_n, and λ_h be the rate of HO arrivals. Let μ_c be the rate at which an ongoing call (new or HO) completes service and let μ_h be the rate at which the MU engaged in the call departs the cell. The channel holding time has an exponential distribution with mean rate $\mu = \mu_c + \mu_h$. Since there are a total of M channels in each cell, K of them is reserved for the HO calls, thus when a HO call arrives, and at least one idle channel is available, it will be accepted, and the channel will be assigned to it. Otherwise, the HO call is blocked. The new call is accepted only if at least one channel is available among (M-K) channels. Otherwise,

the new call is blocked. Where K is the number of reserved channels. We assume that the number of reserved channels, K, is adjustable between [0 and M] and assigned such that the probability of blocking a HO call is less than or equals to a certain threshold T that satisfies the required QoS. The remaining (M-K) channels are shared by both new calls and HO requests, as shown in figure (6.2). Note that a new call request is blocked if the number of available channels in the cell is less than or equal to K, and a HO request is only blocked if no channel is available in the cell. That always gives priority to HO requests.

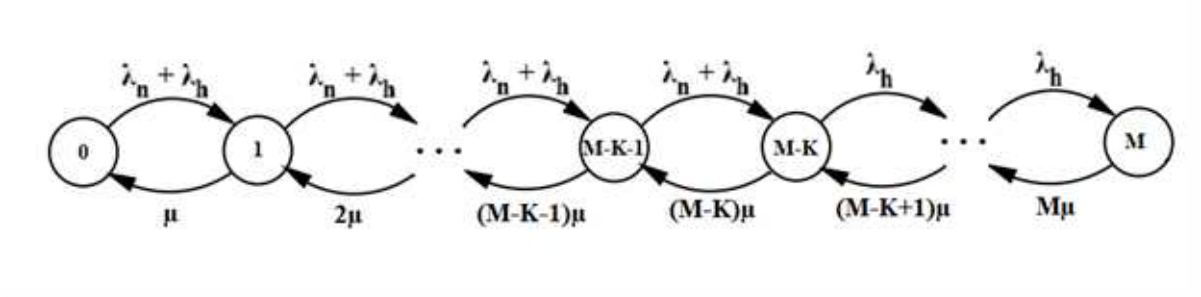

Figure 6.2: The state transition diagram of the Markov Chain for the proposed scheme.

Let's define the state i, (i = 0,1,...,M), as the number of busy channels in the mm-wave BS of the target cell at time t. While P(i) represents the the steady state probability that the mm-wave BS of the target cell is in state i. It is apparent from the above assumptions that i is a one-dimensional Markov chain, which can be determined in the usual way for birth–death processes as shown in figure (6.2). Equilibrium probabilities, P(i), are related to each other through the following state balance equations:

$$\begin{cases} i\mu P(i) = (\lambda_n + \lambda_h)P(i-1) & 0 \leqslant i \leqslant M-K \\ i\mu P(i) = \lambda_h P(i-1) & M-K \leqslant i \leqslant M \end{cases} \tag{6.1}$$

Using equation (6.1) recursively, along with the normalization condition:

$$\sum_{i=0}^{M} P(i) = 1 \tag{6.2}$$

the steady state probability P(i) is given as follows:

$$P(i) = \begin{cases} \frac{(\lambda_n+\lambda_h)^i}{i!\mu^i} P(0) \\ \frac{(\lambda_n+\lambda_h)^{M-K}\lambda_h^{i-(M-K)}}{i!\mu^i} P(0) \end{cases} \tag{6.3}$$

Where, P(0), is given by:

$$P(0) = \left[\sum_{i=0}^{M-K} \frac{(\lambda_n + \lambda_h)^i}{i!\mu^i} + \sum_{i=M-K+1}^{M} \frac{(\lambda_n + \lambda_h)^{M-K} \lambda_h^{i-(M-K)}}{i!\mu^i} \right]^{-1} \tag{6.4}$$

The blocking probability, P_{Hb}, of a HO request is given by:

$$P_{Hb} = P(M) = \frac{(\lambda_n + \lambda_h)^{M-K} \lambda_h^K}{M!\mu^M} P(0) \tag{6.5}$$

The blocking probability, P_{Nb}, for an originating call is given by:

$$P_{Nb} = \sum_{i=M-K}^{M} P(i) \tag{6.6}$$

Note that a blocked HO request call can maintain communication via current mm-wave BS until the received signal strength becomes less than the receiver threshold or the call is terminated before the received signal strength becomes lower than the receiver threshold. However, in this scheme, we aim to prioritize HO requests. Therefore, we adjust the number of reserved channels, K, such that the blocking probability, P_{Hb}, of a HO request is maintained below a certain threshold T. Figure (6.3) shows the flow chart of the mechanism for reserving channels in the HO scheme.

For simplicity, the priority HO scheme can be summarized in the following steps:

1. Initialization: Set $K_n = K_{min}$ as the initial value for the minimum reserved channels in the cell.
2. Solve for P(i) using the Markov Chain in figure (6.2).
3. Using equation (6.5), check if the blocking probability of HO requests is less than or equals the threshold ($P_{Hb} \leqslant T$), then go to step 6. Otherwise, go to step 4.
4. If the blocking probability of HO requests is greater than the threshold ($P_{Hb} > T$), set ($K_n = K_n + 1$).

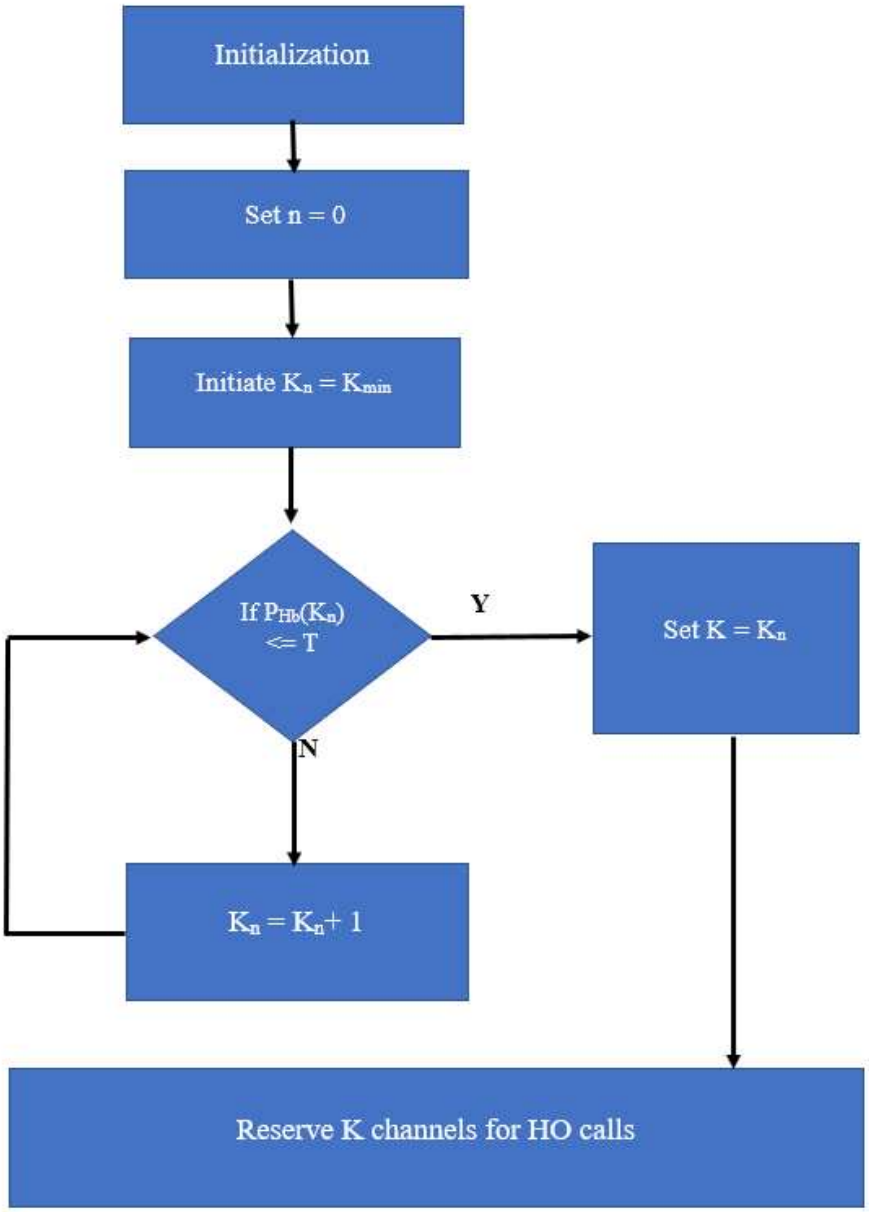

Figure 6.3: Flow chart of the mechanism of reserving channels in the HO scheme.

5. Repeat step 3 until the condition, ($P_{Hb} \leqslant T$), satisfies.
6. Set $K = K_n$ as the number of reserved channels for HO request.

6.4 Performance Evaluation and Discussion

In this section, we present and discuss our analytical results, where the results of the HO scheme are compared with the system performance results using the traditional channel reservation scheme. To obtain the analytical results, we use a single cell model where the number of reserved channels, K, in the target cell is adjusted such that the threshold of the blocking probability of HO calls is satisfied. In the previous chapters, we show that different types of blockages have a remarkable impact on the HO probability. Therefore, we consider the impact of the blockages in our HO scheme such that the number of reserved channels, K, is adjusted according to the variation of the HO requests.

We use the results of HO probability that obtained from the previous chapters, and we assume that the arrival rate of HO calls in each cell is given as follows:

$$\lambda_h = N_M \; P[HO]/N_{BS}/\Delta t \tag{6.7}$$

Where:
N_M: is the number of MUs in area of interest.

$P[HO]$: is the probability of HO for a MU.

N_{BS}: is the number of mm-wave BSs in area of interest.

Δt: is the time unit in which the MU makes a displacement.

From equation (6.7), it is clear that the arrival rate of HO calls in each cell is directly proportional to the HO probability for a MU. Therefore, the HO arrival rate in each cell rises as the HO probability rises as well. Using the results obtained in chapter 4, figure (4.11), where the HO probability is variant with the variation of the blockage lengths, we show the change in the arrival rate of HO calls in each cell. If we assume the following parameters in our area of interest: $N_M = 3000$ MUs, $N_{BS} = 100$ mm-wave BS and Δt =1

unit time. If no blockages are incorporated in the system, and MU makes a displacement of 5m, the $P[HO] = 0.42$. Whereas in the case blockages are incorporated in the system with an average length of 6m, the $P[HO] = 0.85$, and using equation (6.7), the arrival rate of HO calls in each cell is 12.6 and 25.5 respectively. That is an increase of the double, which can be interpreted that the blockages have a significant impact on the arrival rate of HO calls. That depends mainly on the blockages' related parameters, such as blockages length, speed and density, as well as other parameters such as the MU' speed, and the distance between the MU and mm-wave BS.

6.4.1 Numerical Results

In the previous section, we show how blockages affect the arrival rate of HO calls. The arrival rate of HO calls is proportional to HO probability and consequently to the blockages' related metrics, such as; the density and size of blockages and the MU's speed, etc. Our main concern is to prioritize HO calls rather than originating calls. For this purpose, we applied a standard HO priority scheme to show the impact of blockages on resource allocation in the mm-wave cellular network. Therefore, we adjust the number of reserved channels in order to minimize the blocking probability of HO calls.

The results in figure (6.4) show the blocking probability of HO call with different numbers of reserved channels, K, when the arrival rate of HO call equals the arrival rate of new calls. It can be concluded that by increasing the reserved channels, K would decrease the blocking probability of HO calls. As a result, the number of reserved channels needs to be adjusted according to the arrival rate of HO calls, which mainly depends on the parameters related to the HO probability, such as blockages density, size, speed, etc.

The results in figure (6.5) show the blocking probability of HO calls, P_{Hb}, with different number of reserved channels,K, and different ratio between the arrival rate of HO calls and the arrival rate of new calls to the target mm-wave BS, while figure (6.6) shows the blocking probability of HO calls, P_{Hb}, with different values of arrival rate of new calls, λ_n, and different ratio between the arrival rate of HO calls and the arrival rate of new calls to the target mm-wave BS. Figure (6.7) shows the blocking probability of originating calls, P_{Nb}, with different values of the arrival rate of originating calls in the target mm-wave BS, λ_n, and fixed number of reserved channels, K = 5. As the arrival rate of the HO calls

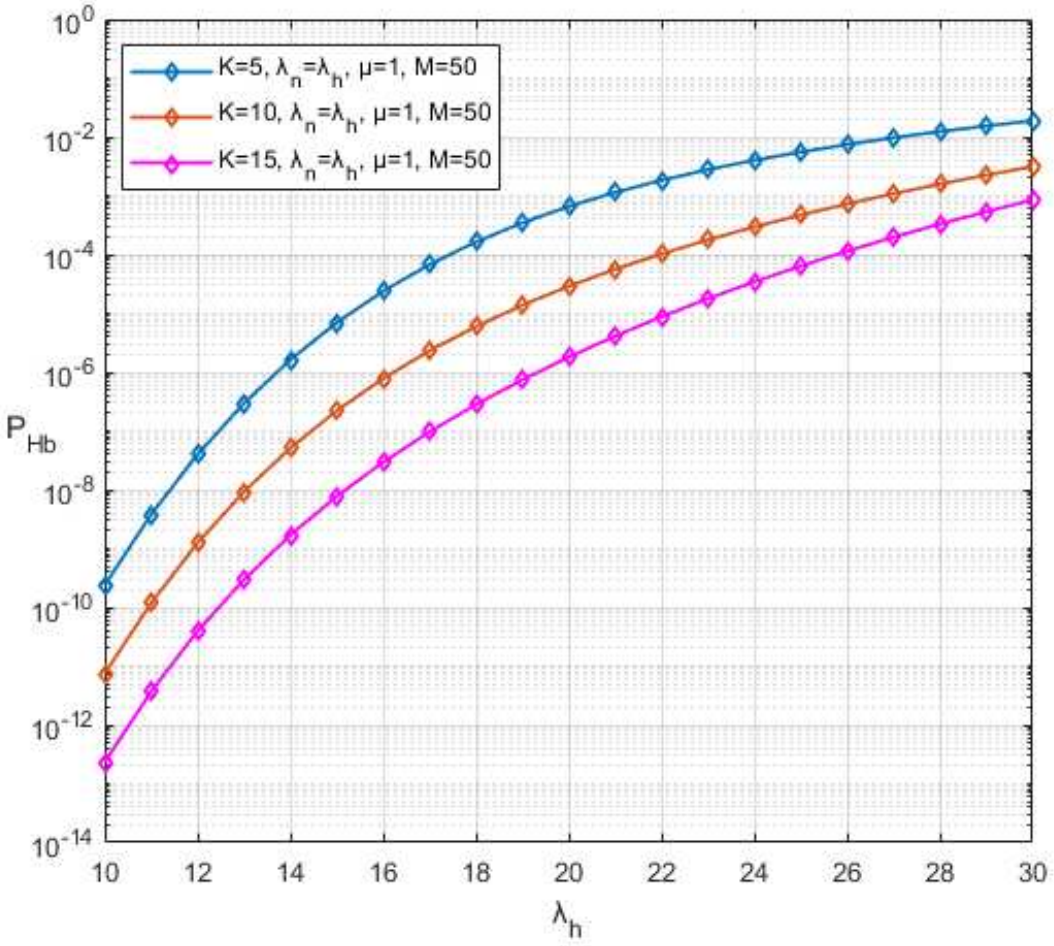

Figure 6.4: Blocking probability of HO calls with different values of λ_h.

gets lower compared to the arrival rate of new calls, the blocking probability of originating calls , P_{Nb}, gets lower as well.

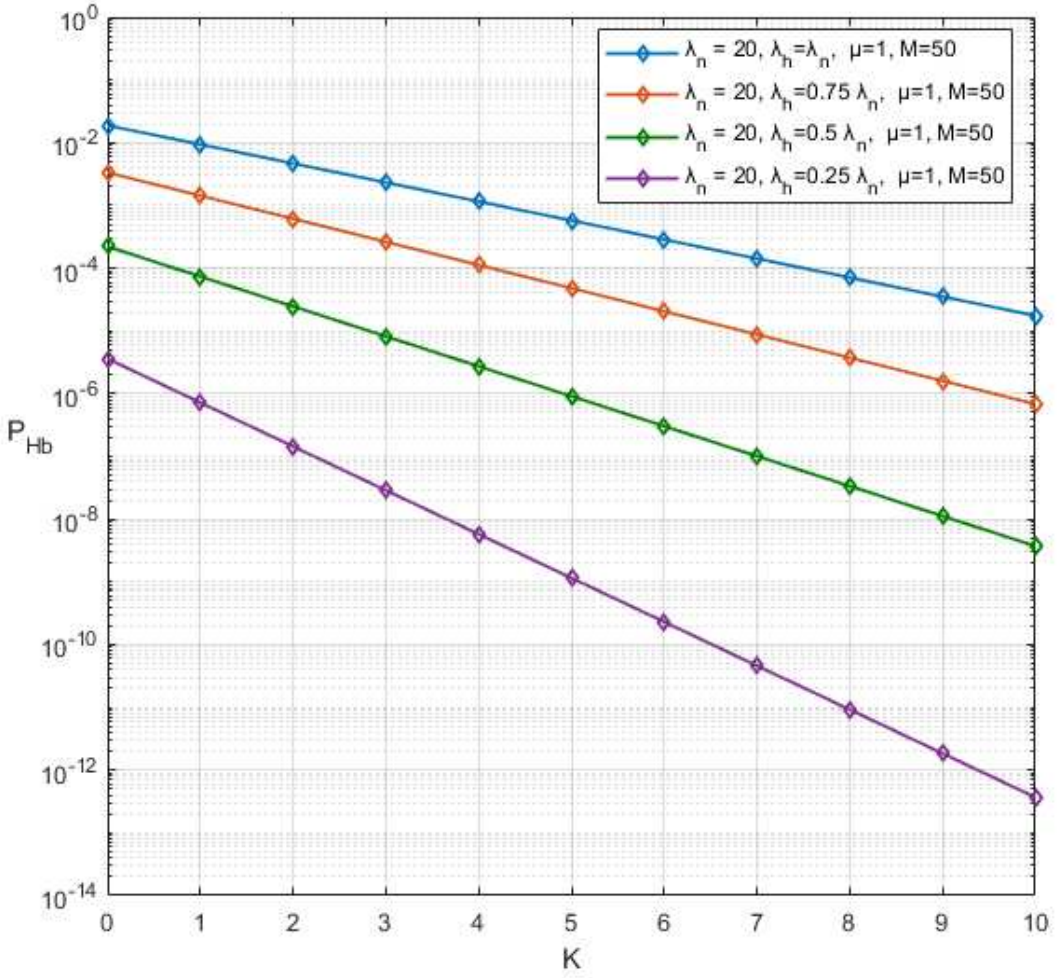

Figure 6.5: Blocking probability of HO calls with different values of K.

From the above results, it can be observed that adjusting the number of reserved channels, K, according to the required threshold of the blocking probability of HO calls, P_{Hb}, would satisfy and guarantee the QoS requirements. For this purpose, we adjust the number of reserved channels, K, such that the blocking probability of HO calls, P_{Hb}, is always maintained under some threshold T. That can be done by following the steps in the flow chart in figure (6.3).

The results in figure (6.8) show the blocking probability of HO calls, P_{Hb}, is maintained under the threshold (T), while the results in figure (6.9) show the required reserved

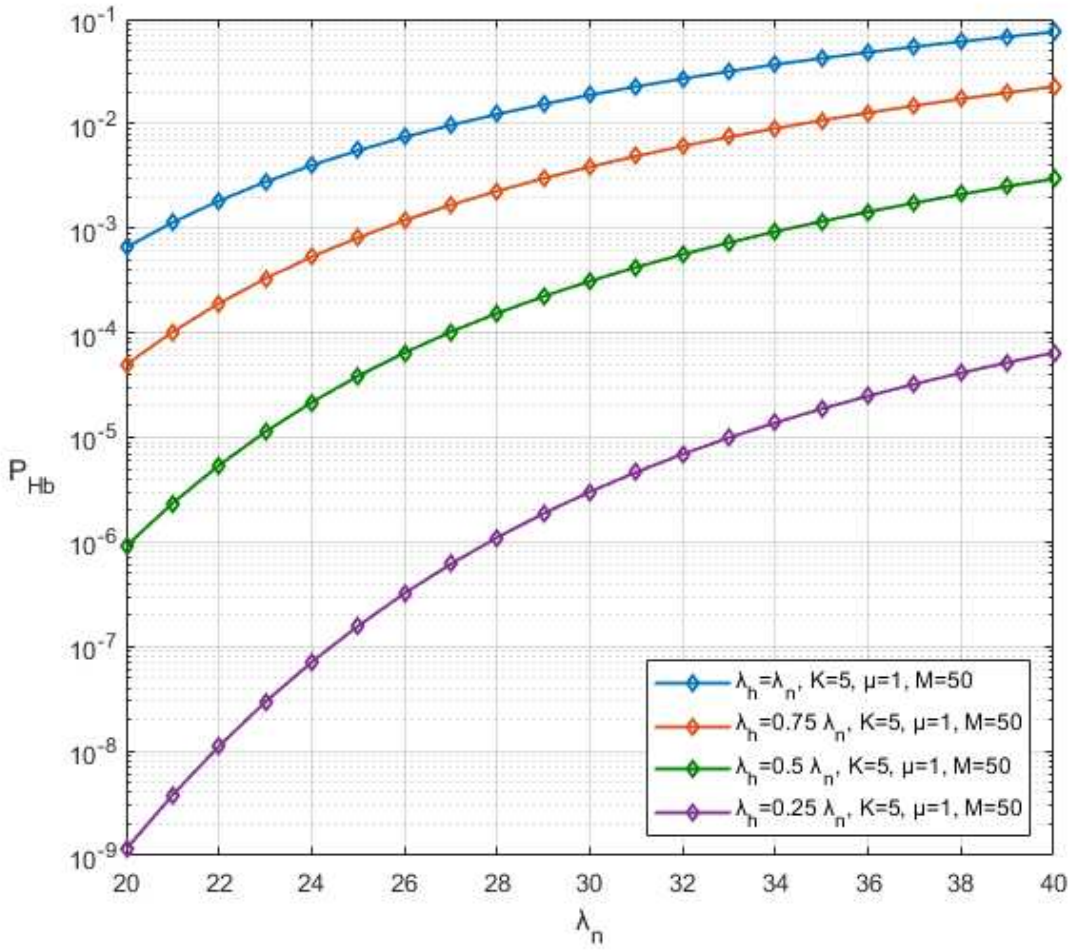

Figure 6.6: Blocking probability of HO calls with different values of λ_n.

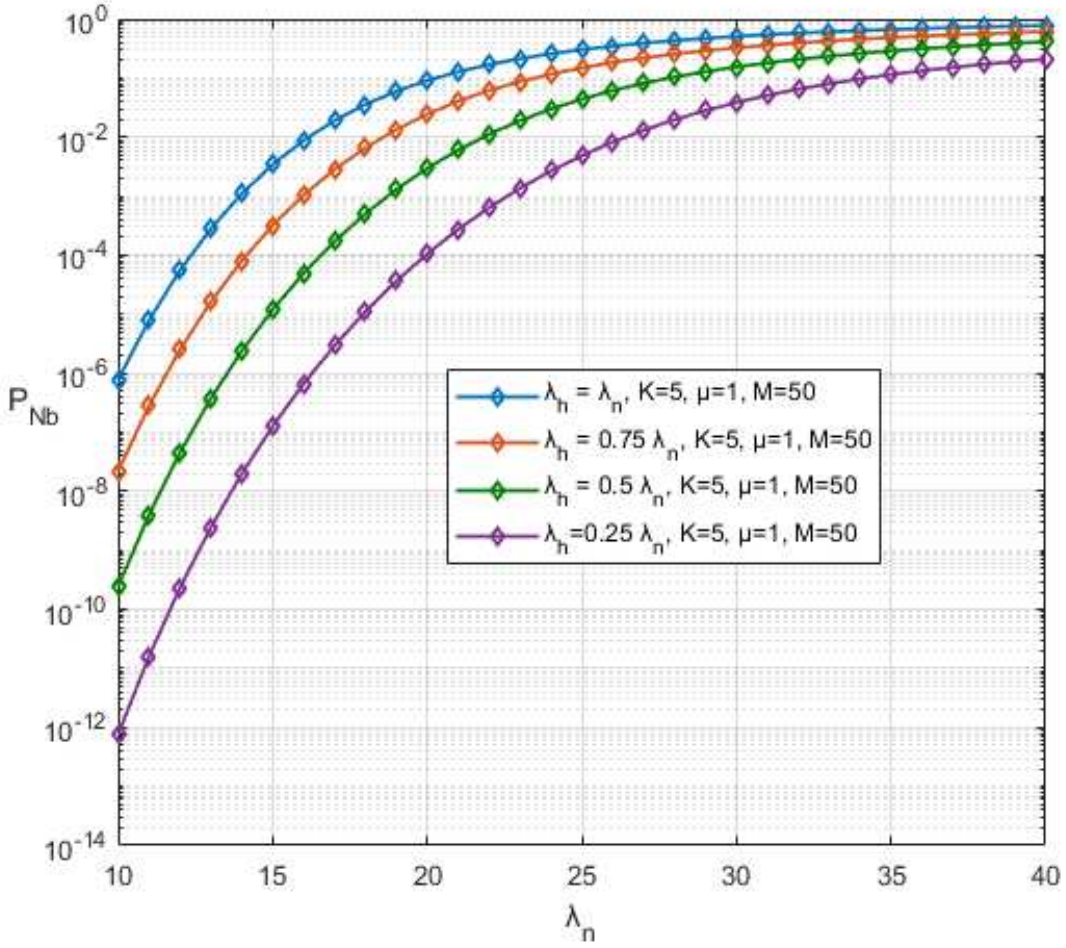

Figure 6.7: Blocking probability of originating calls with different values of λ_n.

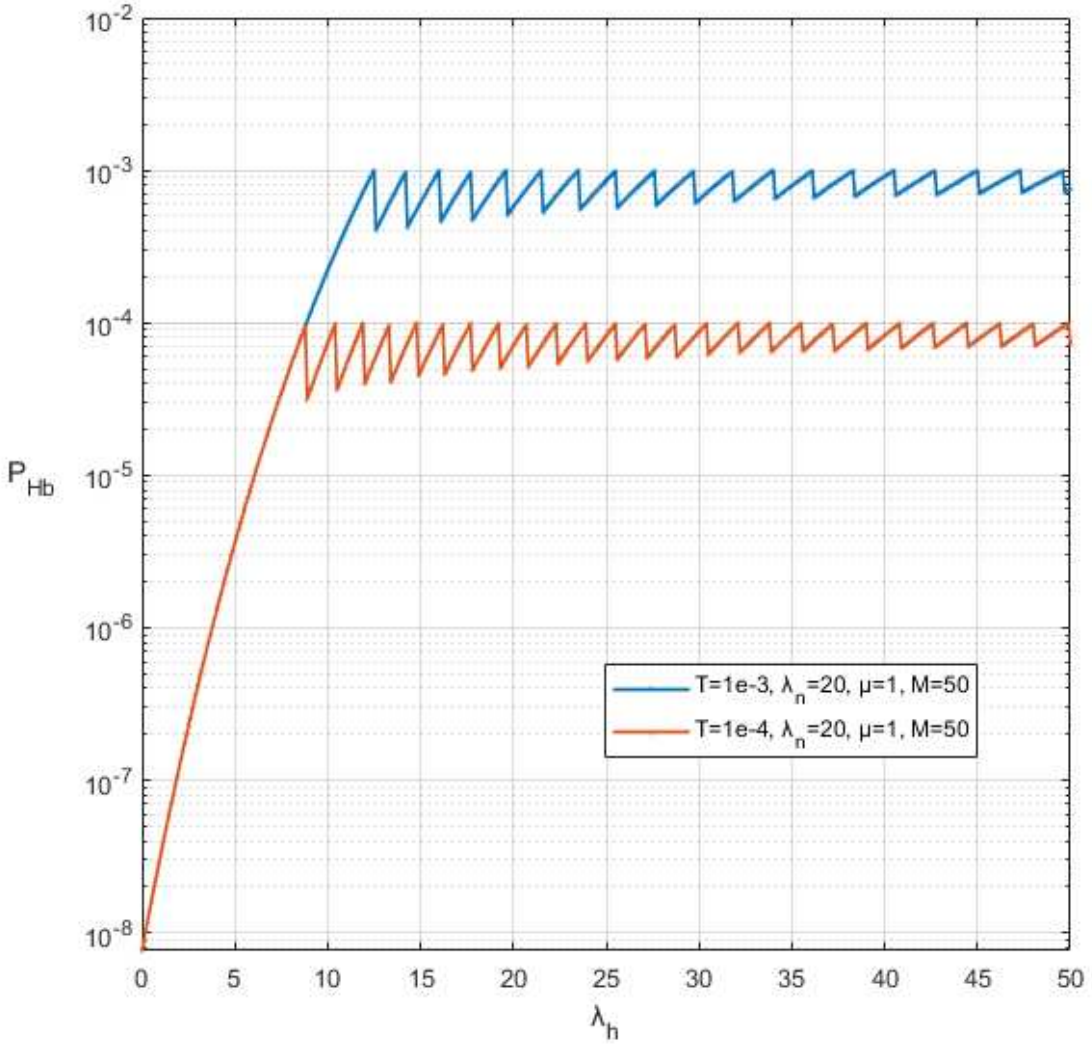

Figure 6.8: Blocking probability of HO calls with different values of λ_h.

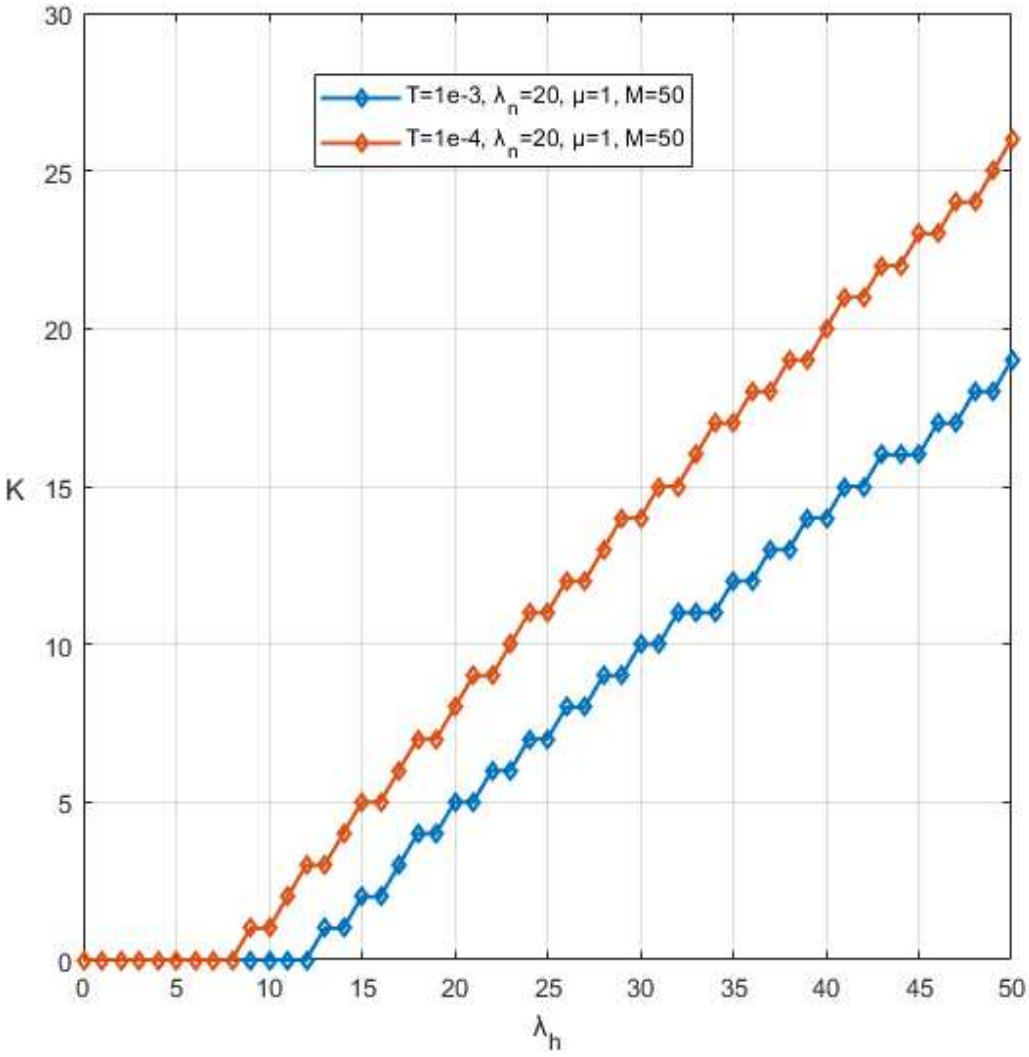

Figure 6.9: The number of reserved channels, K, required to satisfy the threshold, T, with different values of λ_h.

channels to satisfy the required threshold T. We assume two thresholds, T = 1e-3 and T = 1e-4. It can be observed that the required number of reserved channels, K, is getting higher as the threshold T gets lower. The lower the blocking probability of HO call, the higher the number of reserved channels is required. For instance, when the arrival rate of HO calls is 50, it is required 26 reserved channels to satisfy the threshold (T=1e-4), while it is required 18 reserved channels to satisfy the threshold (T=1e-3). Increasing the number of reserved channels would be at the expense of lowering the channels for the originating calls in the target mm-wave cell. That would increase the blocking probability of originating calls. Therefore, a balanced scheme between the admission of HO calls and new calls in an mm-wave cell is required, and we left that for future work.

Chapter 7
Conclusion and Future Work

Conclusion and Future Work

This chapter includes a summary of the work carried out toward the Ph.D thesis, and discusses future works.

7.1 Conclusion

In this thesis, we studied the impact of different types of blockages on the performance of mm-wave cellular networks. Specifically, we focus on the impact of the blockages on the HO probability in mm-wave cellular networks and how that affects the HO calls' blocking probability and the new calls.

We started in chapter 3 by analyzing the impact of a static blockage on the HO probability in the 5G mm-wave cellular system. We began by obtaining the HO probability in the presence of a single static blockage by assuming, first, the MU moving with a certain speed in a radial direction with respect to the direction of the connection, i.e., ($\omega = 0$). Second, the MU is moving in a uniform direction with respect to the direction of the connection, i.e., $\omega \in [0, 2\pi)$. After that, we obtained the HO probability with different densities of mm-wave BSs. We compared our result with the case of no blockages incorporated in the system.

Chapter 4 analyzed the impact of multiple static blockages on the HO probability in the 5G mm-wave cellular system. We consider two cases where the MU is moving in a fixed direction and a uniform direction. The results in both cases show that the blockage impacts the HO probability depending significantly on its location, and the speed and direction of the MU.

Chapter 5 covers the impact of self-blockage on HO probability and the impact of dynamic blockages on blocking probability. The findings show that self-blockage impacts the HO probability depends mainly on the blocking angle, while blocking probability gets higher when dynamic blockages move at a higher speed and density. Since the mm-wave signal is very susceptible to blockage interruption, the work in the previous chapters provides us insights on understanding the effect of different types of blockages on the HO probability. Therefore, the blockage impact on the HO probability needs to be carefully considered in designing efficient HO management schemes and planning the 5G mm-wave cellular system.

In chapter 6, we addressed the problem of HO requests in mm-wave cellular systems. We applied a classical HO priority scheme to show how blockages affect resource allocation in mm-wave cellular systems. We aimed to minimize the blocking probability of HO requests and guarantee the QoS requirement. We adjusted the number of reserved channels that are reserved exclusively for the HO requests, where the threshold of the probability of blocking HO calls is satisfied. The results show that the blocking probability of HO calls gets lower when the number of reserved channels is increased. On the other hand, as the number of reserved channels increased, the blocking probability of originating calls also increased. Therefore, it is required to consider the impact of different types of blockages in designing HO schemes in mm-wave cellular systems, which will enhance the system's overall performance.

7.2 Future Work

The main objective of introducing mm-wave communication in the future generation of cellular systems is to meet the future capacity demands, improve the overall throughput, and guarantee Quality of Service for mobile users. However, several challenges need to be addressed related to the blockages' impact on the performance of the mm-wave cellular systems. Based on our study, there are several interesting new research possibilities which can be summarized as follows:

- The unique propagation characteristics at the mm-wave band may cause more redundant HOs in the mm-wave cellular network. That could bring heavy signaling overhead, low energy efficiency, and increased MU outage probability in the conventional-based HO mechanism. Therefore, a smart HO mechanism is required to mitigate the redundancy of HOs while maintaining user QoS requirements in mm-wave cellular systems.
- One of the most important concerns for a MU is that a service should not be terminated or interrupted during an ongoing call. That can be done but at the expense of increasing the probability of blocking new calls. Therefore, it would be interesting to consider a smart and balanced HO scheme to reduce the blocking probability of both HO calls and the originating calls in a balanced manner.
- Since we considered only one tier mm-wave cellular system in this research, extending these results to a multi-tier cellular system would be interesting.

It would also be interesting to consider the case where the mm-wave BSs are deployed with some relationship to the blockages. For example, small mm-wave BSs could be deployed inside buildings, or they could be deployed on the perimeters of blockages.

- This research assumed uncorrelated and independent blockage events of all the mm-wave BS-MU links. It would be interesting to consider the analysis where one blockage could simultaneously interrupt more than one mm-wave BS.

Bibliography

[1] X. Wang, L. Kong, F. Kong, F. Qiu, M. Xia, S. Arnon, and G. Chen, "Millimeter wave communication: A comprehensive survey," *IEEE Communications Surveys Tutorials*, vol. 20, no. 3, pp. 1616–1653, 2018.

[2] T. S. Rappaport, Y. Xing, G. R. MacCartney, A. F. Molisch, E. Mellios, and J. Zhang, "Overview of millimeter wave communications for fifth-generation (5g) wireless networks—with a focus on propagation models," *IEEE Transactions on Antennas and Propagation*, vol. 65, no. 12, pp. 6213–6230, 2017.

[3] Z. Pi and F. Khan, "An introduction to millimeter-wave mobile broadband systems," *IEEE Communications Magazine*, vol. 49, no. 6, pp. 101–107, 2011.

[4] T. S. Rappaport, S. Sun, R. Mayzus, H. Zhao, Y. Azar, K. Wang, G. N. Wong, J. K. Schulz, M. Samimi, and F. Gutierrez, "Millimeter wave mobile communications for 5g cellular: It will work!" *IEEE Access*, vol. 1, pp. 335–349, 2013.

[5] T. Bai and R. W. Heath, "Coverage and rate analysis for millimeter-wave cellular networks," *IEEE Transactions on Wireless Communications*, vol. 14, no. 2, pp. 1100–1114, 2015.

[6] T. Bai, A. Alkhateeb, and R. W. Heath, "Coverage and capacity of millimeter-wave cellular networks," *IEEE Communications Magazine*, vol. 52, no. 9, pp. 70–77, 2014.

[7] U. T. Virk and K. Haneda, "Modeling human blockage at 5g millimeter-wave frequencies," *IEEE Transactions on Antennas and Propagation*, vol. 68, no. 3, pp. 2256–2266, 2020.

[8] S. Singh, F. Ziliotto, U. Madhow, E. Belding, and M. Rodwell, "Blockage and directivity in 60 ghz wireless personal area networks: from cross-layer model to multihop mac design," *IEEE Journal on Selected Areas in Communications*, vol. 27, no. 8, pp. 1400–1413, 2009.

[9] A. Okaf and D. Qiu, "Analysis of blockage impact on handover rate for user with mobility in 5g mm-wave cellular network," in *2020 International Symposium on Networks, Computers and Communications (ISNCC)*, 2020, pp. 1–6.

[10] A. Okaf, A. Saied, and D. Qiu, "Analysis of self-blockage impact on handover probability for user with mobility in 5g mm-wave cellular network," in *2021 International Symposium on Networks, Computers and Communications (ISNCC)*, 2021, pp. 1–5.

[11] A. N. Uwaechia and N. M. Mahyuddin, "A comprehensive survey on millimeter wave communications for fifth-generation wireless networks: Feasibility and challenges," *IEEE Access*, vol. 8, pp. 62 367–62 414, 2020.

[12] S. He, Y. Zhang, J. Wang, J. Zhang, J. Ren, Y. Zhang, W. Zhuang, and X. Shen, "A survey of millimeter-wave communication: Physical-layer technology specifications and enabling transmission technologies," *Proceedings of the IEEE*, vol. 109, no. 10, pp. 1666–1705, 2021.

[13] H. Friis, "A note on a simple transmission formula," *Proceedings of the IRE*, vol. 34, no. 5, pp. 254–256, 1946.

[14] M. Xiao, S. Mumtaz, Y. Huang, L. Dai, Y. Li, M. Matthaiou, G. K. Karagiannidis, E. Björnson, K. Yang, C.-L. I, and A. Ghosh, "Millimeter wave communications for future mobile networks," *IEEE Journal on Selected Areas in Communications*, vol. 35, no. 9, pp. 1909–1935, 2017.

[15] G. R. Maccartney, T. S. Rappaport, M. K. Samimi, and S. Sun, "Millimeter-wave omnidirectional path loss data for small cell 5g channel modeling," *IEEE Access*, vol. 3, pp. 1573–1580, 2015.

[16] H. Zhao, R. Mayzus, S. Sun, M. Samimi, J. K. Schulz, Y. Azar, K. Wang, G. N. Wong, F. Gutierrez, and T. S. Rappaport, "28 ghz millimeter wave cellular communication measurements for reflection and penetration loss in and around buildings in new york city," in *2013 IEEE International Conference on Communications (ICC)*, 2013, pp. 5163–5167.

[17] S. Collonge, G. Zaharia, and G. E. Zein, "Influence of the human activity on wide-band characteristics of the 60 ghz indoor radio channel," *IEEE Transactions on Wireless Communications*, vol. 3, no. 6, pp. 2396–2406, 2004.

[18] M. Jacob, C. Mbianke, and T. Kürner, "A dynamic 60 ghz radio channel model for system level simulations with mac protocols for ieee 802.11ad," in *IEEE International Symposium on Consumer Electronics (ISCE 2010)*, 2010, pp. 1–5.

[19] R. J. Weiler, M. Peter, W. Keusgen, and M. Wisotzki, "Measuring the busy urban 60 ghz outdoor access radio channel," in *2014 IEEE International Conference on Ultra-WideBand (ICUWB)*, 2014, pp. 166–170.

[20] R. J. Weiler, M. Peter, W. Keusgen, K. Sakaguchi, and F. Undi, "Environment induced shadowing of urban millimeter-wave access links," *IEEE Wireless Communications Letters*, vol. 5, no. 4, pp. 440–443, 2016.

[21] G. R. MacCartney, T. S. Rappaport, and S. Rangan, "Rapid fading due to human blockage in pedestrian crowds at 5g millimeter-wave frequencies," in *GLOBECOM 2017 - 2017 IEEE Global Communications Conference*, 2017, pp. 1–7.

[22] C. Larsson, F. Harrysson, B. Olsson, and J. Berg, "An outdoor-to-indoor propagation scenario at 28 ghz," in *The 8th European Conference on Antennas and Propagation (EuCAP 2014)*, 2014, pp. 3301–3304.

[23] T. R. R. Marins, A. A. D. Anjos, C. R. N. D. Silva, V. M. R. Peñarrocha, L. Rubio, J. Reig, R. A. A. De Souza, and M. D. Yacoub, "Fading evaluation in standardized 5g millimeter-wave band," *IEEE Access*, vol. 9, pp. 67 268–67 280, 2021.

[24] T. Bai, R. Vaze, and R. W. Heath, "Using random shape theory to model blockage in random cellular networks," in *2012 International Conference on Signal Processing and Communications (SPCOM)*, 2012, pp. 1–5.

[25] ——, "Analysis of blockage effects on urban cellular networks," *IEEE Transactions on Wireless Communications*, vol. 13, no. 9, pp. 5070–5083, 2014.

[26] M. Gapeyenko, A. Samuylov, M. Gerasimenko, D. Moltchanov, S. Singh, E. Aryafar, S. Yeh, N. Himayat, S. Andreev, and Y. Koucheryavy, "Analysis of human-body

blockage in urban millimeter-wave cellular communications," in *2016 IEEE International Conference on Communications (ICC)*, 2016, pp. 1–7.

[27] V. Raghavan, L. Akhoondzadeh-Asl, V. Podshivalov, J. Hulten, M. A. Tassoudji, O. H. Koymen, A. Sampath, and J. Li, "Statistical blockage modeling and robustness of beamforming in millimeter-wave systems," *IEEE Transactions on Microwave Theory and Techniques*, vol. 67, no. 7, pp. 3010–3024, 2019.

[28] T. Bai and R. W. Heath, "Analysis of self-body blocking effects in millimeter wave cellular networks," in *2014 48th Asilomar Conference on Signals, Systems and Computers*, 2014, pp. 1921–1925.

[29] I. K. Jain, R. Kumar, and S. S. Panwar, "The impact of mobile blockers on millimeter wave cellular systems," *IEEE Journal on Selected Areas in Communications*, vol. 37, no. 4, pp. 854–868, April 2019.

[30] G. T. 36.331, *"E-UTRA Radio Resource Control (RRC); Protocol specification (Release 9)"*, 2016.

[31] Y. Sun, G. Feng, S. Qin, Y.-C. Liang, and T.-S. P. Yum, "The smart handoff policy for millimeter wave heterogeneous cellular networks," *IEEE Transactions on Mobile Computing*, vol. 17, no. 6, pp. 1456–1468, 2018.

[32] S. Javed and B. Naeem, "Reduction of ping-pong effect in cognitive radio spectrum handoffs using fuzzy logic based inference," in *2018 UKSim-AMSS 20th International Conference on Computer Modelling and Simulation (UKSim)*, 2018, pp. 9–13.

[33] Q.-A. Zeng and D. Agrawal, "Modeling of handoffs and performance analysis of wireless data networks," in *Proceedings International Conference on Parallel Processing Workshops*, 2001, pp. 491–496.

[34] P. N. Dave, A. Amberkar, L. Gangurde, and U. Chanderki, "A novel approach for queuing based handoff for increasing reliablity of mobile communication," in *2019 1st International Conference on Innovations in Information and Communication Technology (ICIICT)*, 2019, pp. 1–5.

[35] K. Tokuyama and N. Miyoshi, "Data rate and handoff rate analysis for user mobility in cellular networks," in *2018 IEEE Wireless Communications and Networking Conference (WCNC)*, 2018, pp. 1–6.

[36] S. Sadr and R. S. Adve, "Handoff rate and coverage analysis in multi-tier heterogeneous networks," *IEEE Transactions on Wireless Communications*, vol. 14, no. 5, pp. 2626–2638, 2015.

[37] X. Lagrange and P. Godlewski, "Performance of a hierarchical cellular network with mobility-dependent hand-over strategies," in *Proceedings of Vehicular Technology Conference - VTC*, vol. 3, 1996, pp. 1868–1872 vol.3.

[38] K. I. Pedersen, P. H. Michaelsen, C. Rosa, and S. Barbera, "Mobility enhancements for lte-advanced multilayer networks with inter-site carrier aggregation," *IEEE Communications Magazine*, vol. 51, no. 5, pp. 64–71, 2013.

[39] A. Iera, A. Molinaro, and S. Marano, "Handoff management with mobility estimation in hierarchical systems," *IEEE Transactions on Vehicular Technology*, vol. 51, no. 5, pp. 915–934, 2002.

[40] S. Nikhat and M. Mehmet-Ali, "A performance evaluation of millimeter-wave cellular networks with user mobility," in *2018 IEEE Canadian Conference on Electrical Computer Engineering (CCECE)*, 2018, pp. 1–6.

[41] R. Cowan, "Objects arranged randomly in space: An accessible theory," *Advances in Applied Probability*, vol. 21, 09 1989.

[42] M. Berman, "Distance distributions associated with poisson processes of geometric figures," *Journal of Applied Probability*, vol. 14, 03 1977.

[43] S. H. Aftabi Momo and M. Munjure Mowla, "Effect of human blockage on an outdoor mmwave channel for 5g communication networks," in *2019 22nd International Conference on Computer and Information Technology (ICCIT)*, 2019, pp. 1–6.

[44] D. Hong and S. Rappaport, "Traffic model and performance analysis for cellular mobile radio telephone systems with prioritized and nonprioritized handoff procedures," *IEEE Transactions on Vehicular Technology*, vol. 35, no. 3, pp. 77–92, 1986.

[45] Y.-B. Lin, S. Mohan, and A. Noerpel, "Queueing priority channel assignment strategies for pcs hand-off and initial access," *IEEE Transactions on Vehicular Technology*, vol. 43, no. 3, pp. 704–712, 1994.

[46] R. Fantacci, "Performance evaluation of prioritized handoff schemes in mobile cellular networks," *IEEE Transactions on Vehicular Technology*, vol. 49, no. 2, pp. 485–493, 2000.

Appendix A

Proof of A':

From Fig.3.2, the area of the sector S_γ is given by:

$$S_\gamma = \frac{R^2\ \gamma}{2} \tag{1}$$

Where γ is given by:

$$\gamma = 2\pi - 2\alpha \tag{2}$$

From Fig. 3.2:

$$R = \sqrt{d^2 + r^2 - 2dr\cos\left(\pi - \omega\right)} \tag{3}$$

$$R^2 = d^2 + r^2 + 2dr\ cos(\omega) \tag{4}$$

$$\beta = \pi - (\alpha + [\pi - \omega]) = \omega - \alpha \tag{5}$$

$$\alpha = \omega - \sin^{-1}\left(\frac{d\ \sin\left(\omega\right)}{R}\right) \tag{6}$$

$$\gamma = 2\pi - 2\left[\omega - \sin^{-1}\left(\frac{d\ \sin\left(\omega\right)}{R}\right)\right] \tag{7}$$

Substituting (7) and (4) in (1), the area of the sector S_γ is given by:

$$S_\gamma = \frac{R^2}{2}\left(2\pi - 2\left[\omega - \sin^{-1}\left(\frac{d\ \sin(\omega)}{R}\right)\right]\right) \tag{8}$$

The area of sector S_ω is given by:

$$S_\omega = R^2(\pi - \omega) \tag{9}$$

The area of triangle A_τ is given by:

$$A_\tau = \frac{r\ d}{2}\ \sin(\omega) \tag{10}$$

Substituting (10), (9), and (8) in (3.3), the excess area A' is given by:

$$A' = \pi R^2 - R^2\left[\omega - \sin^{-1}\left(\frac{d\sin(\omega)}{R}\right)\right] + rdsin(\omega) - r^2(\pi - \omega) \tag{11}$$

The proof is complete.

Appendix B

All cases where MU makes displacements in different directions of (ω) forming different excess areas:

1. System model of single static blockage (Case 1: $(\frac{\pi+\theta_2}{2}) \leq \omega < \pi$):

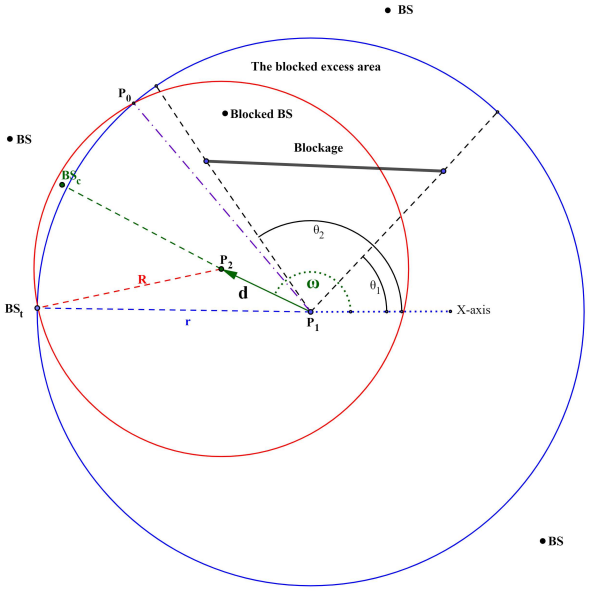

Figure 1: Appendix: System model of single static blockage (Case 1)

2. System model of single static blockage (Case 2: $\theta_2 \leq \omega < (\frac{\pi+\theta_2}{2})$):

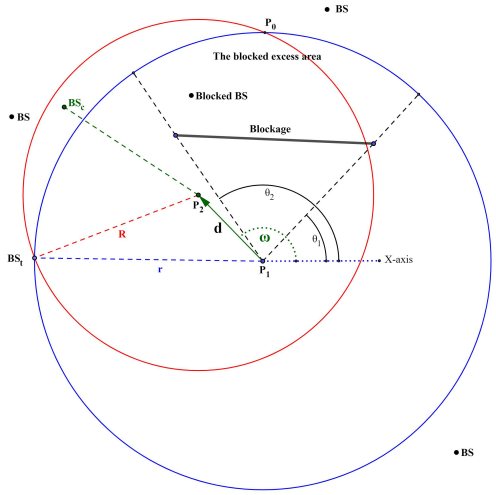

Figure 2: Appendix: System model of single static blockage (Case 2)

3. System model of single static blockage (Case 3: $(\frac{\pi+\theta_1}{2}) \leq \omega < \theta_2$):

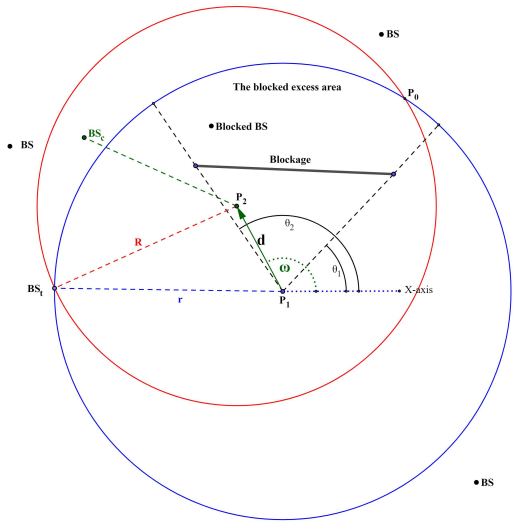

Figure 3: Appendix: System model of single static blockage (Case 3)

4. System model of single static blockage (Case 4: $\theta_1 \leq \omega < (\frac{\pi+\theta_1}{2})$):

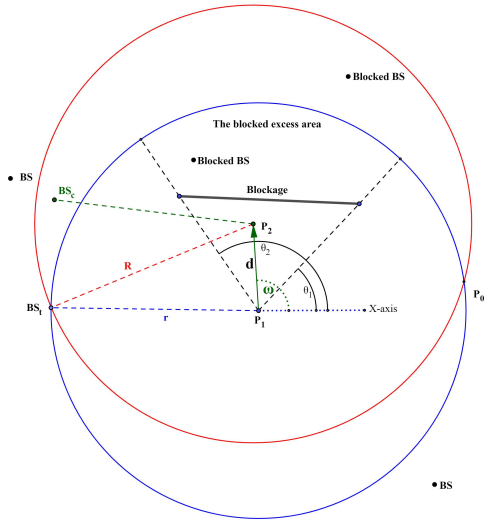

Figure 4: Appendix: System model of single static blockage (Case 4)

5. System model of single static blockage (Case 5: $0 \leq \omega < \theta_1$):

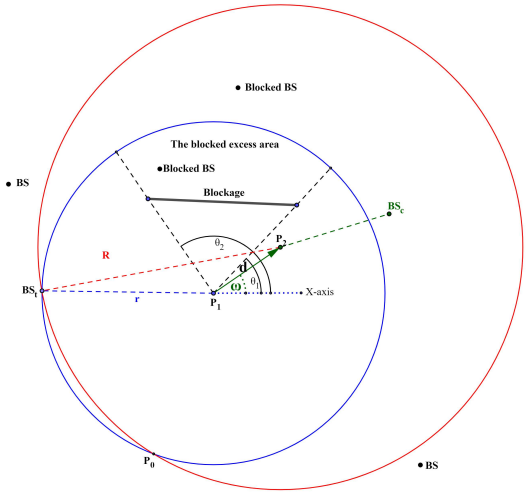

Figure 5: Appendix: System model of single static blockage (Case 5)

6. System model of single static blockage (Case 6: $\pi \leq \omega < (\frac{3\pi+\theta_1}{2})$):

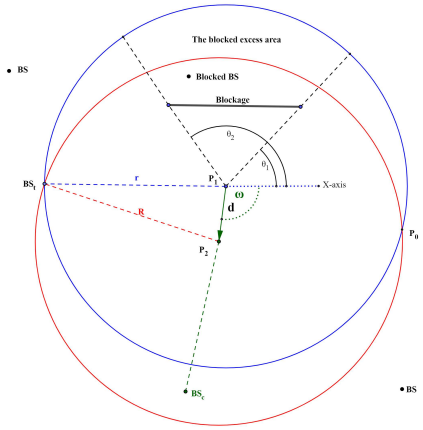

Figure 6: Appendix: System model of single static blockage (Case 6)

7. System model of single static blockage (Case 7: $(\frac{3\pi+\theta_1}{2}) \leq \omega < \theta_{P1}$):

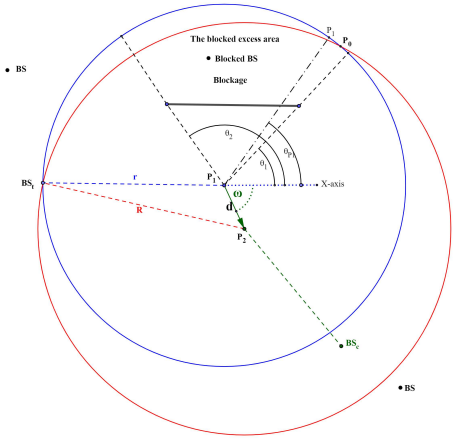

Figure 7: Appendix: System model of single static blockage (Case 7)

8. System model of single static blockage (Case 8: $\theta_{P1} \leq \omega < (\frac{3\pi+\theta_2}{2})$):

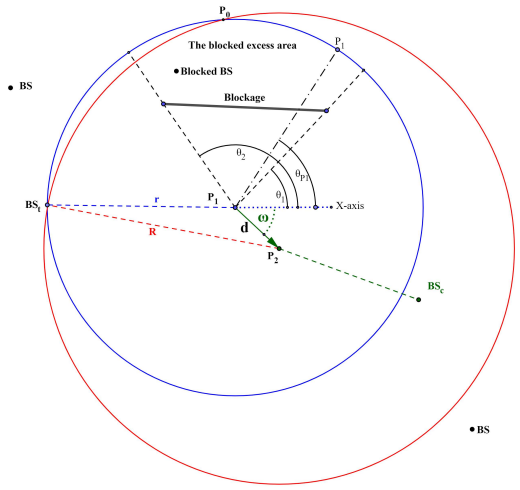

Figure 8: Appendix: System model of single static blockage (Case 8)

9. System model of single static blockage (Case 9: $(\frac{3\pi+\theta_2}{2}) \leq \omega < 0$):

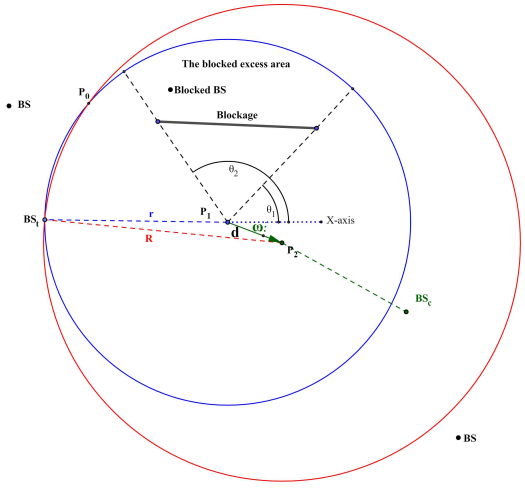

Figure 9: Appendix: System model of single static blockage (Case 9)